RESULTATS

1 EXPRESSIÓ I PURIFICACIÓ DE LES ADH8 MUTANTS

Mitjançant mutagènesi dirigida per PCR, s'obtingueren els mutants simples G223D, T224I, H225N, els dobles mutants G223D/T224I i T224I/H225N, i el triple mutant G223D/T224I/H225N. Els nivells d'expressió de les diferents proteïnes mutants fou d'aproximadament 30 mg per litre de cultiu (Taula 13). La seva purificació mostrà uns rendiments propers al 10 % (Taula 13), obtenint-se una proteïna amb un alt grau de puresa en tots els casos (Fig. 21).

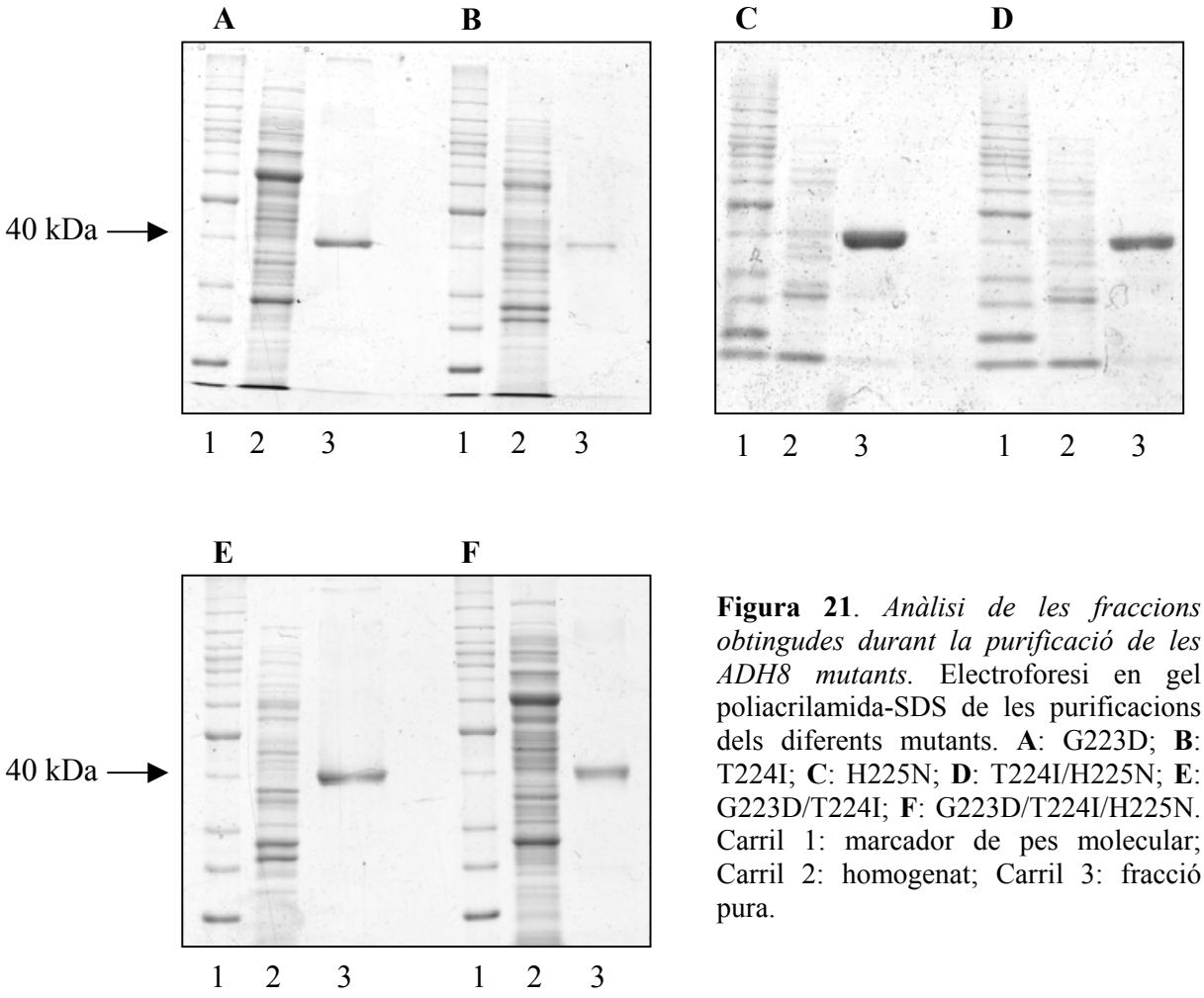

Figura 21. *Anàlisi de les fraccions obtingudes durant la purificació de les ADH8 mutants*. Electroforesi en gel poliacrilamida-SDS de les purificacions dels diferents mutants. **A**: G223D; **B**: T224I; **C**: H225N; **D**: T224I/H225N; **E**: G223D/T224I; **F**: G223D/T224I/H225N. Carril 1: marcador de pes molecular; Carril 2: homogenat; Carril 3: fracció pura.

Taula 13. Purificació dels diferents enzims mutants recombinants

ENZIM	Etapa	ADH (mg)	Activitat total (U)	Rendiment (%)
G223D	Homogenat	36	216	100
	Glutatió-Sepharose	7	42	19,4
	Cibacron Blue	4,3	26	12
T224I	Homogenat	30	318	100
	Glutatió-Sepharose	6	64	20
	Red Sepharose	3	32	10
H225N	Homogenat	35	690	100
	Glutatió-Sepharose	7	138	20
	Cibacron Blue	3,5	69	10
T224I/H225N	Homogenat	34	719	100
	Glutatió-Sepharose	5	104	15
	Cibacron Blue	3,3	69	9,7
G223D/T224I	Homogenat	32	440	100
	Glutatió-Sepharose	5	68,2	15
	Cibacron Blue	2,8	39,6	9
G223D/T224I/H225N	Homogenat	30	810	100
	Glutatió-Sepharose	4	108	13
	Cibacron Blue	2,1	57	7

Les activitats foren determinades utilitzant etanol 1M, en tampó Gly/NaOH 0,1 M, pH 10. Les concentracions de coenzim van ser: $NADP^+$ 1,2 mM per al mutant G223D; $NADP^+$ 2,4 mM per als mutants T224I i H225N; NAD^+ 0,4 mM per al mutant G223D/T224I/H225N i NAD^+ 2,4 mM per als mutants G223D/T224I i T224I/H225N.

2 CARACTERITZACIÓ CINÈTICA DE L'ENZIM SILVESTRE I DELS MUTANTS

Les constants cinètiques per al NAD^+ i $NADP^+$, a pH 10 i pH 7,5, de l'ADH8 silvestre recombinant i dels diferents mutants, determinades a concentracions saturants de substrat, es presenten en les Taules 14 i 15, respectivament. Per altra banda, les constants cinètiques per al NADH i NADPH, a pH 7,5, determinades també a concentracions saturants de substrat, es mostren en la Taula 16. Amb l'objectiu d'il.lustrar les diferències entre les eficiències catalítiques (kcat/Km) dels diferents mutants per a ambdós coenzims, i al mateix temps facilitar la seva comparació, es varen representar en diagrames de barres a la Figura 22.

2.1 CARACTERITZACIÓ CINÈTICA DE L'ADH8 SILVESTRE RECOMBINANT

La caracterització de l'ADH8 silvestre recombinant revelà que les seves constants cinètiques eren força similars a les de l'enzim natiu purificat a partir d'estómac de granota (Peralba i col., 1999a). L'ADH8 recombinant, com ja havia estat observat en l'enzim purificat a partir de teixit, presenta valors de kcat força similars amb NADP(H) i NAD(H), a un mateix pH i amb el mateix substrat. Aquest resultat suggereix que les reaccions d'oxidació/reducció catalitzades per l'enzim presentarien un pas limitant independent del coenzim utilitzat. En canvi, els valors de Km per al NADP(H) foren 10-40 vegades més baixos que per al NAD(H). Així l'ADH8 és un enzim molt més específic per al NADP(H), especialment a pH 7,5.

2.2 CARACTERITZACIÓ CINÈTICA DELS ENZIMS MUTANTS

Respecte a l'efecte de les substitucions en les cinètiques dels coenzims, la majoria de les observacions fetes a pH 10 (Taula 14) podien ser confirmades a pH 7,5, tant per a la reacció d'oxidació (Taula 15) com per a la de reducció (Taula 16). Aquest resultat suggereix que una mateixa mutació genera un efecte similar per a un mateix coenzim, independentment del pH i de l'estat d'oxidació del coenzim. En canvi, una mateixa substitució sí que provocava efectes diferents en funció del coenzim utilitzat, NADP(H) o NAD(H).

2.2.1 Mutants G223D, T224I i H225N

Les mutacions simples només produiren una petita disminució (2-8 vegades) en l'eficiència catalítica (kcat/Km) per al NADP(H). Generalment, això fou degut a un increment en els valors de Km, mentre que els valors de kcat no variaven significativament entre els mutants.

La substitució G223D no impedí la unió del $NADP^+$ ni canvià la kcat significativament, com hauria estat l'esperat, sinó que l'enzim encara preferia el NADP(H) per sobre del NAD(H). Resultats similars s'obtingueren per al mutant T224I. La substitució H225N va ésser ben tolerada, i fou la que tingué menys efecte en les cinètiques amb NADP(H). No s'observaren efectes dependents de pH associats amb aquesta mutació, potser degut a que aquesta His es trobaria desprotonada tant a pH 7,5 com a pH 10.

Les mutacions simples van produir efectes positius en les cinètiques amb NAD(H), amb un moderat increment en els valors de kcat/Km. T224I mostrà la millor eficiència catalítica d'aquests mutants per a aquest coenzim, mentres que H225N exhibí l'eficiència catalítica més baixa, degut principalment a l'elevat valor de Km per al NAD(H). En tots els mutants simples, els valors de kcat per al NAD(H) romanen pràcticament constants, el que suggereix un mateix pas limitant.

A qualsevol dels pHs utilitzats, cap dels tres mutants mostrà una reversió en la seva especificitat de coenzim. Només el mutant T224I presentà una eficiència catalítica molt similar, a pH 10, amb ambdós coenzims.

2.2.2 Mutants T224I/H225N i G223D/T224I

Una doble mutació fou el mínim canvi necessari per observar un clar efecte en l'especificitat de coenzim, tant a pH 7,5 com a pH 10. L'efecte fou molt més marcat en les cinètiques per al NADP(H), especialment en el mutant G223D/T224I. Aquest mutant no va poder ésser saturat amb NADP(H) i, per tant, els seus valors de Km i de kcat no varen poder ésser determinats. Les constants cinètiques només poderen ésser acuradament mesurades per al mutant T224I/H225N en la reacció d'oxidació: els valors de Km per al $NADP^+$ s'incrementaren notablement (més de 200 vegades), i els valors de kcat baixaren 30 vegades. L'eficiència catalítica per al NADP(H) va decréixer de 1500 a 10000 vegades per a G223D/T224I i de 100 a 1400 vegades per a T224I/H225N.

Ambdós mutants varen mostrar un moderat increment en els valors de kcat/Km per al NAD(H), principalment degut a una petita disminució en els valors de Km (més marcada en G223D/T224I). En general, els dobles mutants varen mostrar un canvi en l'especificitat de coenzim, però sense aconseguir-ne una reversió total.

2.2.3 Mutant G223D/T224I/H225N

La triple substitució G223D/T224I/H225N va produir una reversió completa de l'especificitat de coenzim, tant a pH 7,5 com a pH 10. En comparació amb els dobles mutants, l'efecte fou més marcat en les cinètiques amb NAD(H). Així, l'eficiència catalítica del triple mutant per al NAD(H) s'incrementà de 30 a 50 vegades respecte l'enzim silvestre recombinant, i fins i tot fou més gran que el valor de kcat/Km de l'ADH8 per al NADP(H). Aquest resultat fou provocat fonamentalment per una disminució en els valors de Km per al NAD(H).

Per altra banda, el triple mutant no va poder ésser saturat amb NADP(H), presentant aquest enzim una disminució de l'eficiència catalítica per a aquest coenzim del mateix ordre de magnitud que els dobles mutants. Així, el triple mutant es comportà com un enzim dependent de NAD(H), essent molt més específic per a aquest coenzim que l'ADH8 silvestre per al NADP(H).

Taula 14. Constants cinètiques d'ADH8 silvestre i dels enzims mutants amb $NADP^+$ i NAD^+, a pH 10.

Enzim	Coenzim	Km (mM)	kcat (min^{-1})	kcat/Km ($mM^{-1}min^{-1}$)
Silvestre	$NADP^+$	0,050 ± 0,002	1600 ± 80	32000 ± 6600
	NAD^+	0,50 ± 0,05	1490 ± 60	2980 ± 295
G223D	$NADP^+$	0,08 ± 0,01	600 ± 50	7500 ± 1100
	NAD^+	0,42 ± 0,06	1550 ± 50	3690 ± 530
T224I	$NADP^+$	0,20 ± 0,01	900 ± 170	4500 ± 890
	NAD^+	0,44 ± 0,03	2370 ± 10	5390 ± 320
H225N	$NADP^+$	0,16 ± 0,01	1690 ± 76	10560 ± 640
	NAD^+	1,7 ± 0,4	1820 ± 280	1050 ± 270
G223D/T224I	$NADP^+$	N.S.[a]	N.S.	9.0 ± 0.3[b]
	NAD^+	0,130 ± 0,002	1227 ± 40	9440 ± 360
T224I/H225N	$NADP^+$	1,37 ± 0,30	50 ± 3	36 ± 9
	NAD^+	0,20 ± 0,04	1850 ± 70	9250 ± 1840
G223D/T224I/H225N	$NADP^+$	N.S.	N.S.	15 ± 2[b]
	NAD^+	0,020 ± 0,003	2275 ± 70	113750 ± 10700

Les activitats foren mesurades amb etanol 1 M i tampó glicina/NaOH 0,1 M, pH 10.

[a] N.S.: no saturació amb $NADP^+$ 4,8 mM i 9,6 mM, per al G223D/T224I i el G223D/T224I/H225N, respectivament.

[b] kcat/Km fou calculada com el pendent de la representació lineal de V *versus* [S].

Taula 15. Constants cinètiques d'ADH8 silvestre i dels enzims mutants amb $NADP^+$ i NAD^+, a pH 7,5.

Enzim	Coenzim	Km (mM)	kcat (min^{-1})	kcat/Km ($mM^{-1}min^{-1}$)
Silvestre	$NADP^+$	0,045 ± 0,007	640 ± 35	14220 ± 2330
	NAD^+	2,0 ± 0,2	640 ± 15	320 ± 33
G223D	$NADP^+$	0,090 ± 0,008	160 ± 9	1780 ± 430
	NAD^+	0,64 ± 0,02	420 ± 50	655 ± 80
T224I	$NADP^+$	0,07 ± 0,01	330 ± 11	4715 ± 730
	NAD^+	0,36 ± 0,06	560 ± 38	1555 ± 272
H225N	$NADP^+$	0,11 ± 0,01	590 ± 37	5360 ± 640
	NAD^+	3,0 ± 0,2	450 ± 48	150 ± 21
G223D/T224I	$NADP^+$	N.S.[a]	N.S.	1,3 ± 0,1[b]
	NAD^+	0,25 ± 0,03	330 ± 17	1500 ± 220
T224I/H225N	$NADP^+$	9,0 ± 0,7	95 ± 5	10 ± 1
	NAD^+	0,34 ± 0,03	580 ± 31	1700 ± 160
G223D/T224I/H225N	$NADP^+$	N.S.	N.S.	6 ± 1[b]
	NAD^+	0,05 ± 0,01	785 ± 33	15700 ± 2890

Les activitats foren mesurades amb octanol 1,5 mM i tampó fosfat/NaOH 0,1 M, pH 7,5.

[a] N.S.: no saturació amb $NADP^+$ 4,8 mM i 9,6 mM, per al G223D/T224I i el G223D/T224I/H225N, respectivament.

[b] kcat/Km fou calculada com el pendent de la representació lineal de V *versus* [S].

Taula 16. Constants cinètiques d'ADH8 silvestre i dels enzims mutants amb NADPH i NADH, a pH 7,5.

Enzim	Coenzim	Km (mM)	kcat (min^{-1})	Kcat/Km ($mM^{-1}min^{-1}$)
Silvestre	NADPH	0,030 ± 0,006	4000 ± 10	133330 ± 26670
	NADH	0,44 ± 0,07	2455 ± 190	5580 ± 990
G223D	NADPH	0,110 ± 0,008	1765 ± 120	16050 ± 1590
	NADH	0,150 ± 0,006	1610 ± 50	10735 ± 550
T224I	NADPH	0,050 ± 0,001	1920 ± 80	38400 ± 1720
	NADH	0,110 ± 0,008	1920 ± 10	17455 ± 1260
H225N	NADPH	0,080 ± 0,003	4605 ± 110	57560 ± 2535
	NADH	0,660 ± 0,016	2350 ± 70	3560 ± 140
G223D/T224I	NADPH	N.S.[a]	N.S.	89 ± 7[b]
	NADH	0,040 ± 0,002	1500 ± 190	37550 ± 5100
T224I/H225N	NADPH	N.S.	N.S.	1250 ± 50[b]
	NADH	0,150 ± 0,016	2805 ± 100	18700 ± 2100
G223D/T224I/H225N	NADPH	N.S.	N.S.	760 ± 21[b]
	NADH	0,040 ± 0,001	6200 ± 150	155000 ± 4100

Les activitats foren mesurades amb *m*-nitrobenzaldehid 0,2 mM i tampó fosfat/NaOH 0,1 M, pH 7,5.

[a] N.S.: no saturació amb NADPH 1,2 mM.

[b] kcat/Km fou calculada com el pendent de la representació lineal de V *versus* [S].

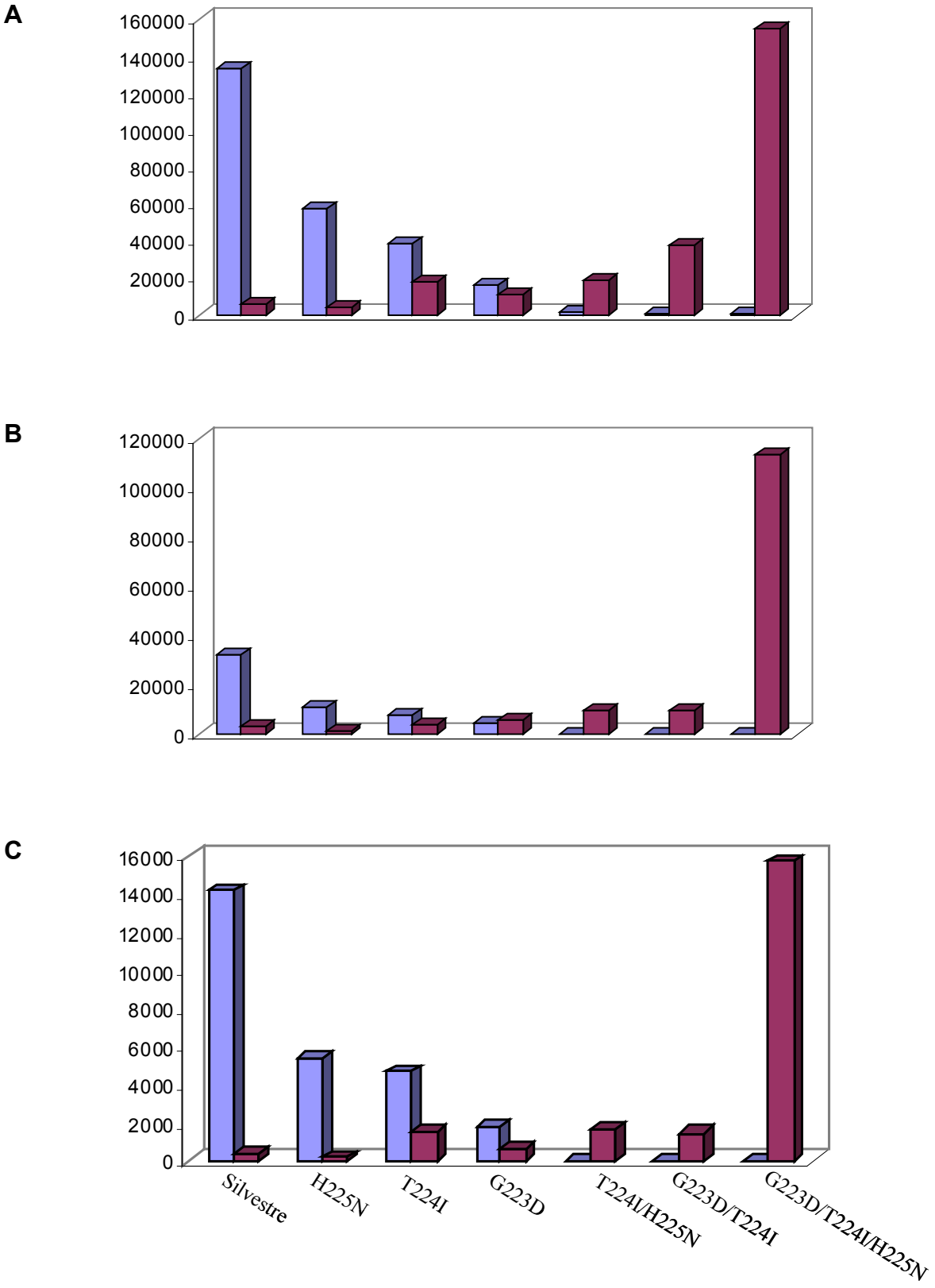

Figura 22. *Eficiències catalítiques* (kcat/Km, $mM^{-1}\cdot min^{-1}$) *de l'enzim silvestre i dels mutants per a les reaccions de reducció* **(A)** *i oxidació a pH 10* **(B)** *i pH 7,5* **(C)**, *utilitzant NADP(H)* (blau) *i NAD(H)* (grana) *com a coenzims.*

3 CINÈTIQUES BISUBSTRAT

Els resultats obtinguts en les cinètiques bisubstrat foren compatibles amb un mecanisme seqüencial Bi-Bi (Taula 17). En els diferents enzims analitzats, els valors de la Km per a l'etanol (Kb) es trobava entre 25 i 110 mM.

Les mutacions simples tingueren un efecte modest en els valors de kcat per al $NADP^+$. Aquesta disminuí, unes 20 vegades en el doble mutant T224I/H225N, i no va poder ésser determinada en el triple mutant G223D/T224I/H225N en no poder-se arribar a saturació. Per al doble mutant, aquest dramàtic canvi en el valor de kcat anà acompanyat d'un increment en les constants de dissociació (Kia) i de Michaelis (Ka) per al $NADP^+$, de 60 i 30 vegades respectivament.

En canvi, el valor de kcat per al NAD^+ romangué relativament constant en totes les formes substituides, suggerint un pas limitant comú. L'eficiència catalítica per al NAD^+, mesurada com kcat/KiaKb (Plapp, 1995), augmentà 30 vegades en el triple mutant, arribant al mateix nivell que la de l'enzim silvestre recombinant.

4 EFECTE ISOTÒPIC

L'efecte isotòpic fou estudiat utilitzant etanol deuterat com a substrat, en presència de cadascun dels coenzims. Un efecte isotòpic ($kcat_H/Km_H/kcat_D/Km_D$) d'aproximadament 2 cops fou observat tant amb $NADP^+$ com en NAD^+ a l'ADH8 silvestre recombinant (Taula 18), suggerint que la transferència de l'ió hidrur podria ser el pas limitant durant la catàlisi.

Respecte els enzims mutants, i quan utilitzem $NADP^+$ com a coenzim, el mateix increment només és vist en els mutants simples. En canvi, els dobles i triple mutants no mostren efecte isotòpic, indicant que la transferència de l'ió hidrur no en seria el pas limitant. Per altra banda, amb NAD^+ com a coenzim, un efecte isotòpic de 2 és observat en totes les formes mutants.

Taula 17. Cinètiques bisubstrat d'ADH8 silvestre i dels enzims mutants amb $NADP^+$ i NAD^+, a pH 10.

Enzim	Coenzim	Kia (mM)	Ka (mM)	Kb (mM)	kcat (min^{-1})	kcat/KiaKb (mM^{-2} min^{-1})
Silvestre	$NADP^+$	0,02	0,042	25	1520	3040
	NAD^+	0,56	0,83	31	1790	103
G223D	$NADP^+$	0,037[a]	0,14	109	570	141
	NAD^+	0,22[a]	0,33	35	1100	143
T224I	$NADP^+$	0,028	0,12	98	900	328
	NAD^+	0,12[a]	0,20	41	2250	457
H225N	$NADP^+$	0,16	0,10	40	1700	265
	NAD^+	0,71	0,88	39	1795	65
T224I/H225N	$NADP^+$	1,22	1,16	56	76	1
	NAD^+	0,12	0,23	68	2090	256
G223D/T224I/H225N	$NADP^+$	N.S.[b]	N.S.	N.S.	N.S.	N.S.
	NAD^+	0,017[a]	0,04	45	2450	3200

Les activitats foren mesurades en tampó glicina/NaOH 0,1 M, pH 10, amb etanol com a substrat.

Els errors estàndard dels ajustos foren menors del 20%, excepte en els valors indicats.

Kia i Ka són les constants de dissociació i de Michaelis per al NAD^+, respectivament.

Kb és la constant de Michaelis per a l'etanol.

[a] Els errors estàndard dels ajustos foren del 20-30%.

[b] N.S.: no saturació amb $NADP^+$ 9,6 mM.

Taula 18. Efecte isotòpic en l'ADH8 silvestre i en els enzims mutants amb $NADP^+$ i NAD^+, a pH 10.

Enzim	**$NADP^+$**		**NAD^+**	
	kcatH/kcatD	**(kcatH/KmH)/ (kcatD/KmD)**	**kcatH/kcatD**	**(kcatH/KmH)/ (kcatD/KmD)**
Silvestre	1,99	1,99	1,85	2,02
G223D	2,04	1,95	1,72	1,86
T224I	1,94	2,04	1,88	2,04
H225N	2,11	2,04	1,87	1,81
G223D/T224I	1,31[a]	1,15[b]	1,78	1,57
T224I/H225N	1,03	1,08	1,60	1,80
G223D/T224I/H225N	0,90[a]	1,02[b]	2,08	1,66

Les activitats foren mesurades amb etanol-*d6* o etanol 1M, com a substrat, i tampó glicina/NaOH, pH 10.

[a] La relació d'activitats fou calculada a una sola concentració de coenzim ($NADP^+$ 4,8 mM), ja que no es podia aconseguir la saturació.

[b] kcat/Km fou calculada com el pendent de la representació lineal de V *versus* [S], ja que no es podia aconseguir la saturació.

5 MODELATGE MOLECULAR

A partir de les coordenades de l'estructura tridimensional del complex ADH8-$NADP^+$, es generaren els models moleculars dels complexos binaris dels mutants G223D, T224I, H225N i T224I/H225N amb $NADP^+$ (Fig. 23), i de l'ADH8 i del triple mutant amb NAD^+ (Fig. 24).

En l'estructura resolta del complex ADH8-$NADP^+$, els àtoms d'oxigen del grup fosfat addicional interaccionen a través de 5 ponts d'hidrogen amb les cadenes laterals de Thr224, His225, Lys228, i amb els àtoms de nitrogen de les cadenes principals de Leu200 i Thr224 (Fig. 23A). En el complex G223D-$NADP^+$, impediments estèrics i electroestàtics generats per la cadena lateral d'Asp223 forcen la reubicació del fosfat del coenzim en el seti d'unió, allunyant-se de Lys228 (comparar Figs. 23A i 23B). Així, com a resultat de la mutació G223D, els ponts d'hidrogen amb Leu200 i Lys228, i amb l'atom de nitrogen de la cadena principal de Thr224, es perden. Però aquestes pèrdues són parcialment compensades per l'existència de dos nous ponts d'hidrogen que realitza un àtom d'oxigen del fosfat teminal amb l'oxigen del grup carbonil de Leu362, i amb l'àtom d'oxigen de Ser364. Així, un àtom d'oxigen del grup fosfat addicional queda sense interaccionar, encara que ho podria fer a través d'una molècula d'aigua.

En els complexos T224I-$NADP^+$ i H225N-$NADP^+$, s'observen petites diferències envers el $NADP^+$ unit a l'enzim silvestre recombinant. En ambdós casos, es perden dos ponts d'hidrogen dels realitzats pel fosfat terminal, però es forma un nou pont d'hidrogen, de manera que tots els àtoms d'oxigen del grup fosfat addicional es troben interaccionant amb algun residu (Fig. 23C i 23D).

En comparar el $NADP^+$ unit al mutant T224I/H225N amb l'unit a l'ADH8 silvestre, s'observa que un àtom d'oxigen del grup fosfat terminal no interaccionaria amb cap residu (Fig. 23E), encara que és possible que ho fés amb alguna molècula d'aigua.

En la simulació de la interacció del $NADP^+$ amb el triple mutant, també es produeix una reubicació del coenzim. En aquest cas però, es perden algunes interaccions proteïna-coenzim (tres ponts d'hidrogen), que no són compensades per la creació de nous ponts d'hidrogen. Com a resultat, un àtom d'oxigen del grup fosfat addicional no interacciona amb cap residu, essent possible la interacció amb molècules d'aigua (Fig. 23F).

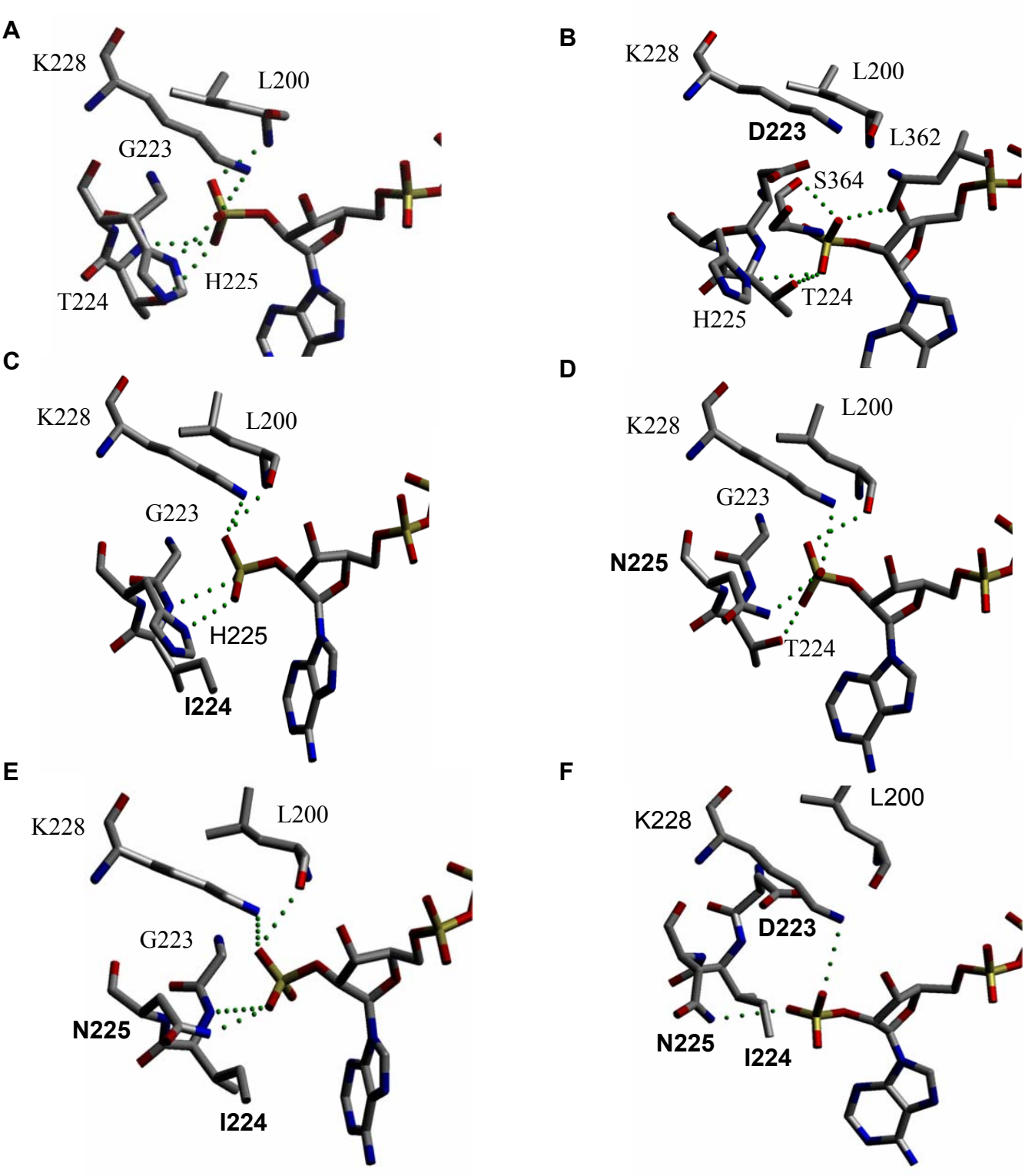

Figura 23. *Representació de l'estructura cristalogàfica del complex binari ADH8-NADP*$^+$ **(A)** *i de les simulacions d'interacció del NADP*$^+$ *amb els mutants G223D* **(B)**, *T224I* **(C)**, *H225N* **(D)**, *H225N/T224I* **(E)** *i G223D/T224I/H225N* **(F)**. En negreta, els residus mutats.

En el complex binari del triple mutant amb NAD^+, Asp223 interacciona amb els àtoms d'oxigen 2' i 3' de la ribosa de l'adenosina. Per altra banda, l'oxigen 3' es troba també unit per pont d'hidrogen a Lys228 (Fig. 24B). Aquests contactes són característics d'ADHs dependents de NAD(H) (Eklund i col., 1984; Hurley i col., 1991; Xie i col., 1997; Svensson i col., 2000). A més, es produeix una interacció hidrofòbica entre l'anell d'adenina i Ile224, que no s'observa en el complex del triple mutant amb $NADP^+$ (Fig. 23A). Aquesta interacció hidrofòbica és també típica d'ADHs dependents de NAD(H), així com d'altres enzims dependents d'aquest coenzim (Carugo i Argos, 1997).

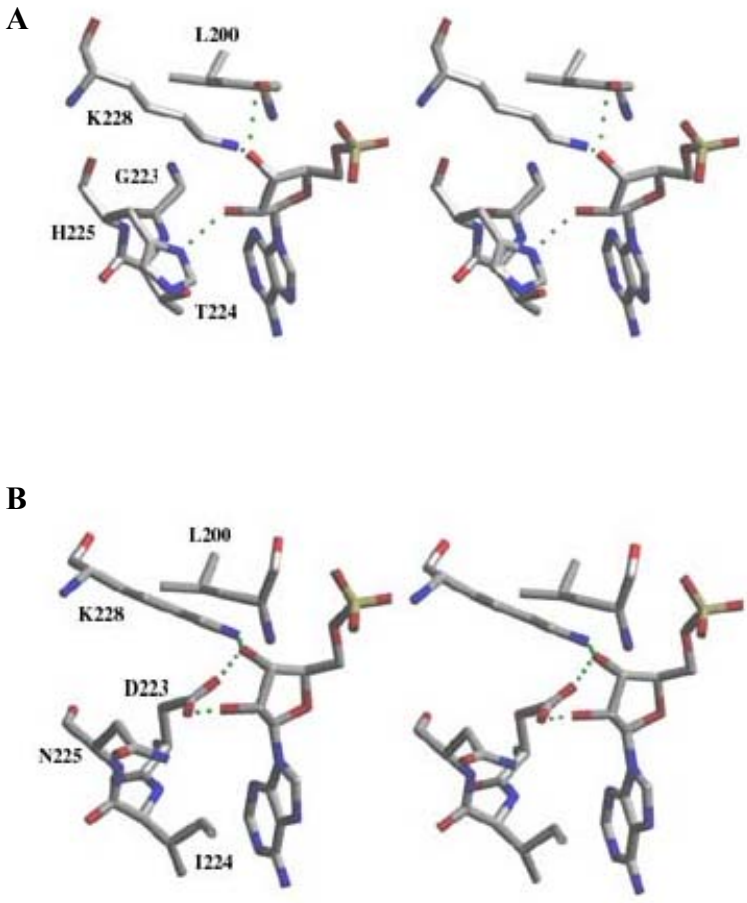

Figura 24. *Representació estereoscòpica del complex binari ADH8-NAD^+* **(A)** *i del complex del mutant G223D/T224I/H225N amb NAD^+* **(B)**.

En el complex ADH8-NAD^+, observem com aquest coenzim pot encaixar fàcilment en el seti d'unió al coenzim. Aquest fet explicaria que ADH8 sigui activa amb el NAD^+ com a coenzim. Les interaccions que realitza el NAD^+ amb la proteïna són equivalents a les que realitza aquest coenzim amb un enzim dependent de NAD(H): 2 ponts d'hidrogen amb els àtoms d'oxigen 2' i 3' (en el model, realitzats per His225 i Leu200, respectivament, Fig. 24A), i la interacció de Lys228 amb l'oxigen 3'. No es conserva, però, la interacció hidrofòbica amb l'anell d'adenina. Els ponts d'hidrogen generats per His225 i Leu200 amb els oxigens 2' i 3', podrien diferir en les seves propietats respecte als realitzats per Asp223, creant condicions no òptimes per a la unió del NAD(H). Això queda reflectit en les baixes eficiències catalítiques d'ADH8 amb NAD(H).

DISCUSSIÓ

ADH8 és l'únic membre de la subfamília de les ADHs d'animals que utilitza preferentment NADP(H) com a coenzim (Peralba i col., 1999a). ADH8 també uneix NAD(H), però amb uns valors de Km 10-40 vegades més elevats que per al NADP(H). La resolució de l'estructura del complex ADH8-$NADP^+$ mostrà que la butxaca d'unió al fosfat estava configurada pels residus no conservats Gly223, Thr224 i His225, i dos residus altament conservats, Leu200 i Lys228.

La contribució individual dels tres primers residus en la discriminació entre NAD(H) i NADP(H) no era coneguda. Resoldre aquest interrogant, així com intentar revertir l'especificitat de coenzim, foren els objectius d'aquest estudi de mutagènesi dirigida. Així, els residus 223, 224 i 225 foren substituïts separadament o en diferents combinacions, i les proteïnes mutants recombinants caracteritzades envers ambdós coenzims.

1 ESTUDI DEL PAS LIMITANT DE LES REACCIONS CATALITZADES PER ADH8

En les ADHs, el pas limitant de la reacció d'oxidació de l'etanol i d'altres alcohols alifàtics és la dissociació del coenzim reduït (Brändén i Eklund, 1980; Stone i col., 1993b). Així, la constant de velocitat de dissociació del coenzim (k_7) sovint determina la constant catalítica de la reacció (kcat).

L'assaig d'efecte isotòpic, però, revelà que la transferència de l'ió hidrur seria el pas limitant de la reacció d'oxidació de l'etanol catalitzada per ADH8, tant amb $NADP^+$ com amb NAD^+ com a coenzims. La transferència de l'ió hidrur també ha estat proposada com a pas limitant en altres ADHs, utilitzant etanol com a substrat, com l'ADH3 humana (Lee i col., 2003) i el mutant I269S de l'ADH1 de cavall (Fan i Plapp, 1995).

1.1 EFECTE DE LES DIFERENTS MUTACIONS EN EL PAS LIMITANT

En els mutants simples, utilitzant $NADP^+$ com a coenzim s'observà un efecte isotòpic de la mateixa magnitud que en l'ADH8 recombinant. Així, la transferència de l'ió l'hidrur també seria el pas limitant per a aquests enzims utilitzant aquest coenzim. Aquest resultat explicaria el descens dels valors de kcat per al NADP(H) d'aquests mutants, malgrat que al mateix temps es produia un increment en els valors de la constant de dissociació (Kia) per el $NADP^+$.

En el mutant T224I/H225N, els valors de kcat sofriren una brusca disminució, que anà acompanyada d'un increment en el valor de Kia per el $NADP^+$. En els mutants G223D/T224I i G223D/T224I/H225N, l'eficiència catalítica disminuí dramàticament, probablement reflectint un increment del valor de la Km per al NADP(H). En aquests tres mutants però, l'assaig d'efecte isotòpic mostrà que la transferència de l'ió l'hidrur no seria el pas limitant. En aquests enzims, un pas limitant encara més lent, com el canvi conformacional associat a la unió del coenzim, en podria ser el responsable. Actualment però, no tenim evidències de que es produeixi un canvi conformacional després de la unió al coenzim, degut a que l'estructura de l'apoenzim mostrà la mateixa conformació que el complex binari. La dissociació del coenzim no seria el nou pas limitant en aquests enzims, degut a que els increments en els valors de Kia no es traduiren en un augment en els valors de kcat.

Quan en els assajos d'efecte isotòpic el NAD^+ fou utilitzat com a coenzim, s'observà un efecte de semblant magnidud en tots els mutants, suggerint que la transferència de l'ió hidrur seria el pas limitant. Aquest resultat era consistent amb el fet que els valors de kcat per al NAD(H) es mantenien relativament invariables per als enzims mutants envers l'ADH8 silvestre recombinant, indicant que el pas limitant era probablement el mateix en totes les formes enzimàtiques quan el NAD^+ era utilitzat com a coenzim.

2 IMPORTÀNCIA DE GLY223, THR224 I HIS225 EN L'ESPECIFICITAT DE COENZIM DE L'ADH8

2.1 EL RESIDU 223 NO ÉS L'ÚNIC RESIDU DETERMINANT EN L'ESPECIFICITAT DE COENZIM

Les deshidrogenases dependents de NAD(H) presenten un residu acídic en l'extrem C-terminal de la segona fulla β del plegament de Rossmann (Bellamacina, 1996), que és Asp223 en ADHs dependents de NAD(H) (Sun i Plapp, 1992). En les estructures resoltes de diferents complexos ADH-NAD^+, aquest residu es troba unit per ponts d'hidrogen als grups hidroxil 2' i 3' de la ribosa de l'adenosina (Eklund i col., 1984; Hurley i col., 1991; Xie i col., 1997; Svensson i col., 2000). La importància d'aquest residu acídic en l'especificitat de coenzim ha estat estudiada des de fa molt de temps, essent considerada la seva presència un tret distintiu dels dominis d'unió al NAD(H) (Rossmann i col., 1974; Ohlsson i col., 1974).

En les deshidrogenases/reductases de cadena mitjana (MDR), Asp223 ha estat proposat com el residu que discriminaria en contra del NADP(H) (Fan i col., 1991). Les MDR dependents de NADP(H) presenten en la posició equivalent un residu menys voluminós i no carregat, normalment Gly, Ala o Ser (Lauvergeat i col., 1995, Lesk, 1995, Edwards i col., 1996; Banfield i col., 2001), que reduiria els impediments estèrics i electroestàtics durant la unió del NADP(H). Així, per revertir l'especificitat de coenzim de diferents MDR, nombrosos estudis de mutagènesi dirigida han estat focalitzats envers aquest residu. En un cas, l'Asp homòleg de l'ADH1 de llevat fou substituït per Gly. El mutant resultant utilitzà els dos coenzims amb similar però molt baixa eficiència (Fan i col., 1991). En la cinamil alcohol deshidrogenasa, enzim dependent de NADP(H), la mutació inversa equivalent, S212D, tampoc canvià l'especificitat de coenzim (Lauvergeat i col., 1995). De forma similar, la substitució del corresponent Asp en altres deshidrogenases dependents de NAD(H) no generà enzims dependents de NADP(H), encara que la substitució millorà l'eficiència catalítica per al $NADP^+$ i l'empitjorà per al NAD^+ (Feeney i col., 1990; Chen i col., 1991).

En el present treball, les mutacions simples G223D, T224I i H225N només proporcionen petits canvis en les cinètiques per als coenzims, que foren moderadament menys eficients per al NADP(H) i lleugerament més eficients per al NAD(H). Per al NADP(H), en general, existí una bona correlació entre la pèrdua de ponts d'hidrogen i d'interaccions electroestàtiques, i modestos increments en els valors de Km i de Kia.

La substitució G223D, tot i generar un enzim amb una més baixa eficiència catalítica per al NADP(H), no impedeix la unió d'aquest coenzim, preferint encara aquest mutant el NADP(H) com a coenzim. El model del complex G223D-$NADP^+$, confirma la generació, per part de la cadena lateral acídica de l'Asp, de condicions estèriques i electroestàtiques desfavorables durant la unió del NADP(H). Sorprenentment, però, el grup fosfat addicional del $NADP^+$ pot encara encabir-se en la butxaca d'unió al coenzim, tot i perdre ponts d'hidrogen i interaccions electrostàtiques favorables. D'acord amb aquests resultats, i confirmant resultats previs en altres MDR (Fan i col., 1991; Lauvergeat i col., 1995 ; Metger i Hollenberg, 1995; Fan i Plapp, 1999), la presència o absència d'un residu acídic en la posició 223 no pot ésser considerat com l'únic factor determinant en l'especificitat de coenzim d'ADH8 i, per tant, podria ser important la seva combinació amb substitucions en altres posicions.

2.2 LA REVERSIÓ COMPLETA DE L'ESPECIFICITAT DE COENZIM NOMÉS ES PRODUEIX EN EL TRIPLE MUTANT

En el triple mutant, els valors de Km, kcat i kcat/Km per al NAD(H), i de Kia per al NAD^+ són del mateix ordre de magnitud que els de l'ADH8 silvestre recombinant per al NADP(H). Així, podem afirmar que hem aconseguit la reversió completa de l'especificitat de coenzim en aquest mutant. Encara més, els valors de kcat/Km del triple mutant són similars als d'altres ADHs dependents de NAD(H) (Taula 19).

En general, el triple mutant és molt més "específic de coenzim" que l'enzim silvestre, com ho il.lustra la representació del logaritme del quocient $kcat/Km_{(NADH)}/kcat/Km_{(NADPH)}$ (Fig. 25). Aquest comportament és típic d'ADHs dependents de NAD(H) de vertebrats, que freqüentment són altament específiques per al NAD(H), encara que també presenten una activitat residual amb NADP(H).

Taula 19. Constants cinètiques d'ADHs per al NAD^+ a pH 7,5.

Enzim	Organisme	Km (mM)	kcat (min^{-1})	kcat/Km ($mM^{-1}min^{-1}$)
	Home			
ADH1A[a]		0,013	54	4154
ADH1B1[a]		0,0074	18	2432
ADH1B2[b]		0,18	800	4444
ADH1B3[b]		0,71	600	845
ADH1C1[a]		0,0079	170	21519
ADH1C2[b]		0,0087	70	8046
ADH2[c]		0,014	40	2857
ADH4[d]		0,18	1510	8390
	Rata			
ADH1[f]		0,17	39	229
ADH2[f]		0,2	300	1500
ADH3[f]		0,04	4	100
ADH4[e]		0,3	300[f]	1000
	Granota			
ADH1[g]		0,03	17	567
ADH8		2	640	320
TM		0,05	785	15700

Les constants foren determinades utilitzant etanol com a substrat, a excepció dels enzims ADH2, ADH3 i ADH4 de rata, ADH8 i TM (Triple Mutant), on ho fou l'octanol. **a** Bosron i col., 1983; **b** Burnell i col. 1989; **c** Bosron i col., 1979; **d** Farrés i col., 1994; **f** Boleda i col., 1991; **g** Peralba i col., 1999b.

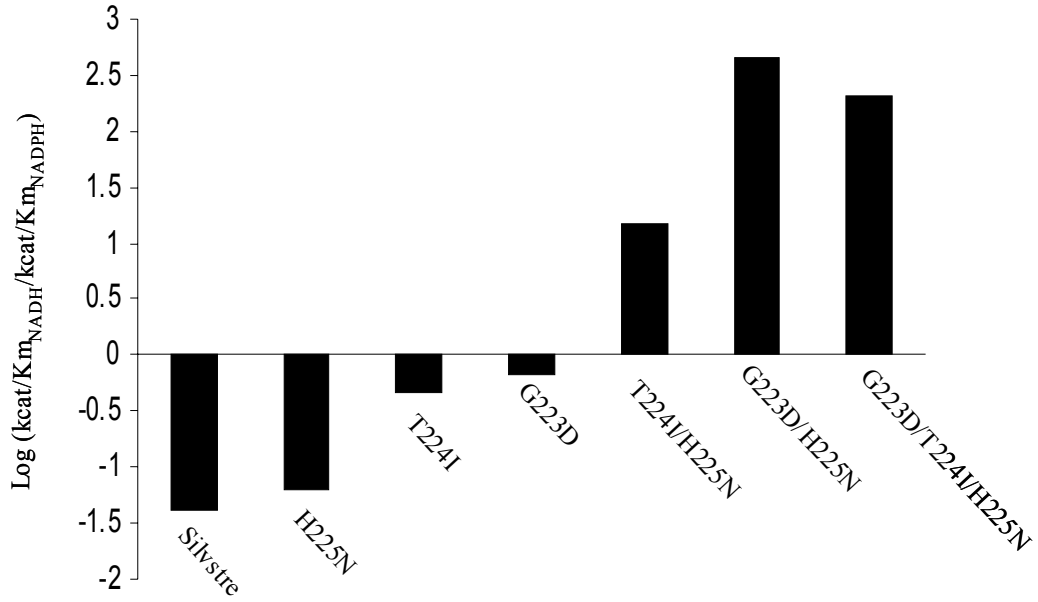

Figura 25. *Grau d'especificitat de coenzim de l'ADH8 silvestre i dels mutants.* Diagrama de barres on es representa el logaritme del quocient entre les eficiències catalítiques amb NADH i NADPH a pH 7,5, utilitzant *m*-nitrobenzaldehid 0,2 mM com a substrat.

En el model molecular del complex del triple mutant amb $NADP^+$, es pot apreciar com el coenzim s'uneix de diferent manera a com ho feia en l'ADH8 silvestre. Això és degut, com en el mutant G223D, als impediments estèrics i electroestàtics que la cadena lateral acídica d'Asp223 genera sobre el grup fosfat addicional del $NADP^+$. Per altra banda, l'entorn d'aquest grup fosfat és menys hidrofílic degut als residus Ile224 i Asn225.

2.3 EFECTES SINÈRGICS ENTRE RESIDUS ADJACENTS DETERMINEN L'ESPECIFICITAT DE COENZIM

Els resultats d'aquest treball destaquen la importància dels efectes sinèrgics que produeixen tres residus adjacents, en les posicions 223, 224 i 225, en el conferiment de l'especificitat de coenzim de l'ADH. Les substitucions simples tenen només efectes limitats sobre l'especificitat de coenzim d'ADH8. Els dobles mutants (T224I/H225N i G223D/T224I) ja presenten un canvi en la seva especificitat de coenzim, i el triple mutant mostra una reversió completa de la mateixa.

La caracterització cinètica dels diferents mutants, així com els seus models moleculars, indiquen que les diferents combinacions possibles de residus en aquestes posicions generen llocs d'unió més específics per a l'adenosina o per a l'adenosina-fosfat, del NAD(H) i NADP(H), respectivament.

El NAD(H) requereix la presència simultània d'Asp223, Ile224 i Asn225, si bé aquest darrer residu no interacciona amb el NAD^+, com ha estat observat en altres complexos ADH-NAD^+. Asp223 forma dos ponts d'hidrogen amb el diol de la ribosa de l'adenosina, a la distància precisa perquè el NAD(H) pugui interaccionar amb Ile224 i Lys228. La interacció hidrofòbica d'Ile224 amb l'anell d'adenina és fonamental per a la seva estabilització. Precisament el paper de Asn225, residu menys voluminós que His225, seria el de facilitar l'espai perquè es produeixi aquesta interació. Per altra banda, la presència d'Asp223 ajuda a discriminar contra el NADP(H)

El NADP(H), en canvi, necessita l'existència al mateix temps de Gly223, Thr224 i His225, interaccionant només amb els dos darrers residus. La petita cadena lateral de Gly223 proporciona l'espai addicional al grup fosfat, permetent al mateix temps la interacció iònica i per pont d'hidrogen amb Lys228. Per altra banda, la presència de

Thr224 i His225 genera un entorn hidrofílic, que es tradueix en les interaccions per pont d'hidrogen que realitzen ambdós residus amb el grup fosfat, essencial per a la seva l'estabilització.

Per altra banda, Lys228, un residu versàtil i altament conservat en les ADHs, presenta una funció dual: la interacció electroestàtica amb el grup fosfat addicional del NADP(H), i la interacció per pont d'hidrogen amb l'àtom d'oxigen 3' de la ribosa del NAD(H).

Com era d'esperar, les interaccions iòniques jugarien un paper predominant en la unió del NADP(H), mentre que els ponts d'hidrogen i les interaccions hidrofòbiques serien més prevalents en la unió del NAD(H). El fet que, només amb la substitució de tres residus ubicats en la zona d'unió de l'adenosina, un enzim dependent de NADP(H) esdevingui dependent de NAD(H), és consistent amb que les conformacions que presenten el $NADP^+$ i el NAD^+, quan es troben units a l'ADH, únicament es diferencien en l'adenosina.

Els canvis més efectius de l'especificitat de coenzim en diferents deshidrogenases han estat provocats per múltiples mutacions en diferents zones del domini d'unió del coenzim (Scrutton i col., 1990; Mittl i col., 1993, 1994; Bocanegra i col., 1993). En canvi, en ADH8, la reversió completa de l'especificitat de coenzim ha estat obtinguda amb la substitució de només tres residus consecutius.

2.4 CONSIDERACIONS EVOLUTIVES

L'absència d'un residu acídic, juntament amb la presència de residus polars al voltant del grup fosfat addicional contribueix a l'especificitat de l'ADH8 per el NADP(H). Diferents MDR dependents de NADP(H) presenten estratègies semblants. Així, poliol deshidrogenases bacterianes (Burdette i col., 1996; Korkhin i col., 1998; Kumar i col., 1992), cinamil alcohol deshidrogenases de fongs i de plantes (Lauvergeat i col., 1995), quinones oxidoreductases bacterianes i d'animals (Edwards i col., 1996) o sorbitol deshidrogenases d'insectes (Banfield i col., 2001), mostren una evolució convergent cap a la utilització del NADP(H), i la seva arquitectura una flexibilitat suficient per satisfer canvis en els requeriments de coenzim.

Els nostres resultats indiquen que l'evolució concertada de residus adjacents (223 a 225) d'un petit segment de la seqüència, que requereix només tres mutacions puntuals en la seqüència del gen, ha permès canviar l'especificitat de coenzim de l'ADH d'amfibi. Aquest fet podria reflectir una enzimogènesi tardana d'ADH8, amb un origen evolutiu relativament recent d'aquest enzim dependent de NADP(H), a partir d'una ADH dependent de NAD(H). L'ADH dependent de NAD(H), amb una major identitat seqüencial amb ADH8, és l'ADH1 de *Rana perezi* (70 % d'identitats; Peralba i col., 1999b). El fet que únicament amb tres canvis, respecte als enzims dependents de NAD(H), ADH8 esdevingui dependent de NADP(H), implicaria també una ràpida adaptació funcional a diferents necessitats metabòliques (reducció d'aldehids com el retinal, en lloc de l'oxidació d'alcohols, Peralba i col., 1999a). La simplicitat d'aquests canvis evolutius ha facilitat el redisseny del seti d'unió al coenzim, i aconseguir així la reversió completa de l'especificitat de coenzim.

CONCLUSIONS GENERALS

1. L'arquitectura general d'ADH8 es troba força conservada respecte a la que presenten les estructures d'alcohol deshidrogenases de vertebrat resoltes fins el moment.

2. ADH8 presenta una via alternativa de transmissió del protó, provinent del substrat, al solvent. Ser51 podria tenir el mateix paper que His51 o His47, actuant com a acceptor/donador de protons. Per altra banda, també hi participaria una molècula d'aigua, que ocupa l'espai existent entre el grup hidroxil 2' de la ribosa de la nicotinamida del coenzim i el grup hidroxil de Ser51.

3. En ADH8, la disposició del llaç Asn114-Gly121, juntament amb la presència de Ser48 i Leu140, generen un seti d'unió al substrat voluminós. Aquest fet explicaria les baixes eficiències catalítiques de l'enzim amb alcohols alifàtics de cadena curta com l'etanol.

4. La simulació de les interaccions amb diferents isòmers de retinoides revelà que el tot-*trans*, el 9-*cis* i el 13-*cis*-retinol poden unir-se productivament a la butxaca d'unió al substrat de l'ADH8.

5. La superposició de la molècula de $NADP^+$ unida a l'ADH8, amb la de NAD^+ present en complexos d'ADHs dependents de NAD(H), revelà que només existeixen desviacions conformacionals significatives entre l'adenosina-fosfat i l'adenosina.

6. La butxaca d'unió del grup fosfat addicional del $NADP^+$ es troba definida per dos residus conservats en ADHs dependents de NAD(H), Leu200 i Lys228, i tres residus propis d'ADH8, Gly223, Thr224 i His225. Tots ells interaccionen amb el grup fosfat a excepció de Gly223.

7. La presència en ADH8 d'un seti d'unió adaptat a interaccionar amb el NADP(H) confereix a aquest enzim una especificitat de coenzim única entre les ADHs de vertebrat. Aquest fet, juntament amb l'existència d'una via alternativa de

transmissió de protons, i d'una butxaca d'unió al substrat amb especial afinitat pels retinoides, recolzen la proposta de considerar ADH8 com una nova classe dins de les alcohol deshidrogenases de vertebrat.

8. La transferència de l'ió hidrur és el pas limitant de la reacció d'oxidació de l'etanol catalitzada per ADH8, tant amb $NADP^+$ com amb NAD^+ com a coenzims. Aquest pas limitant es manté en tots els mutants generats quan el NAD^+ és utilitzat com a coenzim. Quan el coenzim utilitzat és el $NADP^+$, els mutants T224I/H225N, G223D/T224I i G223D/T224I/H225N no presenten la transferència de l'ió hidrur com a pas limitant.

9. L'especificitat d'ADH8 per al NADP(H) no és conferida per un únic residu. Cap de les tres mutacions simples, G223D, T224I i H225N, va revertir l'especificitat de coenzim.

10. La combinació d'un residu apolar i poc voluminós a la posició 223 (Gly), i d'un residu polar a la posició 224 (Thr), seria la principal responsable de l'especificitat de coenzim d'ADH8. Així, la doble mutació G223D/T224I és la que provoca una disminució més acusada de l'eficiència catalítica per al NADP(H) envers l'enzim silvestre.

11. La conversió d'ADH8 en un enzim dependent de NAD(H) requereix la triple substitució G223D/T224I/H225N. En aquest mutant, Asp223 i Ile224 realitzen amb l'adenosina les mateixes interaccions que les observades en enzims dependents de NAD(H). Asn225, malgrat no interaccionar directament amb el coenzim, facilitaria la interacció d'Asp223 i Ile224 amb el NAD^+.

12. La reversió completa de l'especificitat de coenzim d'ADH8 s'ha realitzat amb únicament tres substitucions, el que suggereix un origen evolutiu relativament recent de l'ADH8 a partir d'una ADH dependent de NAD(H).

BIBLIOGRAFIA

Abdallah, A.H. i Roby D.M. (1975) Antagonism of depressant activity of ethanol by DH-524; a comparative study with Bemegride, Doxapram and d-amphetamine. *Proc. Soc. Exp. Biol. Med*. **148**, 819-822.

Algar, E.M., VandeBerg, J.L. i Holmes, R.S. (1992) A gastric alcohol dehydrogenase in the baboon: purification and properties of a 'high-Km' enzyme, consistent with a role in 'first pass' alcohol metabolism. *Alcohol Clin. Exp. Res*. **16**, 922-927.

Al-Karadaghi, S., Cedergren-Zeppezauer, E.S., Petrantos, K., Hovmöller, S., Terry, H., Dauter, Z. i Wilson, K.S. (1994) Refined crystal structure of liver alcohol dehydrogenase-NADH complex at 1.8 Å resolution. *Acta Crystallog. sect.* D, **50**, 793-807.

Allali-Hassani, A., Martínez, S.E., Peralba, J.M., Vaglenova, J., Vidal, F., Richart, C., Farrés J. i Parés, X. (1997) Alcohol dehydrogenase of human and rat blood vessels. Role in ethanol metabolism. *FEBS Lett.* **405**, 26-30.

Allali-Hassani, A., Peralba, J.M., Martras, S., Farrés, J. i Parés, X. (1998) Retinoids, omega-hydroxyfatty acids and cytotoxic aldehydes as physiological substrates, and H2-receptor antagonists as pharmacological inhibitors, of human class IV alcohol dehydrogenase. *FEBS Lett.* **426**, 362-366.

Allali-Hassani, A., Crosas, B., Parés, X. i Farrés, J. (2001) Kinetic effects of a single-amino acid mutation in a highly variable loop (residues 114-120) of class IV ADH. *Chem. Biol. Interact*. **30**, 435-444.

Ang, H.L., Deltour, L., Hayamizu, T.F., Zgombic-Knight, M. i Duester, G. (1996) Retinoic acid synthesis in mouse embryos during gastrulation and craniofacial development linked to class IV alcohol dehydrogenase gene expression. *J. Biol. Chem*. **271**, 9526-9534.

Backer, P.J., Britton, K.L., Rice, D.W., Rob, A. i Stillman, T.J. (1992) Structural consequences of sequence patterns in the fingerprint region of the of the nucleotide binding fold. *J. Mol. Biol.* **228**, 662-671.

Bagchi, D., Bagchi, M., Hassoun, E. i Stohs, S.J. (1993) Carbon-tetrachloride-induced urinary excretion of formaldehyde, malondialdehyde, acetaldehyde and acetone in rats. *Pharmacology* **47**, 209-216.

Banfield, M.J., Salvucci, M.E., Baker, E.N. i Smith, C.A. (2001) Crystal structure of the NADP(H)-dependent ketose reductase from Bemisia argentifolii at 2.3 A resolution. *J. Mol. Biol*. **306**, 239-250.

Bannister, W.H. (1967) The oxidation-reduction state of pyridine nucleotide in isolated frog gastric mucosa. *Experientia*, **23**, 715-716.

Bellamacina, C.R. (1996) The nicotinamide dinucleotide binding motif: a comparison of nucleotide binding proteins. *FASEB J.* **10**, 1257-1269.

Bjorkhem, I., Jörnvall, H i Zeppezauer, E. (1973) Oxidation of omega-hydroxylated fatty acids and steroids by alcohol dehydrogenase. *Biochem. Biophys. Res. Commun.* **52**, 413-420.

Blair, A.H. i Vallee, B.L. (1966) Some catalytic properties of human liver alcohol dehydrogenase. *Biochemistry*, **5**, 2026-2034.

Bocanegra, J.A., Scrutton, N.S. i Perham, R.N. (1993) Creation of an NADP-dependent pyruvate dehydrogenase multienzyme complex by protein engineering. *Biochemistry* **32**, 2737-2740.

Boleda, M.D., Julià, P., Moreno, A. i Parés, X. (1989) Role of extrahepatic alcohol dehydrogenase in rat ethanol metabolism. *Arch. Biochem. Biophys.* **274**, 74-81.

Boleda, M.D., Saubi, N., Farrés, J. i Parés, X. (1993) Physiological substrates for rat alcohol dehydrogenase classes: aldehydes of lipid peroxidation, omega-hydroxyfatty acids, and retinoids. *Arch. Biochem. Biophys.* **307**, 85-90.

Borràs, E., Coutelle, C., Rosell, A., Fernández-Muixí, F., Broch, M., Crosas, B., Hjelmqvist, L., Lorenzo, A., Gutiérrez, C., Santos, M., Szczepanek, M., Heilig, M., Quattrocchi, P., Farrés J, Vidal, F., Richart, C., Mach, T., Bogdal, J., Jörnvall, H., Seitz, H.K., Couzigou, P., i Parés, X. (2000) Genetic polymorphism of alcohol dehydrogenase in europeans: the ADH2*2 allele decreases the risk for alcoholism and is associated with ADH3*1. *Hepatology*, **31**, 984-989.

Bosron, W.F., Li, T.K., Dafeldecker, W.P. i Vallee, B.L. (1979) Human liver pi-alcohol dehydrogenase: kinetic and molecular properties. *Biochemistry*, **20**, 1101-1105.

Bosron, W.F., Magnes, L.J. i Li, T.K. (1983) Kinetic and electrophoretic properties of native and recombined isoenzymes of human liver alcohol dehydrogenase. *Biochemistry* **22**, 1852-1857.

Bosron, W.F., Yin, S.J. i Li, T.K. (1985a) Purification and characterization of human liver beta 1 beta 1, beta 2 beta 2 and beta Ind beta Ind alcohol dehydrogenase isoenzymes. *Prog. Clin. Biol. Res*. **174**, 193-206.

Bosron, W.F., Gaither, J.W. i Magnes, L.J. (1985b) Kinetic characterization of two classes of dog liver alcohol dehydrogenase isoenzymes. *Alcohol Clin. Exp. Res*. **9**, 228-234.

Bradford, M.M. (1976) A rapid and sensitive method for the quantitation of microgram quantities of protein utilizing the principle of protein-dye binding. *Anal. Biochem*. **72**, 248-254.

Brändén, C.I. i Eklund, H. (1980) Structure and mechanism of liver alcohol dehydrogenase, lactate dehydrogenase and glyceraldehyde-3-phosphate dehydrogenase. *Experientia Suppl*. **36**, 40-84.

Brünger, A.T., Adams, P.D., Clore, G.M., DeLano, W.L., Gros, P., Grosse-Kunstleve, R.W., Jiang, J.S., Kuszewski, J., Nilges, M. i Pannu, N.S. (1998) Crystallography & NMR system: a new software suite for macromolecular structure determination. *Acta Crystallog. sect.* D, **54**, 905-921.

Bühler, R. i von Wartburg, J.P. (1984) Differential susceptibility of human alcohol dehydrogenase isoenzymes to anions. *FEBS Lett*. **178,** 249-252.

Burdette, D.S, Vieille, C. i Zeikus, J.G. (1996) Cloning and expression of the gene encoding the *Thermoanaerobacter ethanolicus* 39E secondary-alcohol dehydrogenase and biochemical characterization of the enzyme. *Biochem. J.* **316**, 115-122.

Burnell, J.C., Li, T.K. i Bosron, W.F. (1989) Purification and steady-state kinetic characterization of human liver beta 3 beta 3 alcohol dehydrogenase. *Biochemistry* **28**, 6810-6815.

Cañestro, C., Hjelmqvist, L., Albalat, R., Garcia-Fernandez, J., Gonzalez-Duarte, R. i Jörnvall, H. (2000) Amphioxus alcohol dehydrogenase is a class 3 form of single type and of structural conservation but with unique developmental expression. *Eur. J. Biochem*. **267**, 6511-6518.

Cañestro, C., Albalat, R., Hjelmqvist, L., Godoy, L., i Jörnvall, H. (2001) Ascidian and Amphioxus Adh genes correlate functional and molecular features of the ADH family expansion during vertebrate evolution. *J. Mol. Evol.* **53**, 987-998.

Carugo, O. i Argos, P. (1997) NADP-dependent enzymes. I: Conserved stereochemistry of cofactor binding. *Proteins*,**28**, 10-28.

Chen, Z., Lu, L., Shirley, M., Lee, W.R. i Chang, S.H. (1990) Site-directed mutagenesis of glycine-14 and two "critical" cysteinyl residues in *Drosophila* alcohol dehydrogenase. *Biochemistry* **29**, 1112-1118.

Chen, C.S. i Yoshida, A. (1991) Enzymatic properties of the protein encoded by newly cloned human alcohol dehydrogenase ADH6 gene. *Biochem. Biophys. Res. Commun*. **181**, 743-747.

Chen, Z., Lee, W.R. i Chang, S.H. (1991) Role of aspartic acid 38 in the cofactor specificity of Drosophila alcohol dehydrogenase. *Eur. J. Biochem.* **202**, 263-267.

Cho, H., Ramaswamy, S. i Plapp, B.V (1997) Flexibility of liver alcohol dehydrogenase in stereoselective binding of 3-butylthiolane 1-oxides. *Biochemistry* **36**, 382-389.

Chu, R., Lin, Y., Rao, M.S. i Reddy, J.K. (1995a) Cooperative formation of higher order peroxisome proliferator-activated receptor and retinoid X receptor complexes on the peroxisome proliferator responsive element of the rat hydratase-dehydrogenase gene. *J. Biol. Chem.* **270**, 29636-29639.

Chu, R., Madison, L.D., Lin, Y., Kopp, P., Rao, M.S., Jameson, J.L. i Reddy, J.K. (1995b) Thyroid hormone (T3) inhibits ciprofibrate-induced transcription of genes encoding beta-oxidation enzymes: cross talk between peroxisome proliferator and T3 signaling pathways. *Proc. Natl. Acad. Sci. USA* **92**, 11593-11597.

Cleland, W.W. (1979) Statistical analysis of enzyme kinetic data. *Methods Enzymol.* **63**, 103-138.

Colonna-Cesari, F., Perahia, D., Karplus, M., Eklund, H., Brändén, C.I. i Tapia, O. (1986) Interdomain motion in liver alcohol dehydrogenase. Structure and energetic analysis of the hinge bending mode. *J. Biol. Chem.* **261**, 15273-15280.

Consalvi, V., Mårdh, G. i Vallee, B.L. (1986) Human alcohol dehydrogenases and serotonin metabolism. *Biochem. Biophys. Res. Commun*. **139**, 1009-1016.

Costaridis, P., Horton, C., Zeitlinger, J., Holder, N. i Maden, M. (1996) Endogenous retinoids in the zebrafish embryo and adult. *Dev. Dyn.* **205**, 41-51.

Crabb, D.W., Bosron, W.F. i Li, T.K (1987) Ethanol metabolism. *Pharmacol Ther.* **34**, 59-73.

Cronholm, T., Larsen, C., Jörnvall, H., Theorell, H., i Akeson, A. (1975) Steroid oxidoreductase activity of alcohol dehydrogenases from horse, rat, and human liver. *Acta Chem. Scand. B*, **29**, 571-576.

Crosas, B., Allali-Hassani, A., Martínez, S.E., Martras, S., Persson, B., Jörnvall, H., Parés, X. i Farrés, J. (2000) Molecular basis for differential substrate specificity in class IV alcohol dehydrogenases: A conserved function in retinoid metabolism but not in ethanol metabolism. *J. Biol. Chem.* **275**, 25180-25187.

Dafeldecker, W.P., Meadow, P.E., Parés, X. i Vallee, B.L. (1981) Simian liver alcohol dehydrogenase: isolation and characterization of isoenzymes from Macaca mulatta. *Biochemistry* **20**, 6729-6734.

Danielsson, O. i Jörnvall, H. (1992) Enzymogenesis: Classical liver alcohol dehydrogenase origin from the glutathione-dependent formaldehyde dehydrogenase line. *Proc. Natl. Acad. Sci. USA* **89**, 9247-9251.

Danielsson, O., Eklund, H. i Jörnvall, H. (1992) The major piscine liver alcohol dehydrogenase has class-mixed properties in relation to mammalian alcohol dehydrogenases of classes I and III. *Biochemistry*, **31**, 3751-3759.

Danielsson, O., Shafqat, J., Estonius, M. i Jörnvall, H. (1994) Alcohol dehydrogenase class III contrasted to class I. Characterization of the cyclostome enzyme, the existence of multiple forms as for the human enzyme, and distant cross-species hybridization. *Eur. J. Biochem*. **225**, 1081-1088.

Davis, G.J., Carr, L.G., Hurley, T.D., Li, T.K. i Bosron, W.F. (1994) Comparative roles of histidine 51 in human beta 1 beta 1 and threonine 51 in pi pi alcohol dehydrogenases. *Arch. Biochem. Biophys.* **311**, 307-312.

Davis, G.J., Bosron, W.F., Stone, C.L., Owusu-Dekyi, K. i Hurley, T.D. (1996) X-ray structure of human beta3beta3 alcohol dehydrogenase. The contribution of ionic interactions to coenzyme binding. *J. Biol. Chem*. **271**, 17057-17061.

Deetz, J.S., Luehr, C.A. i Vallee, B.L. (1984) Human liver alcohol dehydrogenase isozymes: reduction of aldehydes and ketones. *Biochemistry* **23**, 6822-6828.

Deltour, L., Haselbeck, R.J., Ang, H.L. i Duester, G. (1997) Localization of class I and class IV alcohol dehydrogenases in mouse testis and epididymis: potential retinol dehydrogenases for endogenous retinoic acid synthesis. *Biol. Reprod.* **56**, 102-109.

Ditlow, C.C., Holmquist, B., Morelock, M.M. i Vallee, B.L. (1984) Physical and enzymatic properties of a class II alcohol dehydrogenase isozyme of human liver: π-ADH. *Biochemistry* **23**, 6363-6368.

Duester, G. (1996) Involvement of alcohol dehydrogenase, short-chain dehydrogenase/reductase, aldehyde dehydrogenase, and cytochrome P450 in the control of retinoid signaling by activation of retinoic acid synthesis. *Biochemistry* **35**, 12221-12227.

Duester, G., Farrés, J., Felder, M.R., Holmes, R.S., Höög, J.O., Parés, X., Plapp, B.V., Yin, S.J. i Jörnvall, H. (1999) Recommended nomenclature for the vertebrate alcohol dehydrogenase gene family. *Biochem. Pharmacol*. **58**, 389-395.

Duester, G. (2000) Families of retinoid dehydrogenases regulating vitamin A function production of visual pigment and retinoic acid. *Eur. J. Biochem*. **267**, 4315-4524.

Duester, G. (2001) Genetic dissection of retinoid dehydrogenases. *Chem. Biol. Interact.* **132**, 469-480.

Edenberg, H.J. (2000) Regulation of the mammalian alcohol dehydrogenase genes. *Prog. Nucleic Acid Res. Mol. Biol.* **64**, 295-341.

Edwards, K.J., Barton, J.D., Rossjohn, J., Thorn, J.M., Taylor, G.L. i Ollis, D.L. (1996) Structural and sequence comparisons of quinone oxidoreductase, zeta-crystallin, and glucose and alcohol dehydrogenases. *Arch. Biochem. Biophys.* **328**, 173-183.

Ehrig, T., Hurley, T.D., Edenberg, H.J. i Bosron, W.F. (1991) General base catalysis in a glutamine for histidine mutant at position 51 of human liver alcohol dehydrogenase. *Biochemistry* **30**, 1062-1068.

Eklund, H., Nordstrom, B., Zeppezauer, E., Soderlund, G., Ohlsson, I., Boiwe, T., Soderberg, B.O., Tapia, O., Brändén, C.I. i Akeson, A. (1976) Three-dimensional structure of horse liver alcohol dehydrogenase at 2-4 A resolution. *J. Mol. Biol.* **102**, 27-59.

Eklund, H. i Brändén, C.I. (1979) Structural differences between apo- and holoenzyme of horse liver alcohol dehydrogenase. *J. Biol. Chem.* **254**, 3458-3461.

Eklund, H., Samama, J.P., Wallén, L., Brändén, C.I., Åkeson, Å. i Jones, T.A. (1981) Structure of a horse triclinic ternary complex with liver alcohol dehydrogenase at 2.9 Å. *J. Mol. Biol.* **146**, 561-587.

Eklund, H., Plapp, B.V., Samama, J.P. i Brändén, C.I. (1982) Binding of substrate in a ternary complex of horse liver alcohol dehydrogenase. *J. Biol. Chem.* **257**, 14349-14358.

Eklund, H., Samama. J.P. i Jones, T.A. (1984) Crystallographic investigations of nicotinamide adenine dinucleotide binding to horse liver alcohol dehydrogenase. *Biochemistry* **23**, 5982-5996.

Eklund, H. i Brändén, C.I. (1987) Alcohol dehydrogenase. In: Biological Macromolecules and Assemblies (Jurnak, F.A. & McPherson, A., eds.), pp. 73-142, John Wiley & Sons Inc., London.

Eklund, H., Horjales, E., Vallee, B.L. i Jörnvall, H. (1987) Computer-graphics interpretations of residue exchanges between the alpha, beta and gamma subunits of human-liver alcohol dehydrogenase class I isoenzymes. *Eur. J. Biochem.* **167**, 185-193.

Eklund, H., Muller-Wille, P., Horjales, E., Futer, O., Holmquist, B., Vallee, B.L., Höög, J.O., Kaiser, R. i Jörnvall, H. (1990) Comparison of three classes of human liver alcohol dehydrogenase. Emphasis on different substrate binding pockets. *Eur. J. Biochem*. **193**, 303-310.

Estonius, M., Karlsson, C., Fox, E.A., Höög, J.O., Holmquist, B., Vallee, B.L., Davidson, W.S. i Jörnvall, H. (1990) Avian alcohol dehydrogenase: the chicken liver enzyme. Primary structure, cDNA-cloning, and relationships to other alcohol dehydrogenases. *Eur. J. Biochem*. **194**, 593-602.

Estonius, M., Hjelmqvist, L. i Jörnvall, H. (1994a) Diversity of vertebrate class I alcohol dehydrogenase. Mammalian and non-mammalian enzyme functions correlated through the structure of a ratite enzyme. *Eur. J. Biochem.* 224, 373-378.

Estonius, M., Höög, J.O., Danielsson, O. i Jörnvall, H. (1994b) Residues specific for class III alcohol dehydrogenase. Site-directed mutagenesis of the human enzyme. *Biochemistry* **33**, 15080-15085.

Estonius, M., Svensson, S. i Höög, J.O. (1996) Alcohol dehydrogenase in human tissues. Localisation of transcripts coding for five classes of the enzyme. *FEBS Lett*. **397**, 338-342.

Fan, F., Lorenzen, J.A. i Plapp, B.V. (1991) An aspartate residue in yeast alcohol dehydrogenase I determines the specificity for coenzyme. *Biochemistry* **30**, 6397-6401.

Fan, F. i Plapp, B.V. (1995) Substitutions of isoleucine residues at the adenine binding site activate horse liver alcohol dehydrogenase. *Biochemistry* **34**, 4709-4713.

Fan, F. i Plapp, B.V. (1999) Probing the affinity and specificity of yeast alcohol dehydrogenase I for coenzymes. *Arch. Biochem. Biophys.* **367**, 240-249.

Farrés, J., Moreno, A., Crosas, B., Peralba, J.M., Allali-Hassani, A., Hjelmqvist, L., Jörnvall, H. i Parés, X. (1994) Alcohol dehydrogenase of class IV (σσ-ADH) from human stomach. cDNA sequence and structure/function relationships. *Eur. J. Biochem.* **224**, 549-557.

Feeney, R., Clarke, A.R. i Holbrook, J.J. (1990) A single amino acid substitution in lactate dehydrogenase improves the catalytic efficiency with an alternative coenzyme. *Biochem. Biophys. Res. Commun*. **166**, 667-672.

Fernández, M.R., Jörnvall, H., Moreno, A., Kaiser, R., i Parés, X. (1993) Cephalopod alcohol dehydrogenase: purification and enzymatic characterization. *FEBS Lett*. **328**, 235-238.

Fernández, M.R., Biosca, J.A., Norin, A., Jörnvall, H. i Parés, X. (1995) Class III alcohol dehydrogenase from Saccharomyces cerevisiae: Structural and enzymatic features differ toward the human/mammalian forms in a manner consistent with functional needs in formaldehyde detoxification. *FEBS Lett*. **370**, 23-26.

Fernández, M.R., Biosca, J.A., Torres, D., Crosas, B. i Parés, X. (1999) A double residue substitution in the coenzyme-binding site accounts for the different kinetic properties between yeast and human formaldehyde dehydrogenases. *J. Biol. Chem*. **274**, 37869-37875.

Fernández, M.R., Biosca, J.A. i Parés X. (2003) S-nitrosoglutathione reductase activity of human and yeast glutathione-dependent formaldehyde dehydrogenase and its nuclear and cytoplasmic localisation. *Cell. Mol. Life. Sci.* **60**,1013-1028.

Foglio, M.H. i Duester, G. (1999) Molecular docking studies on interaction of diverse retinol structures with human alcohol dehydrogenases predict a broad role in retinoid ligand synthesis. *Biochim. Biophys. Acta*. **1432**, 239-250.

Frey, W.A. i Vallee, B.L. (1980) Digitalis metabolism and human liver alcohol dehydrogenase. *Proc. Natl. Acad. Sci. USA* **77**, 924-927.

Fries, R.W., Bohlken, D.P. i Plapp, B.V. (1979) 3-substituted pyrazole derivatives as inhibitors and inactivators of liver alcohol dehydrogenase. *J. Med. Chem.* **22**, 356-359.

Glassner, J.D., Kocher, T.D. i Collins, J.J. (1995) *Caenorhabditis elegans* contains genes encoding two new members of the Zn-containing alcohol dehydrogenase family. *J. Mol. Evol.* **41**, 46-53.

Gomi, T., Date, T., Ogawa, H., Fujioka, M., Akszmit, R.R., Backlund, P.S. i Cantoni, G.L. (1989) Expression of rat liver S-adenosylhomocysteinase cDNA in *Escherichia coli* and mutagenesis at the putative NAD binding site. *J. Biol. Chem.* **264**, 16138-16142.

Gotoh, Y., Sumimoto, H. i Minakami, S. (1990) Formation of 20-oxoleukotriene B4 by an alcohol dehydrogenase isolated from human neutrophils. *Biochim. Biophys. Acta*. **1043**, 52-56.

Gudas, L.J., Sporn, M.B. i Roberts, A.B. (1994) Cellular biology and biochemistry of the retinoids. En Sporn, A.B., Roberts, A.B., i Goodman, D.S. (eds), *The Retinoids: biology, chemistry, and medicine*, 2nd edition. Raven Press Ltd, New York, pp. 443-520.

Gutheil, W.G., Holmqvist, B., i Vallee, B.L. (1992) Purification, characterization, and partial sequence of the glutathione-dependent formaldehyde dehydrogenase from *Escherichia coli*: A class III alcohol dehydrogenase. *Biochemistry* **31**, 475-481.

Han, C.L., Liao, C.S., Wu, C.W., Hwong, C.L., Lee, A.R. i Yin, S.J. (1998) Contribution to first-pass metabolism of ethanol and inhibition by ethanol for retinol oxidation in human alcohol dehydrogenase family-implications for etiology of fetal alcohol syndrome and alcohol-related diseases. *Eur. J. Biochem*. **254**, 25-31.

Hanukoglu, I. i Gutfinger, T. (1989) cDNA sequence of adrenodoxin reductase. Identification of NADP-binding sites in oxidoreductases. *Eur. J. Biochem.* **180**, 479-484.

Haselbeck, R.J. i Duester, G. (1997a) Regional restriction of alcohol/retinol dehydrogenases along the mouse gastrointestinal epithelium. *Alcohol Clin. Exp. Res.* **21**, 1484-1490.

Haselbeck, R.J., Ang, H.L. i Duester, G. (1997b) Class IV alcohol/retinol dehydrogenase localization in epidermal basal layer: potential site of retinoic acid synthesis during skin development. *Dev. Dyn*. **208**, 447-453.

Haselbeck, R.J., Ang, H.L., Deltour, L. i Duester, G. (1997c) Retinoic acid and alcohol/retinol dehydrogenase in the mouse adrenal gland: a potential endocrine source of retinoic acid during development. *Endocrinology*, **138**, 3035-3041.

Hjelmqvist, L., Estonius, M. i Jörnvall, H (1995a) The vertebrate alcohol dehydrogenase system: Variable class II type form elucidates separate stages of enzymogenesis. *Proc. Natl. Acad. Sci. USA* **92**, 10905-10909.

Hjelmqvist, L., Metsis, M., Persson, H., Höög, J.O., McLennan, J. i Jörnvall, H. (1995b) Alcohol dehydrogenase of class I: kiwi liver enzyme, parallel evolution in separate vertebrate lines, and correlation with 12S rRNA patterns. *FEBS Lett.* **367**, 306-310.

Hjelmqvist, L., Shafqat, J., Siddiqi, A.R. i Jörnvall, H. (1995c) Alcohol dehydrogenase of class III: consistent patterns of structural and functional conservation in relation to class I and other proteins. *FEBS Lett.* **373**, 212-216.

Hjelmqvist, L., Shafqat, J., Siddiqi, A.R. i Jörnvall, H. (1996) Linking of isozyme and class variability patterns in the emergence of novel alcohol dehydrogenase functions. Characterization of isozymes in *Uromastix hardwickii*. *Eur. J. Biochem*. **236**, 563-570.

Holmes, R.S., Courtney, Y.R. i VandeBerg, J.L. (1986) Alcohol dehydrogenase isozymes in baboons: tissue distribution, catalytic properties, and variant phenotypes in liver, kidney, stomach, and testis. *Alcohol Clin. Exp. Res*. **10**, 623-630.

Höög, J.O., Eklund, H. i Jornvall, H. (1992) A single-residue exchange gives human recombinant beta beta alcohol dehydrogenase gamma gamma isozyme properties. *Eur. J. Biochem.* **205**, 519-526.

Höög, J.O. i Brandt, M. (1995) Mammalian class VI alcohol dehydrogenase. Novel types of the rodent enzymes. *Adv. Exp. Med. Biol*. **372**, 355-364.

Hoop, M.D., Asgeirsdottir, S., Blaauw, M., Veenhuis, M., Cregg, J., Gleeson, M. i Ab, G. (1991) Mutations in the FAD-binding fold of alcohol oxidase from *Hansenula polymorpha*. *Protein Eng.* **4**, 821-829.

Hurley, T.D., Bosron, W.F., Hamilton, J.A. i Amzel, L.M. (1991) Structure of human beta 1 beta 1 alcohol dehydrogenase: catalytic effects of non-active-site substitutions. *Proc. Natl. Acad. Sci. USA* **88**, 8149-8153.

Hurley, T.D. i Bosron, W.F. (1992) Human alcohol dehydrogenase: dependence of secondary alcohol oxidation on the amino acids at positions 93 and 94. *Biochem. Biophys. Res. Commun.* **183**, 93-99.

Hurley, T.D., Bosron, W.F., Stone, C.L. i Amzel, L.M. (1994) Structures of three human beta alcohol dehydrogenase variants. Correlations with their functional differences. *J. Mol. Biol*. **239**, 415-429.

Iborra, F.J., Renau-Piqueras, J., Portoles, M., Boleda, M.D., Guerri, C. i Parés, X. (1992) Immunocytochemical and biochemical demonstration of formaldehyde dehydrogenase (class III alcohol dehydrogenase) in the nucleus. *J. Histochem. Cytochem.* **12**, 1865-1878.

Jensen, D.E., Belka, G.K. i Du Bois, G.C. (1998) S-Nitrosoglutathione is a substrate for rat alcohol dehydrogenase class III isoenzyme. *Biochem. J.* **331**, 659-668.

Jones, T.A., Zou, J.Y., Cowan, S. i Kjeldgaard, M. (1991) Improved methods for building protein models in electron density maps and the location of errors in these models. *Acta Crystallog. sect. A*, **47**, 110-119.

Jörnvall, H., Danielsson, O., Eklund, H., Hjelmqvist, L., Höög, J.O., Parés, X. i Shafqat, J. (1993) Enzyme and isozyme developments within the medium-chain alcohol dehydrogenase family. *Adv. Exp. Med. Biol*. **328**, 533-544.

Jörnvall, H. i Höög, J.O. (1995) Nomenclature of alcohol dehydrogenases. *Alcohol. Alcohol*. **30**, 153-161.

Jörnvall, H. (1999) Multiplicity and complexity of SDR and MDR enzymes. *Adv. Exp. Med. Biol.* **1463**, 359-364.

Jörnvall, H., Hoog, J.O. i Persson B. (1999) SDR and MDR: completed genome sequences show these protein families to be large, of old origin, and of complex nature. *FEBS Lett*. **445,** 261-264.

Jörnvall, H., Shafqat, J. i Persson, B. (2001) Variations and constant patterns in eukaryotic MDR enzymes. Conclusions from novel structures and characterized genomes. *Chem. Biol. Interact.* **30**, 491-498.

Julià, P., Farrés, J. i Parés, X. (1983) Purification and partial characterization of a rat retina alcohol dehydrogenase active with ethanol and retinol. *Biochem. J*. **213**, 547-550.

Julià, P., Farrés, J. i Parés, X. (1986) Ocular alcohol dehydrogenase in the rat: Regional distribution and kinetics of the ADH-1 isoenzyme with retinol and retinal. *Exp. Eye Res.* **42**, 305-314.

Julià, P., Farrés, J. i Parés, X. (1987) Characterization of three isoenzymes of rat alcohol dehydrogenase. Tissue distribution and physical and enzymatic properties. *Eur. J. Biochem*. **162**, 179-189.

Kaiser, R., Nusseallah, B.A., Dam, R., Wagner, F.W, i Jörnvall, H. (1990) Avian alcohol dehydrogenase. Characterization of the quail enzyme, functional interpretations, and relationships to the different classes of mammalian alcohol dehydrogenase. *Biochemistry* **29**, 8365-8371.

Kaiser, R., Fernández, M.R., Parés, X. i Jörnvall, H. (1993) Origin of the human alcohol dehydrogenase system: implications from the structure and properties of the octopus protein. *Proc. Natl. Acad. Sci. USA* **90**, 11222-11226.

Kedishvili, N.Y., Gough, W.H., Chernoff, E.A., Hurley, T.D., Stone, C.L., Bowman, K.D., Popov, K.M., Bosron, W.F. i Li, T.K. (1997) cDNA sequence and catalytic properties of a chick embryo alcohol dehydrogenase that oxidizes retinol and 3beta,5alpha-hydroxysteroids. *J. Biol. Chem*. **272**, 7494-7500.

Kedishvili, N.Y., Gough, W.H., Davis, W.I., Parsons, S., Li, T.K. i Bosron, W.F. (1998) Effect of cellular retinol-binding protein on retinol oxidation by human class IV retinol/alcohol dehydrogenase and inhibition by ethanol. *Biochem. Biophys. Res. Commun*. **249**, 191-196.

Keung, W.M. i Yip, P.K. (1989) Rabbit liver alcohol dehydrogenase: Isolation and characterization of class I isozymes. *Biochem. Biophys. Res. Commun.* **158**, 445-453.

Keung, W.M., Kunze, L. i Holmquist, B. (1995) Rabbit liver class III alcohol dehydrogenase: a cathodic isoform with formaldehyde dehydrogenase activity. *Alcohol. Clin. Exp. Res.* **19**, 860-866.

Koivusalo, M., Baumann, M. i Uotila, L. (1989) Evidence for the identity of glutathione-dependent formaldehyde dehydrogenase and class III alcohol dehydrogenase. *FEBS Lett*. **257**, 105-109.

Korkhin, Y., Kalb (Gilboa), A.J., Peretz, M., Bogin, O., Burstein, Y. i Frolow, F. (1998) NADP-dependent bacterial alcohol dehydrogenases: crystal structure, cofactor-binding and cofactor specificity of the ADHs of *Clostridium beijerinckii* and *Thermoanaerobacter brockii*. *J. Mol. Biol.* **278**, 967-981.

Kumar, A., Shen, P.S., Descoteaux, S., Pohl, J., Bailey, G. i Samuelson, J. (1992) Cloning and expression of an NADP(+)-dependent alcohol dehydrogenase gene of *Entamoeba histolytica*. *Proc. Natl. Acad. Sci. USA* **89**, 10188-10192.

Labrecque, J., Dumas, F., Lacroix, A. i Bhat, P.V. (1995) A novel isoenzyme of aldehyde dehydrogenase specifically involved in the biosynthesis of 9-*cis* and all-*trans* retinoic acid. *Biochem. J.* **305**, 681-684.

Lauvergeat, V., Kennedy, K., Feuillet, C., McKie, J.H., Gorrichon, L., Baltas, M., Boudet, A.M., Grima-Pettenati i Douglas, K.T. (1995) Site-directed mutagenesis of a serine residue in cinnamyl alcohol dehydrogenase, a plant NADPH-dependent dehydrogenase, affects the specificity for the coenzyme. *Biochemistry* **34**, 12426-12434.

Lee, S.L., Wang, M.F., Lee, A.I. i Yin, S.J. (2003) The metabolic role of human ADH3 functioning as ethanol dehydrogenase. *FEBS Lett.* **544**, 143-147.

Lesk, A.M. (1995) NAD-bining domains of dehydrogenases. *Curr. Opin. Struct. Biol.* **5**, 775-783.

Li, T.K., Bosron, W.F., Dafeldecker, W.P., Lange, L.G. i Vallee, B.L. (1977) Isolation of pi-alcohol dehydrogenase of human liver: is it a determinant of alcoholism? *Proc. Natl. Acad. Sci. USA* **74**, 4378-4381.

Light, D.R., Dennis, M.S., Forsythe, I.J., Liu, C.C., Green, D.W., Kratzer, D.A. i Plapp, B.V. (1992) Alpha-isoenzyme of alcohol dehydrogenase from monkey liver. Cloning, expression, mechanism, coenzyme, and substrate specificity. *J. Biol. Chem.* **267**, 12592-12599.

Luque, T., Atrian, S., Danielsson, O., Jörnvall, H. i González-Duarte, R. (1994) Structure of the Drosophila melanogaster glutathione-dependent formaldehyde dehydrogenase/octanol dehydrogenase gene (class III alcohol dehydrogenase). Evolutionary pathway of the alcohol dehydrogenase genes. *Eur. J. Biochem*. **225**, 985-993.

Maden, M. (1994) Vitamin A in embryonic development. *Nutr. Rev.* **52**, 3-12.

Mårdh, G., Luehr, C.A. i Vallee, B.L. (1985) Human class I alcohol dehydrogenases catalyze the oxidation of glycols in the metabolism of norepinephrine. *Proc. Natl. Acad. Sci. USA* **82**, 4979-4982.

Mårdh, G. i Vallee, B.L. (1986) Human class I alcohol dehydrogenases catalyze the interconversion of alcohols and aldehydes in the metabolism of dopamine. *Biochemistry* **25**, 7279-7282.

Mårdh, G., Dingley, A.L., Auld, D.S. i Vallee, B.L. (1986) Human class II (pi) alcohol dehydrogenase has a redox-specific function in norepinephrine metabolism. *Proc. Natl. Acad. Sci. USA* **83**, 8908-8912.

Maret, W. (1989) Cobalt (II)-substituted class III alcohol and sorbitol dehydrogenases from human liver. *Biochemistry* **28**, 9944-9949.

Marschall, H.U., Oppermann, U.C., Svensson, S., Nordling, E., Persson, B., Hoog, J.O. i Jornvall, H. (2000) Human liver class I alcohol dehydrogenase gammagamma isozyme: the sole cytosolic 3beta-hydroxysteroid dehydrogenase of iso bile acids. *Hepatology*, **31**, 990-996.

Martínez, M.C., Achkor, H., Persson, B., Fernández, M.R., Shafqat, J., Farrés, J., Jörnvall, H. i Parés, X. (1996) Arabidopsis formaldehyde dehydrogenase. Molecular properties of plant class III alcohol dehydrogenase provide further insights into the origins, structure and function of plant class P and liver class I alcohol dehydrogenases. *Eur. J. Biochem*. **241**, 849-857.

Martras, S., Alvarez, R., Martínez, S.E, Torres, D., Gallego, O., Duester, G., Farrés, J., de Lera, A.R i Parés, X. (2004) The specificity of alcohol dehydrogenase with *cis*-retinoids. Activity with 11-*cis*-retinol and localization in retina. *Eur. J. Biochem.* **271**, 1-11.

McEvily, A.J., Holmquist, B., Auld, D.S. i Vallee, B.L. (1988) 3β-Hydroxy-5β-steroid dehydrogenase activity of human liver alcohol dehydrogenase is specific to gamma-subunits. *Biochemistry* **27**, 4284-4288.

Meijers, R., Morris, R.J., Adolph, H.W., Merli, A., Lamzin, V.S. i Cedergren-Zeppezauer, E.S. (2001) On the enzymatic activation of NADH. *J. Biol. Chem.* **276**, 9316-9321.

Metzger, M.H. i Hollenberg, C.P. (1995) Amino acid substitutions in the yeast Pichia stipitis xylitol dehydrogenase coenzyme-binding domain affect the coenzyme specificity. *Eur. J. Biochem.* **228**, 50-54.

Mittl, P.R., Berry, A., Scrutton, N.S., Perham, R.N. i Schulz, G.E. (1993) Structural differences between wild-type NADP-dependent glutathione reductase from Escherichia coli and a redesigned NAD-dependent mutant. *J. Mol. Biol.* **231**, 191-201.

Mittl, P.R., Berry, A., Scrutton, N.S., Perham, R.N. i Schulz, G.E. (1994) Anatomy of an engineered NAD-binding site. *Protein Sci.* **3**, 1504-1514.

Molotkov, A., Fan, X., Deltour, L., Foglio, M.H., Martras, S., Farrés, J., Parés, X. i Duester, G. (2002) Stimulation of retinoic acid production and growth by ubiquitously expressed alcohol dehydrogenase Adh3. *Proc. Natl. Acad. Sci. USA*. **99**, 5337-5342.

Moreno, A. i Parés, X. (1991) Purification and characterization of a new alcohol dehydrogenase from human stomach. *J. Biol. Chem*. **266**, 1128-1133.

Moreno, A., Farrés, J., Parés, X., Jörnvall, H. i Persson, B. (1996) Molecular modelling of human gastric alcohol dehydrogenase (class IV) and substrate docking: differences towards the classical liver enzyme (class I). *FEBS Lett*. **395**, 99-102.

Napoli, J.L. (1996) Biochemical pathways of retinoid transport, metabolism, and signal transduction. *Clin. Immunol. Immunopathol.* **80**, 52-62.

Napoli, J.L. (1999) Interactions of retinoid binding proteins and enzymes in retinoid metabolism. *Biochim. Biophys. Acta* **1440**, 139-162.

Nelson, M. i McClelland, M. (1992) Use of DNA methyltransferase/endonuclease enzyme combinations for megabase mapping of chromosomes. *Methods Enzymol.* **216**, 279-303.

Niederhut, M.S., Gibbons, B.J., Pérez-Miller, S. i Hurley, T.D. (2001) Three-dimensional structures of the three human class I alcohol dehydrogenases. *Protein Sci.* **10**, 697-706.

Nordling, E., Jörnvall, H. i Persson, B. (2002) Medium-chain dehydrogenases/reductases (MDR). Family characterizations including genome comparisons and active site modeling. *Eur. J. Biochem.* **269**, 4267-4276.

Nussrallah, B.A., Dam, R. i Wagner, F.W. (1989) Characterization of Coturnix quail liver alcohol dehydrogenase enzymes. *Biochemistry* **28**, 6245-6251.

Ohlsson, I., Nordstrom, B. i Brändén, C.I. (1974) Structural and functional similarities within the coenzyme binding domains of dehydrogenases. *J. Mol. Biol.* **89**, 339-354.

Parés, X., Farrés, J., Moreno, A., Saubi, N., Boleda, M.D., Cederlund, E., Hoog, J.O. i Jörnvall, H. (1993) Class IV alcohol dehydrogenase: structure and function. *Adv. Exp. Med. Biol.* **328**, 475-480.

Parés, X., Cederlund, E., Moreno, A., Hjelmqvist, L., Farrés, J. i Jörnvall, H. (1994) Mammalian class IV alcohol dehydrogenase (stomach alcohol dehydrogenase): structure, origin, and correlation with enzymology. *Proc. Natl. Acad. Sci. USA*. **91**, 1893-1897.

Park, D.H. i Plapp, B.V. (1991) Isoenzymes of horse liver alcohol dehydrogenase active on ethanol and steroids. cDNA cloning, expression, and comparison of active sites. *J. Biol. Chem*. **266**, 13296-32302.

Peralba, J.M., Cederlund, E., Crosas, B., Moreno, A., Julià, P., Martínez, S.E., Persson, B., Farrés, J., Parés, X. i Jörnvall, H. (1999a) Structural and enzymatic properties of a gastric NADP(H)-dependent and retinal-active alcohol dehydrogenase. *J. Biol. Chem.* **274**, 26021-26026.

Peralba, J.M., Crosas, B., Martínez, S.E., Julià, P., Farrés, J. i Parés, X. (1999b) Amphibian alcohol dehydrogenase. Purification and characterization of classes I and III from *Rana perezi*. *Adv. Exp. Med. Biol*. **463**, 343-350.

Perham, R.N., Scrutton, N.S. i Berry, A. (1991) New enzymes for old: redesigning the coenzyme and substrate specificities of glutathione reductase. *BioEssays* **13**, 515-525.

Persson, B., Bergman, T., Keung, W.M., Waldenstrom, U., Holmquist, B., Vallee, B.L. i Jörnvall, H. (1993) Basic features of class-I alcohol dehydrogenase: variable and constant segments coordinated by inter-class and intra-class variability. Conclusions from characterization of the alligator enzyme. *Eur. J. Biochem*. **216**, 49-56.

Pietruszko, R., Crawford, K. i Lester, D. (1973) Comparison of substrate specificity of alcohol dehydrogenases from human liver, horse liver, and yeast towards saturated and 2-enoic alcohols and aldehydes. *Arch. Biochem. Biophys*. **159**, 50-60.

Pietruszko, R. (1979) Nonethanol substrates of alcohol dehydrogenase. Biochemistry and Pharmacology of Ethanol vol I (Majchrowicz, E. i Noble, E.P., eds), Plenum Press, New York, pp 87-106.

Pietruszko, R. (1982) Alcohol dehydrogenase from horse liver, steroid-active SS isozyme. *Methods Enzymol.* **89**, 428-434.

Plapp, B.V., Sogin, D.C., Dworschack, R.T., Bohlken, D.P., Woenckhaus, C. i Jeck, R. (1986) Kinetics of native and modified liver alcohol dehydrogenase with coenzyme analogues: isomerization of enzyme-nicotinamide adenine dinucleotide complex. *Biochemistry* **25**, 5396-5402.

Plapp, B.V. (1995) Site-directed mutagenesis: a tool for studying enzyme catalysis. *Methods Enzymol.* **249**, 91-119.

Popescu, G. i Napoli, J.L. (2000) Analysis of rat cytosolic 9-*cis*-retinol dehydrogenase activity and enzymatic characterization of rat ADHII. *Biochim. Biophys. Acta* **1476**, 43-52.

Quadro, L., Blaner, W.S., Salchow, D.J., Vogel, S., Piantedosi, R., Gouras, P., Freeman, S., Cosma, M.P., Colantuoni, V. i Gottesman, M.E. (1999) Impaired retinal function and vitamin A availability in mice lacking retinol-binding protein. *EMBO J.* **18**, 4633-4644.

Ramaswamy, S., Eklund, H. i Plapp, B.V. (1994a). Structures of horse liver alcohol dehydrogenase complexed with NAD+ and substituted benzyl alcohols. *Biochemistry* **33**, 5230-5237.

Ramaswamy, S., el-Ahmad, M., Danielsson, O., Jörnvall, H. i Eklund, H. (1994b) Crystallisation and crystallographic investigations of cod alcohol dehydrogenase class I and class III enzymes. *FEBS Lett.* **350**, 122-124.

Ramaswamy, S., el Ahmad, M., Danielsson, O., Jörnvall, H. i Eklund, H. (1996) Crystal structure of cod liver class I alcohol dehydrogenase: substrate pocket and structurally variable segments. *Protein Sci*. **5**, 663-671.

Raner, G.M., Vaz, A.D. i Coon, M.J. (1996) Metabolism of all-trans, 9-*cis*, and 13-*cis* isomers of retinal by purified isozymes of microsomal cytochrome P450 and mechanism-based inhibition of retinoid oxidation by citral. *Mol. Pharmacol.* **49**, 515-522.

Rao, S.T i Rossmann, M.G. (1973) Comparison of super-secondary structure in proteins. *J. Mol. Biol.* **76**, 241-256.

Ray, W.J., Bain, G., Yao, M. i Gottlieb, D.I. (1997) CYP26, a novel mammalian cytochrome P450, is induced by retinoic acid and defines a new family. *J. Biol. Chem.* **272**, 18702-18708.

Riveros-Rosas, H., Julian-Sanchez, A., Villalobos-Molina, R., Pardo, J.P. i Pina, E. (2003) Diversity, taxonomy and evolution of medium-chain dehydrogenase/reductase superfamily. *Eur. J. Biochem*. **270**, 3309-3334.

Roberts, E.S., Vaz, A.D. i Coon, M.J. (1992) Role of isozymes of rabbit microsomal cytochrome P-450 in the metabolism of retinoic acid, retinol, and retinal. *Mol. Pharmacol*. **41**, 427-433.

Ross, S.A., McCaffery, P.J., Drager, U.C. i De Luca, L.M. (2000) Retinoids in embryonal development. *Physiol. Rev.* **80**, 1021-1054.

Rossmann, M.G., Moras, D. i Olsen, K.W. (1974) Chemical and biological evolution of nucleotide-binding protein. *Nature* **250**, 194-199.

Samama, J.P., Zeppezauer, E., Biellmann, J.F. i Brändén, C.I. (1977) The crystal structure of complexes between horse liver alcohol dehydrogenase and the coenzyme analogues 3-iodopyridine-adenine dinucleotide and pyridine-adenine dinucleotide. *Eur. J. Biochem.* **81**, 403-409.

Sanghani, P.C., Bosron, W.F., i Hurley, T.D. (2002) Human glutathione-dependent formaldehyde dehydrogenase. Structural changes associated with ternary complex formation. *Biochemistry* **41**, 15189-15194.

Sarau, H.M., Foley, J., Moonsammy, G. i Wiebelhaus, V.D. (1975) Metabolism of dog gastric mucosa. Nucleotide levels in parietal cells. *J. Biol. Chem.* **250**, 8321-8329.

Scadding, S.R. i Maden, M. (1994) Retinoic acid gradients during limb regeneration. *Dev. Biol.* **162**, 608-617.

Scrutton, N.S., Berry, A. i Perham, R.N. (1990) Redesign of the coenzyme specificity of a dehydrogenase by protein engineering. *Nature* **343**, 38-43.

Seeley, T.L. i Holmes, R.S. (1984) Purification and molecular properties of a Class II alcohol dehydrogenase (ADH-C2) from horse liver. *Int. J. Biochem*. **16**, 1037-1042.

Seeley, T.L., Mather, P.B. i Holmes, R.S. (1984) Electrophoretic analyses of alcohol dehydrogenase, aldehyde reductase, aldehyde oxidase and xanthine oxidase from horse tissues. *Comp. Biochem. Physiol.* **78B**, 131-139.

Sellin, S., Holmquist, B., Mannervik, B. i Vallee, B.L. (1991) Oxidation and reduction of 4-hydrixyalkenals catalyzed by isozyme of human alcohol dehydrogenase. *Biochemistry* **30**, 2514-2518.

Shafqat, J., Hjelmqvist, L. i Jörnvall, H. (1996a) Liver class-I alcohol dehydrogenase isozyme relationships and constant patterns in a variable basic structure. Distinctions from characterization of an ethanol dehydrogenase in cobra, Naja naja. *Eur. J. Biochem*. **236**, 571-578.

Shafqat, J., El-Ahmad, M., Danielsson, O., Martínez, M.C., Persson, B., Parés, X. i Jörnvall, H. (1996b) Pea formaldehyde-active class III alcohol dehydrogenase: common derivation of the plant and animal forms but not of the corresponding ethanol-active forms (classes I and P). *Proc. Natl. Acad. Sci. USA*. **93**, 5595-5599.

Sloan, D.L., Young, J.M. i Mildvan, A.S. (1975) Nuclear magnetic resonance studies of substrate interaction with cobalt substituted alcohol dehydrogenase from liver. *Biochemistry* **14**, 1998-2008.

Stone, C.L., Burnell, J.C., Li, T.K. i Bosron, W.F. (1989) Relationships between the kinetics of alcohol or coenzyme oxidoreduction and amino acid sequence of human liver alcohol dehydrogenase isoenzymes. *Prog. Clin. Biol. Res.* **290**, 155-165.

Stone, C.L., Thomasson, H.R., Bosron, W.F. i Li, T.K. (1993a) Purification and partial amino acid sequence of a high-activity human stomach alcohol dehydrogenase. *Alcohol Clin. Exp. Res*. **17**, 911-918.

Stone, C.L., Bosron, W.F. i Dunn, M.F. (1993b) Amino acid substitutions at position 47 of human beta 1 beta 1 and beta 2 beta 2 alcohol dehydrogenases affect hydride transfer and coenzyme dissociation rate constants. *J. Biol. Chem.* **268**, 892-9.

Stromberg, P. i Hoog, J.O. (2000) Human class V alcohol dehydrogenase (ADH5): A complex transcription unit generates C-terminal multiplicity. *Biochem. Biophys. Res. Commun*. **278**, 544-549.

Sun, H.W. i Plapp, B.V. (1992) Progresive sequence alignment and molecular evolution of the Zn-containing alcohol dehydrogenase family. *J. Mol. Evol.* **34**, 522-535.

Svensson, S., Stromberg, P. i Höög, J.O. (1999) A novel subtype of class II alcohol dehydrogenase in rodents. Unique Pro(47) and Ser(182) modulates hydride transfer in the mouse enzyme. *J. Biol. Chem*. **274**, 29712-29719.

Svensson, S., Höög, J.O., Schneider, G. i Sandalova, T. (2000) Crystal structures of mouse class II alcohol dehydrogenase reveal determinants of substrate specificity and catalytic efficiency. *J. Mol. Biol*. **302**, 441-453.

Thatcher, D.R. (1980) The complete amino acid sequence of three alcohol dehydrogenase alleloenzymes (AdhN-11, AdhS and AdhUF) from the fruitfly *Drosophila melanogaster*. *Biochem. J*. **187**, 875-883.

Theorell, H. i Chance, B. (1951) Studies on liver alcohol dehydrogenase. II. The kinetics of the compound of horse liver alcohol dehydrogenase and reduced diphosphopyridine nucleotide. *Acta Chem. Scand*. **5**, 1127-1144.

Thorn, J.M., Barton, J.D., Dixon, N.E., Ollis, D.L. i Edwards, K.J. (1995) Crystal structure of Escherichia coli QOR quinone oxidoreductase complexed with NADPH. *J. Mol. Biol.* **249**, 785-799.

Tolf, B.R., Siddiqi, M.T. i Dahlbom, R. (1982) Synthetic inhibitors of alcohol dehydrogenase. Pyrazoles containing polar substituents in the 4-position. *Eur. J. Med. Chem. Chim. Ther.* **17**, 395-402.

Vallee, B.L. i Bazzone, T.J. (1983) Isozymes of human liver alcohol dehydrogenase. *Isozymes Curr. Top. Biol. Med. Res*. **8**, 219-244.

von Lintig, J. i Vogt, K. (2000) Filling the gap in vitamin A research. Molecular identification of an enzyme cleaving beta-carotene to retinal. *J. Biol. Chem*. **275**, 11915-11920.

von Wartburg, J.P., Bethune, J.L. i Vallee, B.L. (1964) Human liver-alcohol dehydrogenase. Kinetic and physicochemical properties. *Biochemistry* **3**, 1775-1782.

Wagner, F.W., Burger, A.R. i Vallee, B.L. (1983) Kinetic properties of human liver alcohol dehydrogenase: oxidation of alcohols by class I isoenzymes. *Biochemistry* **22**, 1857-1863.

Wagner, F.W., Parés, X., Holmquist, B. i Vallee, B.L. (1984) Physical and enzymatic properties of a class III isozyme of human liver alcohol dehydrogenase: χ-ADH. *Biochemistry* **23**, 2193-2199.

Wallace, A.C., Laskowski, R.A. i Thornton, J.M. (1995) LIGPLOT: a program to generate schematic diagrams of protein-ligand interactions. *Protein Eng*. **8**, 127-134.

White, J.A., Beckett-Jones, B., Guo, Y.D., Dilworth, F.J., Bonasoro, J., Jones, G. i Petkovich, M. (1997) cDNA cloning of human retinoic acid-metabolizing enzyme (hP450RAI) identifies a novel family of cytochromes P450. *J. Biol. Chem.* **272**, 18538-18541.

White, J.A., Ramshaw, H., Taimi, M., Stangle, W., Zhang, A., Everingham, S., Creighton, S., Tam, S.P., Jones, G. i Petkovich, M. (2000) Identification of the human cytochrome P450, P450RAI-2, which is predominantly expressed in the adult cerebellum and is responsible for all-trans-retinoic acid metabolism. *Proc. Natl. Acad. Sci. USA* **97**, 6403-6408.

Wierenga, R.K., De Maeyer, M.C.H. i Hol, W.G.J. (1985) Interaction of pyrophosphate moieties with α-helixes in dinucleotide binding proteins. *Biochemistry* **24**, 1346-1357.

Wierenga, R.K., Terpstra, P. i Hol, W.G.J. (1986) Prediction of the occurrence of the ADP-binding beta alpha beta-fold in proteins, using an amino acid sequence fingerprint. *J. Mol. Biol.*, **187**, 101-107.
Williamson, D.H. i Brosnan, J.T. (1974) Concentrations of metabolites in animal tissues. Methods of Enzymatic Analysis vol IV (Hans Ulrich ed.), Academic Press, pp 2266-2302.

Wratten, C.C. i Cleland, W.W. (1963) Product inhibition studies on yesat and liver alcohol dehydrogenases. *Biochemistry* **2**, 935-941.

Xie, P., Parsons, S.H., Speckhard, D.C., Bosron, W.F. i Hurley, T.D. (1997) X-ray structure of human class IV σσ alcohol dehydrogenase. Structural basis for substrate specificity. *J. Biol. Chem*. **272**, 18558-18563.

Yang, Z.N., Davis, G.J., Hurley, T.D., Stone, C.L., Li, T.K. i Bosron, W.F. (1994) Catalytic efficiency of human alcohol dehydrogenases for retinol oxidation and retinal reduction. *Alcohol. Clin. Exp. Res*. **18**, 587-591.

Yang, Z.N., Bosron, W.F. i Hurley, T.D. (1997) Structure of human chi chi alcohol dehydrogenase: a glutathione-dependent formaldehyde dehydrogenase. *J. Mol. Biol*. **265**, 330-343.

Yasunami, M., Chen, C.S. i Yoshida, A. (1991) A human alcohol dehydrogenase gene (ADH6) encoding an additional class of isozyme. *Proc. Natl. Acad. Sci. USA* **88**, 7610-7614.

Yin, S.J., Han, C.L., Liao, C.S. i Wu, C.W. (1997) Expression, activities, and kinetic mechanism of human stomach alcohol dehydrogenase. Inference for first-pass metabolism of ethanol in mammals. *Adv. Exp. Med. Biol.* **414**, 347-355.

Yu, P.H., Lai, C.T. i Zuo, D.M. (1997) Formation of formaldehyde from adrenaline in vivo; a potential risk factor for stress-related angiopathy. *Neurochem. Res*. **22**, 615-620.

Zheng, Y.W., Bey, M., Liu, H. i Felder, M.R. (1993) Molecular basis of the alcohol dehydrogenase-negative deer mouse. Evidence for deletion of the gene for class I enzyme and identification of a possible new enzyme class. *J. Biol. Chem*. **268**, 24933-24939.

ANNEX

ARTICLES PUBLICATS COM A RESULTAT
D' AQUESTA TESI

ARTICLE I

Acta Crystallographica Section D
Biological Crystallography
ISSN 0907-4449

Crystallization and preliminary X-ray analysis of NADP(H)-dependent alcohol dehydrogenases from *Saccharomyces cerevisiae* and *Rana perezi*

Eva Valencia,[a] Albert Rosell,[b] Carolina Larroy,[b] Jaume Farrés,[b] Josep A. Biosca,[b] Ignacio Fita,[a] Xavier Parés[b] and Wendy F. Ochoa[a]*

[a]IBMB-CSIC, Jordi Girona 18-26, E-08034 Barcelona, Spain, and [b]Departament de Bioquímica i Biologia Molecular, Universitat Autònoma de Barcelona, E-08193 Bellaterra (Barcelona), Spain

Correspondence e-mail: wfocri@ibmb.csic.es

Received 9 July 2002
Accepted 12 September 2002

Different crystal forms diffracting to high resolution have been obtained for two NADP(H)-dependent alcohol dehydrogenases, members of the medium-chain dehydrogenase/reductase superfamily: ScADHVI from *Saccharomyces cerevisiae* and ADH8 from *Rana perezi*. ScADHVI is a broad-specificity enzyme, with a sequence identity lower than 25% with respect to all other ADHs of known structure. The best crystals of ScADHVI diffracted beyond 2.8 Å resolution and belonged to the trigonal space group $P3_121$ (or to its enantiomorph $P3_221$), with unit-cell parameters $a = b = 102.2$, $c = 149.7$ Å, $\gamma = 120^\circ$. These crystals were produced by the hanging-drop vapour-diffusion method using ammonium sulfate as precipitant. Packing considerations together with the self-rotation function and the native Patterson map seem to indicate the presence of only one subunit per asymmetric unit, with a volume solvent content of about 80%. ADH8 from *R. perezi* is the only NADP(H)-dependent ADH from vertebrates characterized to date. Crystals of ADH8 obtained both in the absence and in the presence of $NADP^+$ using polyethylene glycol and lithium sulfate as precipitants diffracted to 2.2 and 1.8 Å, respectively, using synchrotron radiation. These crystals were isomorphous, space group $C2$, with approximate unit-cell parameters $a = 122$, $b = 79$, $c = 91$ Å, $\beta = 113^\circ$ and contain one dimer per asymmetric unit, with a volume solvent content of about 50%.

1. Introduction

Most alcohol dehydrogenases (ADHs) of wide substrate specificity from yeast and vertebrates are members of the medium-chain dehydrogenase/reductase (MDR) superfamily, which has been divided into different enzyme families with regard to structural and functional relationships (Jörnvall *et al.*, 2001).

The classical *S. cerevisiae* ADHs involved in alcohol production and assimilation are tetrameric enzymes structurally related to vertebrate ADHs (Ciriacy, 1997). We have recently reported the characterization of a new yeast ADH, named ADHVI, presumably a dimer of molecular weight 80 kDa, with only 26% sequence identity to the tetrameric enzyme family (Larroy *et al.*, 2002). Primary structure analysis shows that ADHVI belongs to a different family within the MDRs, the cinnamyl alcohol dehydrogenases (CADs; 37% identity). Consistent with this, ADHVI uses NADP(H) as a cofactor, exhibits a broad substrate specificity with aromatic and linear hydrophobic alcohols and shows high activity towards cinnamyl alcohol and cinnamyl aldehyde. In plants, CAD enzymes participate in the synthesis of cinnamyl alcohol derivatives in the last steps of lignin biosynthesis (Luderitz & Grisebach, 1981). Since *S. cerevisiae* does not synthesize lignin, we hypothesized that the yeast ADHVI could contribute to lignin degradation and the last step of the synthesis of fusel alcohols derived from amino-acid and α-ketoacid metabolism (Larroy *et al.*, 2002). No crystallographic structure has been reported for any member of the CAD family. The closest known structures to ADHVI (25% identity) are of a NADP(H)-dependent ketose reductase from the whitefly *Bemisia argentifolii* (Banfield *et al.*, 2001) and human ADH4 (Xie *et al.*, 1997).

In vertebrates, ADHs constitute a family of eight different classes involved in ethanol metabolism and also in the transformation of a variety of alcohols and aldehydes of physiological importance, such as retinoids, steroids and cytotoxic aldehydes (Duester *et al.*, 1999). All ADHs from vertebrates are dimers of about 80 kDa and contain two Zn atoms per subunit. In mammals, ADH1 and ADH4 have been the most studied classes because of their wide expression level in tissue and their activity towards ethanol and retinol (Boleda *et al.*, 1993). The oxidation of retinol to retinal is the initial step in the synthesis of retinoic acid, an important modulator of gene expression. While ADH1 is present in all vertebrate

groups, ADH4 has only been described in mammals. In our search for an ADH4-type enzyme in amphibians, we found an enzyme with similar kinetic properties to those of ADH4 but, surprisingly, with specificity towards NADP(H) instead of NAD(H), the common coenzyme for all previously described vertebrate ADHs. This enzyme (ADH8) was isolated from the stomach of *R. perezi* and exhibited high activity towards retinal (Peralba *et al.*, 1999). In consequence, we proposed a physiological function in retinal reduction for ADH8, which is also supported by the high cellular NADPH:NADP$^+$ ratio.

Several crystallographic structures of vertebrate ADHs are known: horse ADH1 (Eklund *et al.*, 1976), human ADH1B1, ADH1B2 and ADH1B3 (Hurley *et al.*, 1994), human ADH1A and ADH1C2 (Niederhut *et al.*, 2001), cod ADH1 (Ramaswamy *et al.*, 1996), mouse ADH2 (Svensson *et al.*, 2000), human ADH3 (Yang *et al.*, 1997) and human ADH4 (Xie *et al.*, 1997). All of them correspond to NAD(H)-dependent enzymes and exhibit less than 57% identity with the present amphibian ADH8. Crystallization and structure determination of ADH8 would provide the basis for the unique cofactor specificity of this enzyme and for its particularly high activity towards retinal.

In the present report, we describe the crystallization and the crystal properties of two ADHs from the MDR superfamily: *S. cerevisiae* ADHVI, an NADP(H)-dependent ADH and the first member crystallized of the CAD family, and amphibian ADH8, the first NADP(H)-dependent ADH member of the vertebrate ADH family.

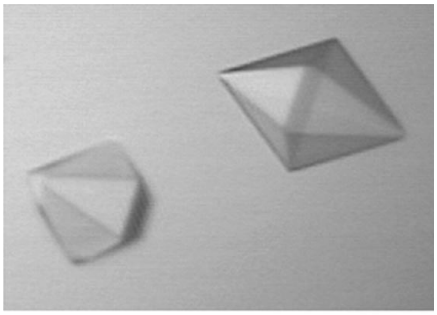

(*a*)

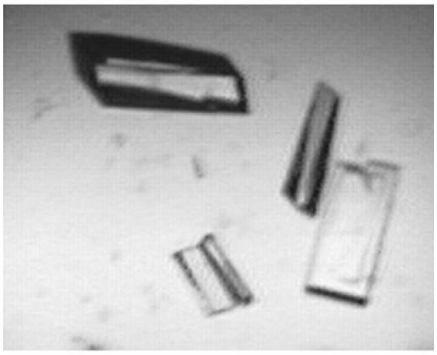

(*b*)

Figure 1
Crystals of (*a*) ScADHVI and (*b*) ADH8. Despite the size and good morphology of the ScADHVI crystals, diffraction was extremely weak beyond approximately 2.8 Å resolution, which may be related to the high solvent content.

Table 1
Data-collection statistics.

Values in parentheses refer to the outer shell.

	ADH8	ADH8 (NADP$^+$)	ScADHVI
Space group	*C*2	*C*2	$P3_121$ or $P3_221$
Unit-cell parameters (Å, °)	$a = 122.5$, $b = 79.5$, $c = 91.9$, $\beta = 113.1$	$a = 122.2$, $b = 79.5$, $c = 91.8$, $\beta = 112.8$	$a = b = 102.2$, $c = 149.7$, $\gamma = 120$
No. measured reflections	150436	254342	120598
No. unique reflections	79197	140960	22735
Resolution (Å)	2.20 (2.28–2.20)	1.80 (1.86–1.80)	2.80 (2.90–2.80)
$R_{\rm merge}$† (%)	11.3 (44.7)	4.8 (33.1)	7.7 (40.0)
Completeness (%)	98.4 (99.0)	96.1 (74.2)	99.8 (99.8)
$\langle I/\sigma(I)\rangle$	11.8 (2.6)	14.4 (1.6)	24.3 (2.2)
Mosaicity (°)	0.4	0.4	0.2

† $R_{\rm merge} = \sum|I_i - \langle I\rangle|/\sum I_i$, where I_i is the measured intensity of an individual reflection and $\langle I\rangle$ is the average intensity of the symmetry-related measurements of this reflection.

2. Experimental results

2.1. Crystallization, data collection and X-ray analysis

2.1.1. NADP(H)-dependent ADHVI from *S. cerevisiae* (ScADHVI). ScADHVI was obtained from yeast cells by a modification of a previously described protocol (Larroy *et al.*, 2002). The modification consisted of performing the DEAE-Sepharose chromatography at pH 8.0 instead of pH 7.0, which resulted in increased purity and allowed bypassing of the hydroxyapatite column. Pure enzyme was used in crystallization screening using the hanging-drop vapour-diffusion method. 1 µl drops of concentrated sample (6 mg ml^{-1}) were mixed with the same volume of a reservoir solution containing 2 *M* ammonium sulfate (AS) and equilibrated at 293 K against a reservoir volume of 1 ml. Well developed bipyramidal hexagonal crystals reaching 0.4 × 0.4 × 0.6 mm in size appeared in 2 d (Fig. 1). These crystals belong to space group $P3_121$ (or to its enantiomorph $P3_221$), with unit-cell parameters $a = b = 102.2$, $c = 149.7$ Å, $\gamma = 120°$). An X-ray diffraction data set was collected using synchrotron radiation and a MAR CCD detector at ESRF (Grenoble, France) at 100 K with 20%(*v*/*v*) glycerol as cryoprotectant. Data were processed and scaled with the programs *DENZO* and *SCALEPACK* (Otwinowski & Minor, 1996), respectively, giving an overall $R_{\rm merge}$ of 7.7% and a completeness of 99% at 2.8 Å (Table 1). An X-ray fluorescence scan of one of the crystals (performed on beamline BM14) showed a clear absorption edge with the peak at 9671.4 eV, strongly supporting the existence of Zn ions in ScADHVI (Kim & Howard, 2002).

Packing considerations indicate that, assuming a protein-subunit molecular weight of about 40 kDa, these crystals could contain one, two or three subunits per asymmetric unit, with corresponding volume solvent contents ranging from 80 to 42% (Matthews, 1968). In turn, the absence of significant peaks in both the native Patterson map and in the self-rotation function (Fig. 2) makes the existence of non-crystallographic symmetry unlikely, although molecular twofold axes oriented almost parallel to the crystallographic twofold axis are still possible. The weakness of the diffraction at high resolution despite the good morphology and size of the ScADHVI crystals could also be related to a high solvent content. Even if these crystals contain only one subunit per asymmetric unit, the ScADHVI molecules could be homodimers as suggested by Larroy *et al.* (2002) if the molecular and crystallographic twofold axes coincide.

No solution has yet been obtained by molecular replacement with the programs *AMoRe* (Navaza, 1994) and *BEAST* (Read, 2001) using search models derived from human ADH1B1 (Hurley *et al.*, 1991), human ADH4 (Xie *et al.*, 1997), horse ADH1 (Adolph *et al.*, 2000) and ketose reductase (Banfield *et al.*, 2001) and from combinations of the N-terminal catalytic and coenzyme-binding domains of these structures. All ADH molecules used as search models exhibit sequence identities with ScADHVI of below 25% which, together

with the difficulties in finding a molecular-replacement solution, suggests significant structural differences. Searches for heavy-atom derivatives and MAD experiments at the Zn edge are now under way.

2.1.2. NADP(H)-dependent ADH from *R. perezi* (ADH8). Wild-type ADH8 cDNA was obtained from isolated poly(A)$^+$ RNA and cloned into pBluescript II SK (+) (Peralba *et al.*, 1999). Cloning into pGEX 4T-2 (Amersham Pharmacia Biotech) was performed by amplification of the coding region using the polymerase chain reaction (PCR) with two specific primers, RanaL (5′-TTATA**GGATCC**ATGTGCACTGCGGG-AAAAGAT-3′) and RanaR (5′-CCAC-CT**GAATTC**TTAGTATATCATAATGCT-TCG-3′), including restriction sites (bold) for *Bam*HI and *Eco*RI, respectively. The resulting PCR product was purified by means of the Concert Rapid Gel Extraction System (Life Technologies) and then cloned into the *Bam*HI and *Eco*RI sites of pGEX 4T-2. *Escherichia coli* BL21 competent cells were transformed with the construct.

Expression and batchwise purification were carried out by means of the GST Gene Fusion System (Amersham Pharmacia Biotech). Wild-type cDNA was expressed by inoculating 2×YT liquid medium, containing 75 µg ml^{-1} ampicillin, with an overnight culture (1:100 dilution) of BL21 cells containing the pGEX 4T-2 harbouring the ADH8 cDNA. Cells were grown at 276 K until an absorbance of 0.8–1.0 at 600 nm was reached. Isopropyl β-D-thiogalactoside was then added to a final concentration of 0.1 m*M*. Bacteria were incubated for 15 h at 296 K and then harvested by centrifugation and stored at 193 K. The pellet was resuspended (100 ml per litre of culture) in cold phosphate-buffered saline (1×PBS; 1.8 m*M* KH_2PO_4, 10 m*M* NaH_2PO_4, 140 m*M* NaCl, 2.7 m*M* KCl pH 7.3) containing 2.5 m*M* dithiothreitol (DTT). Cells were treated with a 1 mg ml^{-1} final concentration of lysozyme for 30 min at 277 K, sonicated, incubated with bovine DNAse for 30 min at 277 K and finally treated with 1%(*v*/*v*) Triton X-100 for 30 min at 277 K to aid in solubilization of the fusion protein. Cell debris was separated by centrifugation at 12 000*g* for 15 min at 277 K.

A batchwise purification of the fusion protein was carried out by incubation of the cleared cell lysate with glutathione Sepharose 4B (2 ml 50% matrix per litre of culture) at room temperature for 90 min with gentle agitation. The suspension was centrifuged at 500*g* for 5 min at 277 K and the supernatant was discarded. The matrix containing bound protein was washed three times with 1×PBS by gentle agitation. All centrifugations for washing and elution were performed as described above. Fusion protein bound to matrix was cleaved with thrombin (50 U per litre of culture) by agitation for 15 h at room temperature. Following incubation, the suspension was centrifuged to pellet Sepharose beads. The GST portion of the fusion protein remained bound to the matrix, while the eluate contained ADH8. The purification buffer was exchanged using Centricon Plus-20 (Millipore) to 10 m*M* sodium phosphate/NaOH pH 6.5 containing 2.5 m*M* DTT. The protein was then further concentrated and stored at 193 K. The fraction containing ADH activity was subjected to an additional affinity chromatography step in Red Sepharose CL-6B (Amersham Pharmacia Biotech) to eliminate thrombin. This purification was performed in batches as described above, but ADH8 was eluted in the presence of 0.6 *M* NaCl. This fraction was subjected to SDS–PAGE and Coomassie Blue staining to assess the degree of purity.

Samples of ADH8 with an initial protein concentration of 12 mg ml^{-1} (Bradford, 1976) were used in crystallization screening with the hanging-drop vapour-diffusion method. Monoclinic crystals belonging to space group *C*2 were obtained in about a week using 20% PEG 4000 and 0.2 *M* $LiSO_4$ as precipitants in 0.1 *M* Tris–HCl pH 8 (Fig. 1). The size of the crystals increased, reaching 0.2 × 0.2 × 0.3 mm, when methanol was used as an additive. Crystals with the same morphology and about the same size were also obtained at 277 K under similar crystallization conditions from ADH8 samples that had been incubated overnight with 1 *M* $NADP^+$ (Table 1).

Diffraction data were collected to 2.2 Å using synchrotron radiation at ESRF (Grenoble) from ADH8 crystals grown without nucleotide and flash-cooled to liquid-nitrogen temperature. The cryobuffer was prepared from the crystallization solution supplemented with glycerol to a final concentration of 25%(*v*/*v*) in three steps. In a similar way, a diffraction data set to 1.8 Å was collected from ADH8 crystals grown in the presence of $NADP^+$. Both data sets were processed and scaled with the programs *DENZO* and *SCALEPACK* (Otwinowski & Minor, 1996), giving overall $R_{\rm merge}$ values of

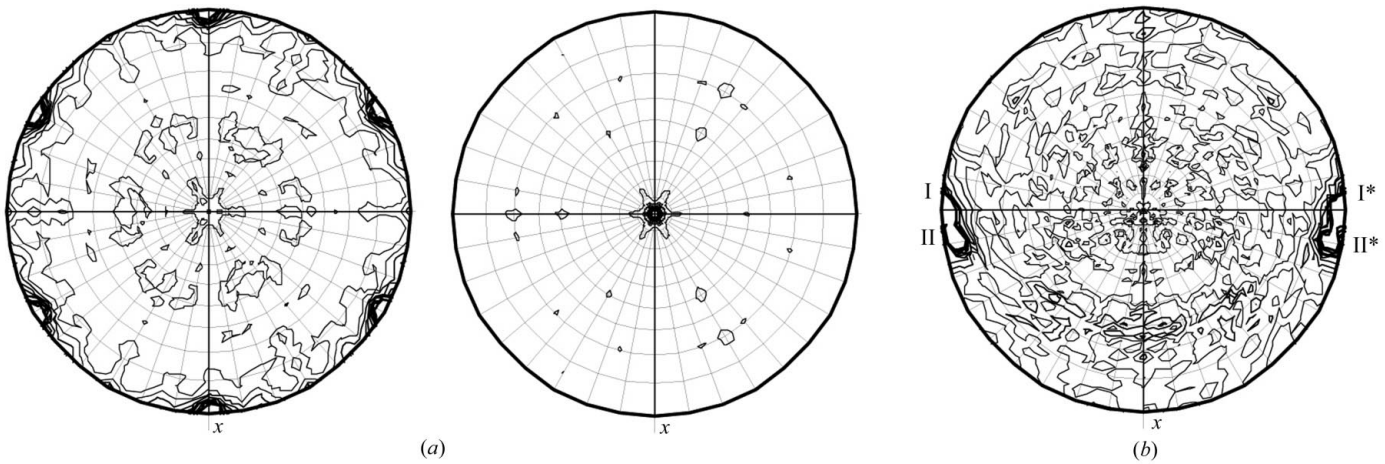

Figure 2
(*a*) Representation of the $\kappa = 180^\circ$ (left) and $\kappa = 120^\circ$ (right) sections containing the only significant peaks found in the self-rotation function of the ScADHVI crystals, which confirm the 3*m* point-group symmetry. (*b*) Representation of the $\kappa = 180^\circ$ section of the self-rotation function of ADH8 crystals. The largest peak, indicated I in the figure, corresponds to the crystallographic twofold axis. The second peak (II in the figure) corresponds to the molecular twofold axis. All self-rotation calculations were performed in the resolution range 20–3 Å with an integration radius of 30 Å.

11.3 and 4.8 and completenesses of 98 and 96%, respectively (Table 1). These crystals contain two protein subunits, corresponding to one molecule, in the crystal asymmetric unit, with the molecular twofold axis approximately 10° from the crystallographic twofold axis (Fig. 2). A clear molecular-replacement solution, where the first peak in the rotation function was about twice the intensity of the second, has been found using the program *AMoRe* (Navaza, 1994) with a search model derived from the structure of human ADH1B1 (PDB code 1deh; Hurley *et al.*, 1991).

3. Conclusions

Different crystal forms diffracting to high resolution have been obtained for two NADP(H)-dependent alcohol dehydrogenases: ScADHVI from *S. cerevisiae* and ADH8 from *R. perezi*. ScADHVI is a broad-specificity ADH (Larroy *et al.*, 2002), a member of the CAD enzymatic family, with a sequence identity lower than 25% with respect to all other ADHs of known structure. No molecular-replacement solution has yet been found, which suggests important structural differences from the available ADH structures. In turn, a preliminary molecular-replacement solution has already been found for ADH8, the only NADP(H)-dependent ADH from vertebrates characterized to date.

The structure determination at high resolution of both ScADHVI and ADH8 would clarify the molecular peculiarities of the NADP(H)-dependent ADHs, particularly their cofactor preference. Moreover, the ScADHVI structure would provide the first three-dimensional approach to explain the structure–function relationships in the cinnamyl alcohol dehydrogenase family.

This work was supported by grants PB98-0855 to XP, BMC2000-0132 to JAB and BIO099-0865 to IF. Many thanks are given to X. Carpena for assistance with data collection.

References

Adolph, H. W., Zwart, P., Meijers, R., Hubatsch, I., Kiefer, M., Lamzin, V. & Cedergren-Zeppezauer, E. (2000). *Biochemistry*, **39**, 12885–12897.
Banfield, M. J., Salvucci, M. E., Baker, E. N. & Smith, C. A. (2001). *J. Mol. Biol.* **306**, 239–250.
Boleda, M. D., Saubi, N., Farrés, J. & Parés, X. (1993). *Arch. Biochem. Biophys.* **307**, 85–90.
Bradford, M. M. (1976). *Anal. Biochem.* **72**, 248–254.
Ciriacy, M. (1997). *Yeast Sugar Metabolism: Biochemistry, Genetics, Biotechnology and Applications*, edited by F. K. Zimmermann & K. D. Entian, pp. 213–223. Lancaster, Pennsylvania, USA: Technomic Publishing Co. Inc.
Duester, G., Farrés, J., Felder, M. R., Holmes, R. S., Höög, J. O., Parés, X., Plapp, B. V., Yin, S. J. & Jörnvall, H. (1999). *Biochem. Pharmacol.* **58**, 389–395.
Eklund, H., Nordström, B., Zeppezauer, E., Söderlund, G., Ohlsson, I., Boiwe, T., Söderberg, B. O., Tapia, O., Brändén, C. I. & Åkeson, Å. (1976). *J. Mol. Biol.* **102**, 27–59.
Hurley, T. D., Bosron, W. F., Hamilton, J. A. & Amzel, L. M. (1991). *Proc. Natl Acad. Sci. USA*, **88**, 8149–8153.
Hurley, T. D., Bosron, W. F., Stone, C. L. & Amzel, L. M. (1994). *J. Mol. Biol.* **239**, 415–429.
Jörnvall, H., Shaqfat, J. & Persson, B. (2001). *Chem. Biol. Interact.* **30**, 491–498.
Kim, K. & Howard, A. J. (2002). *Acta Cryst.* D**58**, 1332–1334.
Larroy, C., Fernandez, M. R., Gonzalez, E., Pares, X. & Biosca, J. A. (2002). *Biochem. J.* **361**, 163–172.
Luderitz, T. & Grisebach, H. (1981). *Eur. J. Biochem.* **119**, 115–124.
Matthews, B. W. (1968). *J. Mol. Biol.* **33**, 491–497.
Navaza, J. (1994). *Acta Cryst.* A**50**, 157–163.
Niederhut, M. S., Gibbons, B. J., Pérez-Miller, S. & Hurley, T. D. (2001). *Protein Sci.* **10**, 697–706.
Otwinowski, Z. & Minor, W. (1996). *Methods Enzymol.*, **276**, 307–326.
Peralba, J. M., Cederlund, E., Crosas, B., Moreno, A., Julià, P., Martínez, S. E., Persson, B., Farrés, J., Parés, X. & Jörnvall, H. (1999). *J. Biol. Chem.* **274**, 26021–26026.
Ramaswamy, S., El-Ahmad, M., Danielsson, O., Jörnvall, H. & Eklund, H. (1996). *Protein Sci.* **5**, 663–671.
Read, R. J. (2001). *Acta Cryst.* D**57**, 1373–1382.
Svensson, S., Höög, J. O., Schneider, G. & Sandalova, T. (2000). *J. Mol. Biol.* **302**, 441–453.
Xie, P., Parsons, S. H., Speckhard, D. C., Bosron, W. F. & Hurley, T. D. (1997). *J. Biol. Chem.* **272**, 18558–63.
Yang, Z. N., Bosron, W. F. & Hurley, T. D. (1997). *J. Mol. Biol.* **265**, 330–343.

ARTICLE II

doi:10.1016/S0022-2836(03)00431-5 J. Mol. Biol. (2003) 330, 75–85

JMB

Available online at www.sciencedirect.com

SCIENCE DIRECT®

Crystal Structure of the Vertebrate NADP(H)-dependent Alcohol Dehydrogenase (ADH8)

Albert Rosell[1]†, Eva Valencia[2]†, Xavier Parés[1], Ignacio Fita[2] Jaume Farrés[1] and Wendy F. Ochoa[2]*

[1]*Departament de Bioquímica i Biologia Molecular, Universitat Autònoma de Barcelona, 08193 Bellaterra, Barcelona, Spain*

[2]*IBMB-CSIC, Jordi-Girona 18-26, 08034 Barcelona, Spain*

**Corresponding author*

The amphibian enzyme ADH8, previously named class IV-like, is the only known vertebrate alcohol dehydrogenase (ADH) with specificity towards NADP(H). The three-dimensional structures of ADH8 and of the binary complex ADH8–$NADP^+$ have been now determined and refined to resolutions of 2.2 Å and 1.8 Å, respectively. The coenzyme and substrate specificity of ADH8, that has 50–65% sequence identity with vertebrate NAD(H)-dependent ADHs, suggest a role in aldehyde reduction probably as a retinal reductase. The large volume of the substrate-binding pocket can explain both the high catalytic efficiency of ADH8 with retinoids and the high K_m value for ethanol. Preference of NADP(H) appears to be achieved by the presence in ADH8 of the triad Gly223-Thr224-His225 and the recruitment of conserved Lys228, which define a binding pocket for the terminal phosphate group of the cofactor. NADP(H) binds to ADH8 in an extended conformation that superimposes well with the NAD(H) molecules found in NAD(H)-dependent ADH complexes. No additional reshaping of the dinucleotide-binding site is observed which explains why NAD(H) can also be used as a cofactor by ADH8. The structural features support the classification of ADH8 as an independent ADH class.

Keywords: amphibian ADH; crystal structure; alcohol dehydrogenases; NAD(H); NADP(H)

Introduction

Medium-chain alcohol dehydrogenases (ADH) constitute in vertebrates a complex enzymatic system composed of at least seven NAD(H)-dependent classes: ADH1–ADH7.[1,2] Recently, an ADH was described in the amphibian *Rana perezi* with a distinct NADP(H) specificity ($k_{cat}/K^+_{mNADP} = 5900$ $mM^{-1}\,min^{-1}$ *versus* $k_{cat}/K^+_{mNAD} = 200$ $mM^{-1}\,min^{-1}$.[3] This enzyme, that displays about 60% sequence identity with NAD(H)-dependent ADHs of known structures, was tentatively designed as an ADH4-like form. However, the unique cofactor dependence, for a member of the animal and plant ADH family, together with its position in the phylogenetic trees raised the possibility that the enzyme represented a new ADH class which was then named class VIII or ADH8.[3,4] This nomenclature is used in the present work.

The finding, in vertebrates, of an ADH with NADP(H) dependence opens a number of questions regarding particularly to the specific role of the enzyme, the structural and evolutionary relationships with the other, all NAD(H)-dependent, vertebrate ADHs and to the reasons for its unique detection in amphibians. ADH8, similarly to other NADP(H)-dependent enzymes, is expected to participate in the reductive metabolism mainly because of the low $NADP^+$/NADPH concentration ratio in frog tissues,[5] but also because aldehydes are much better substrates than the corresponding alcohols for this enzyme.[3] ADH8 could also have a significant role in the retinal metabolism, since all physiological retinals assayed were excellent substrates for the enzyme.[3] In particular, the catalytic efficiency for all-*trans*-retinal ($33.8\ \mu M^{-1}\,min^{-1}$) is the highest ever reported for an ADH from vertebrates.[4] Thus, it has been proposed[3] that ADH8 could act as retinaldehyde dehydrogenase, converting retinal, the major

† These two authors contributed equally to this work.
Abbreviations used: ADH, alcohol dehydrogenase.
E-mail address of the corresponding author: wendy@scripps.edu

0022-2836/03/$ - see front matter

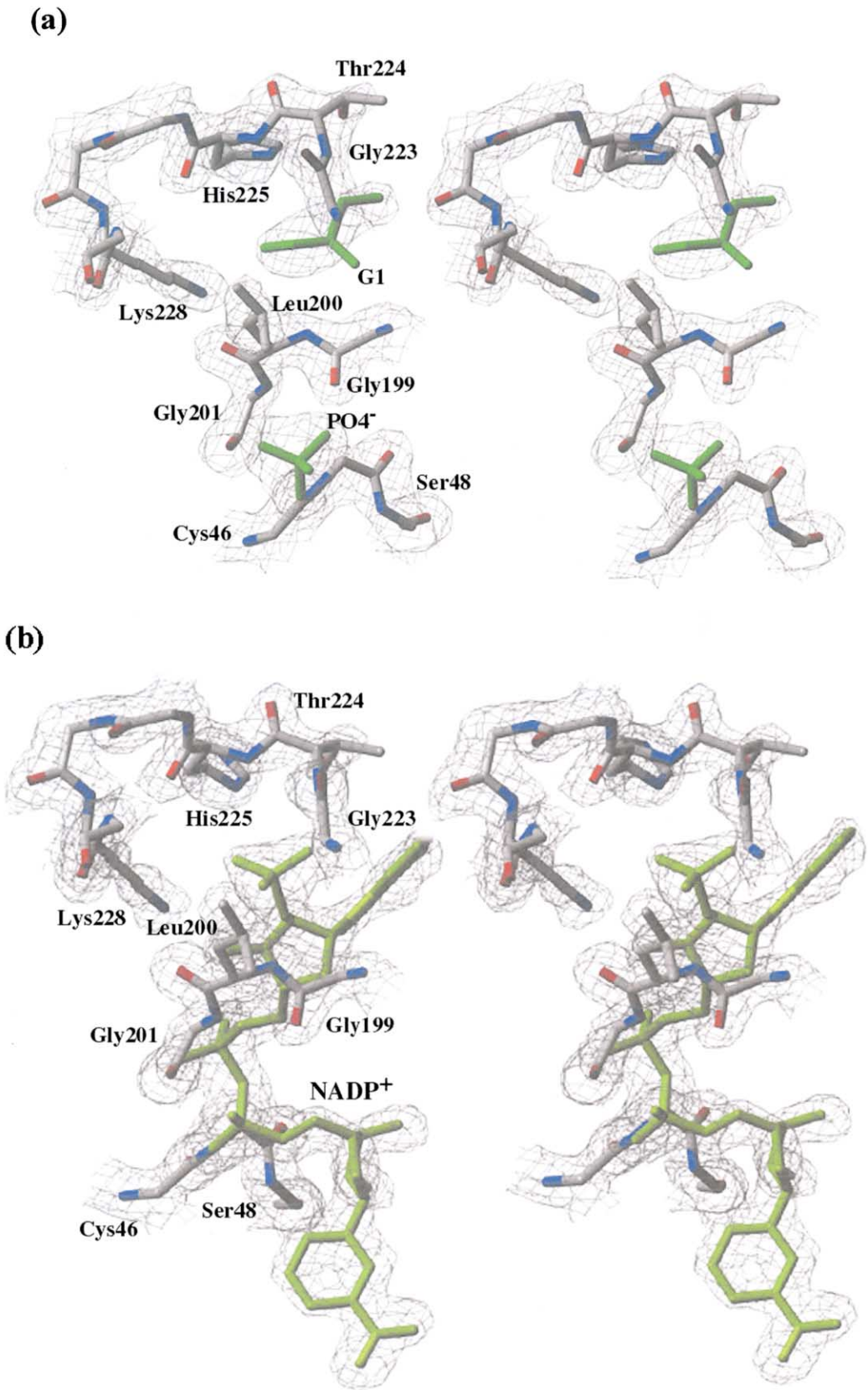

Figure 1. Stereo views of the cofactor-binding pocket in the crystal structures of the (a) *apo*-ADH8 and of the (b) ADH8–$NADP^+$ complex. Molecular models are represented by solid sticks with protein atoms colored according to their atom type. Bound phosphate and glycerol molecules, in the *apo*-ADH8 structure, and the $NADP^+$ molecule, in the ADH8–$NADP^+$ structure, are displayed in green. Electron densities, corresponding to the final $2F_o - F_c$ maps, are also shown, at 1σ level, with a chicken box representation.

retinoid form in amphibian egg and embryo, to retinol that, when esterified, represents the major retinoid form in adults.[6,7]

Within the animal and plant ADH family, only three-dimensional structures for NAD(H)-dependent enzymes were available.[8–13] Each ADH subunit contains a catalytic and a coenzyme-binding domains. The coenzyme-binding domain is composed of a six-stranded parallel β-pleated sheet, similar to those found in other NAD(H)-dependent dehydrogenases.[14] It has been proposed that the active-site cleft closes upon coenzyme binding by a rigid body rotation of the catalytic domain towards the coenzyme-binding domain.[15,16] In fact, the structure of horse *apo*-ADH1 presents an open conformation,[17] while binary or ternary complexes from horse and human ADH1 forms[8,18,19] and from human ADH4[13] exhibit a closed conformation. However, binary or ternary complexes from cod ADH1,[9] mouse ADH2[10] and human ADH3[11] show structures that were defined as semi-open conformations. Structural rearrangements upon dinucleotide binding conform a hydrophobic substrate-binding pocket where the substrate can achieve direct coordination with the catalytic zinc ion by displacing water molecules. The zinc-bound substrate allows the direct hydride transfer to the C4 atom of the nicotinamide ring,[20] while it has been suggested that the hydroxyl proton from the substrate is eliminated *via* a proton-relay pathway which connects the active site with the bulk solvent. The release of cofactor, often the catalytic rate-limiting step, will complete the cycle returning the enzyme to the initial conformation.

The crystal structure of the *apo*-form of ADH8 and of the binary complex with $NADP^+$ have now been determined and refined at resolutions of 2.2 Å and 1.8 Å, respectively. These are the first three-dimensional structures for an NADP(H)-dependent member of the animal and plant ADH family. Results define the molecular architecture of ADH8 providing a framework to explain the cofactor and the substrate preferences of this amphibian enzyme and giving support to its classification as a new ADH class. Structural relationships of ADH8 with NAD(H)-dependent ADHs and with microbial NADP(H)-dependent ADHs are also analyzed.

Results and Discussion

Overall structure

The crystal structure of the *apo* form of ADH8 was solved by molecular replacement using as a search model the coordinates from human ADH1B1.[21] The asymmetric unit of the crystal contained the two protein subunits that correspond to a molecular dimer. The quality of the final electron density maps allowed to position with confidence most residue side-chains (Figure 1(a)). The final molecular model comprises all the 372 amino acid residues, one phosphate group, one glycerol

Table 1. Data and model refinement statistics

	apo-ADH8	ADH8–$NADP^+$
Space group	*C*2	*C*2
Cell parameters (Å; deg.)	$a = 122.7$, $b = 78.8$, $c = 91.6$, $\beta = 112.9$	$a = 122.2$, $b = 79.5$, $c = 91.8$, $\beta = 112.8$
Resolution range (Å)[a]	2.2 (2.1)	1.8 (1.9)
Number of reflections		
Total	150,436	254,342
Unique	79,197	140,960
R_{sym} (%)[b]	11.3 (44.7)	4.8 (33.1)
Completeness (%)	98.4 (99)	96.1 (74)
Average $I/\sigma(I)$	11.8 (2.6)	14.4 (2.0)
R_{work} (%)[c]	20.1	19.9
R_{free}(%)[d]	24.0	22.3
Number of protein residues	2372	2372
Number of water molecules	317	400
Average thermal factor (Å^2)		
Protein	27.6	24.6
Water	32.6	31.6
Zn	35.4[e]	25.4
$NADP^+$	–	31.5
Glycerol	65.7	43.9
$PO4^-$	26.8	–
Geometry deviation		
rmsd bonds (Å)	0.005	0.004
rmsd angles (deg.)	1.31	1.23

[a] Values in parentheses are data for the highest resolution shell.
[b] $R_{sym} = \sum_{hkl} \sum_i |I_{hkl,i} - \langle I_{hkl}\rangle| / \sum_{hkl} \sum_i I_{hkl,i}$, where $I_{hkl,i}$ is the observed intensity and $-\langle I_{hkl}\rangle$ is the average intensity of multiple observations of symmetry-related reflections.
[c] $R_{work} = \sum_{hkl} ||F_o| - |F_c|| / \sum_{hkl} |F_o|$, where F_o and F_c are the observed and calculated structure factors, respectively.
[d] R_{free} same definition as R_{work} for a cross-validation set of about 5% of the reflections.
[e] Occupancy of the catalytic zinc ions was 50% in the two crystallographically independent subunits.

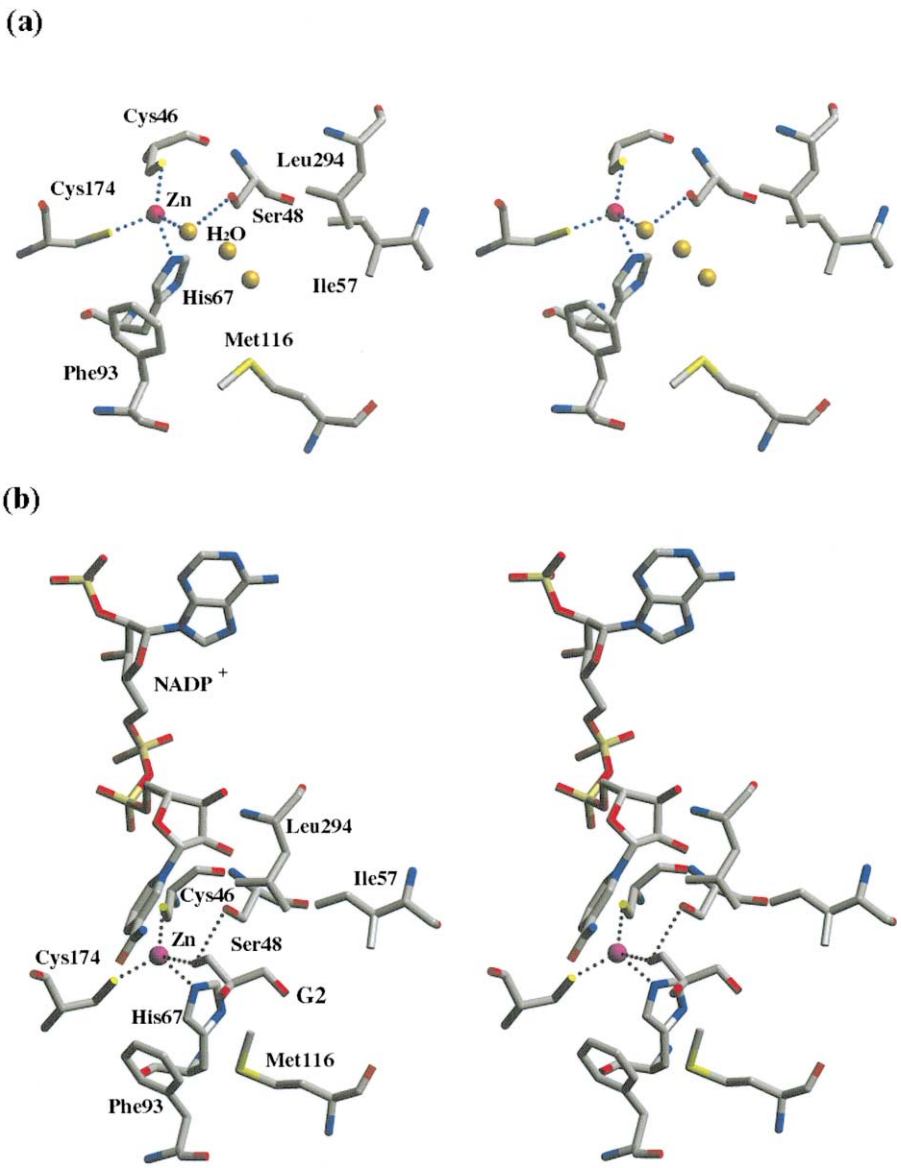

Figure 2. Stereo views of the inner part of the active site in the structures of (a) *apo*-ADH8 and (b) ADH7–$NADP^+$. Coordination of the catalytic zinc ion, depicted as a pink sphere, is indicated with dashed lines. Water molecules, seen in the *apo*-ADH8 structure, are represented as yellow spheres. The $NADP^+$ cofactor and a glycerol molecule (labeled G2) found in the ADH8–$NADP^+$ structure are also shown.

molecule and two zinc ions per protein subunit (Table 1). Occupancy of the zinc ion in the active site was refined to 50% in the two subunits. The model, that also includes 317 water molecules, presents overall crystallographic agreement factors R_{work} and R_{free} of 20.1% and 24.0%, respectively, for data to 2.2-Å resolution (Table 1).

The structure of the binary complex with $NADP^+$ has also been determined from crystals, obtained by co-crystallization of the enzyme with $NADP^+$, that were isomorphous to the *apo* form crystals (Table 1). Positions of the two protein subunits in the asymmetric unit of the crystal of the complex were refined with a rigid body search starting with the coordinates from the structure of the *apo*-enzyme. Iterative positional and isotropic temperature factor refinement of individual atoms resulted in a molecular model with overall crystallographic agreement factors R_{work} and R_{free} of 19.9% and 22.3%, respectively, for data to 1.8-Å resolution (Table 1). The final electron density map was clear for most residue side chains and for the $NADP^+$ cofactor (Figure 1(b)). The final molecular model comprises the two protein subunits and 400 well-ordered water molecules. Each of the protein subunits contains all the 372 residues, one $NADP^+$ coenzyme, one glycerol molecule and two zinc ions, both with full occupancy (Table 1). Attempts to obtain high resolution diffraction from crystals of ADH8–NADPH complexes, prepared either by co-crystallization or by soaking, were unsuccessful.

The relative positioning of the two domains is similar in the *apo* and the ADH8–$NADP^+$ structures, with r.m.s.d. values between the C^α atoms of the two structures of about 0.64 Å In the two

crystal structures the conformation of the ADH8 subunits is similar to the one defined as "closed" in the ternary complex of horse ADH.[16,22] In *apo*-ADH8 the "closed" conformation found might be due to the presence of a phosphate group (likely from the sodium phosphate buffer used during the purification) and of a glycerol molecule (from the cryo-buffer) mimicking in part a bound cofactor (Figure 1(a)). In any event, it seems that the binding of $NADP^+$ to ADH8 can be achieved with only small protein rearrangements.

The catalytic zinc ion displays a tetrahedral coordination with residues Cys46, His67 and Cys174 (henceforth residue numbering will correspond to that of horse ADH1 with the Swiss Prot entry P00327). In the *apo*-ADH8 structure the

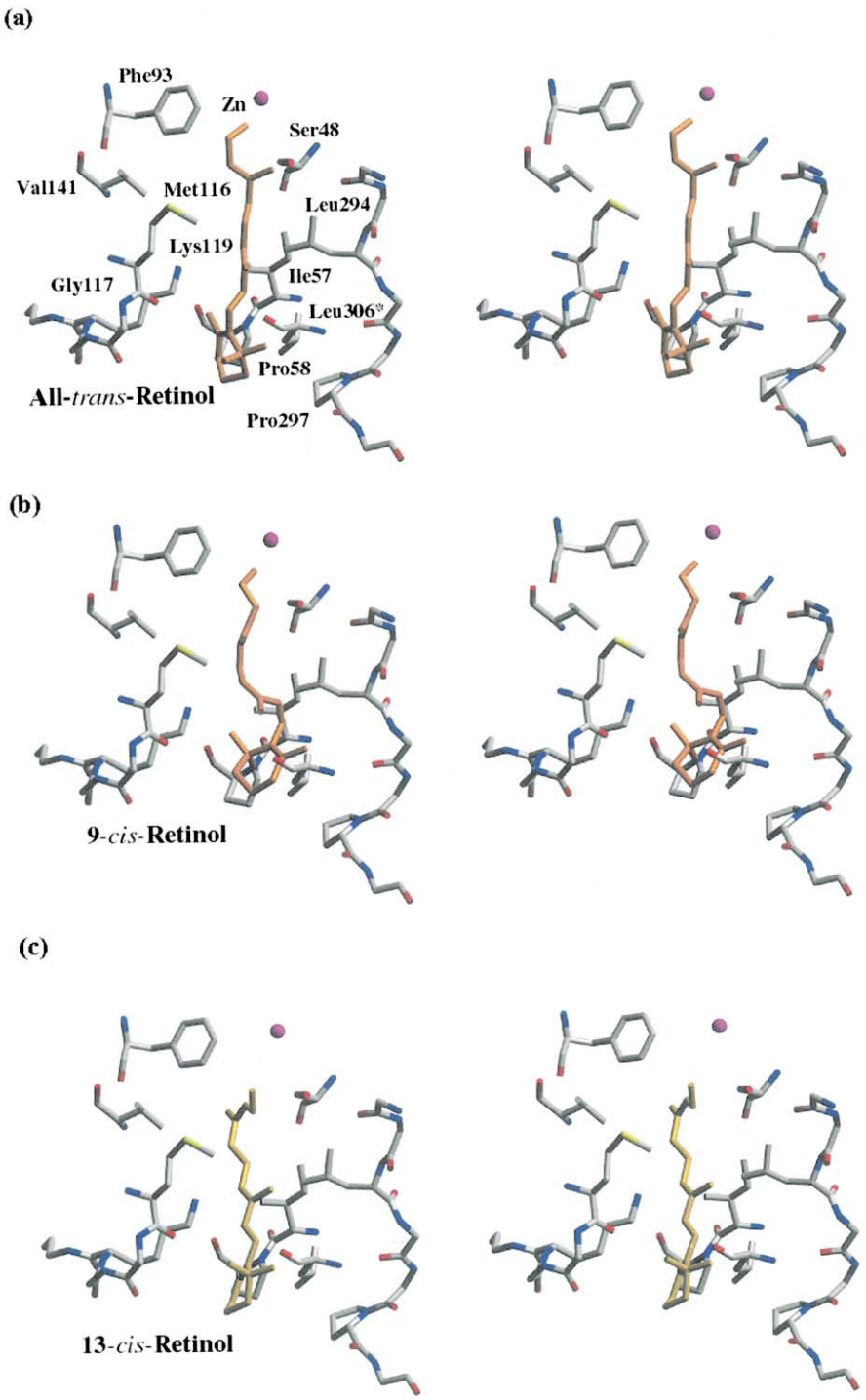

Figure 3. Stereo views of the (a) all-*trans*-retinol. (b) 9-*cis*-retinol and (c) 13-*cis*-retinol, modeled inside the ADH8 substrate-binding pocket. The nature and disposition of residues that conform the substrate-binding site allow the docking of these large, in some cases non-linear, substrates which had been experimentally observed (see in the text). Interaction of the substrate aliphatic chain with the protein is hydrophobic while the polar head approaches to the catalytic zinc ion.

fourth coordination position is occupied by a water molecule (Figure 2(a)), while in the ADH8–$NADP^+$ complex this fourth position corresponds to a density that was interpreted as a glycerol molecule (Figure 2(b)). The low occupancy of the catalytic zinc ion only in the *apo* ADH8 structure suggests that the absence of a bound cofactor could facilitate the loss of the catalytic zinc ion.

The substrate-binding site

In the ADH8–$NADP^+$ complex the glycerol molecule is located at the appropriate distance of the catalytic zinc ion for productive catalysis to occur (Figure 2(b)). In fact, the enzyme was found to be slightly active with glycerol as a substrate (data not shown), but saturation could not be achieved using concentrations up to 4 M. Comparisons of the substrate-binding site of ADH8 with those of human ADH1B1 and ADH4 indicate that the main difference corresponds to the loop 114–121 which, despite having residue Gly117 as in ADH1B1, leaves a cavity volume even larger than in ADH4, where a sequence gap is found at position 117. The change from Phe140, present in ADH1B1 and ADH4, to a leucine together with the presence of a serine at position 48 appears to explain the comparatively large-binding pocket of ADH8. A direct relationship between the size of the substrate-binding site and the K_m values has been demonstrated in ADH enzymes for ethanol and short-chain aliphatic substrates[13,23–25] and can also explain the high K_m (600 mM) of ADH8 for ethanol.

ADH8 displays very good catalytic efficiency with medium- or long-chain substrates, such as hexanal, *trans*-2-hexenal, and several retinoid isomers, with higher values for the retinals than for the corresponding retinols.[3] The catalytic efficiency for all-*trans*-retinal (33.8 $\mu M^{-1}\,min^{-1}$) is the highest reported for vertebrate ADHs with any retinoid.[4] Most ADHs are active with all-*trans*-retinal and 9-*cis*-retinal, but display very low activity with 13-*cis*-retinal ($k_{cat}/K_m < 0.5\ \mu M^{-1}\,min^{-1}$;[26] Martras *et al*., unpublished results). In contrast, 13-*cis*-retinal is a much better substrate for ADH8 ($k_{cat}/K_m = 4.2\ \mu M^{-1}\,min^{-1}$). Different retinol isomers were modeled into the substrate-binding site of the ADH8 structure (Figure 3). The model with all-*trans*-retinol shows hydrophobic interactions between the aliphatic chain of the retinoid and residues in the middle part of the binding site: Ile57, Pro58, Leu294, and Pro297, and Leu306 from the second subunit (Figure 3(a)). From the modeling is also clear that the ADH8-binding site is large enough to accommodate a 9-*cis*-retinol molecule (Figure 3(b)). In this model the terminal ionone ring of the retinoid is positioned away from proline residues 58 and 297 interacting instead with Leu306 from the other subunit. Docking of 13-*cis*-retinol into ADH8 presents new hydrophobic interactions, in particular with Met141 (Figure 3(c)), and appears to require some of the space inside the substrate-binding site pocket that is occupied by Phe140 in both ADH1B1 and ADH4.

The proton-relay system

In ADH enzymes catalysis occurs in a closed molecular conformation where the reaction is not in direct contact with the bulk solvent.[8,13,18,19] The existence of proton-relay pathways would facilitate the transfer of the substrate hydroxyl proton to the bulk solvent. A hydrogen-bonding network consisting of the hydroxyl group of residue 48 (Ser/Thr), the 2′-hydroxyl of the nicotinamide ribose from NAD(H) and, acting as a general base catalyst, the imidazole of either His47 or His51, was proposed to develop this function in several ADHs.[16,27,28] However, ADH8 does not have histidine at either of these positions but Gly47 and Ser51.[3] Other enzymes, such as rodent ADH2, rabbit ADH2B, human ADH5 and rodent ADH6, also lack histidines in positions 47 and 51.[10,29–31] In the ADH8–$NADP^+$ complex, glycerol interacts with the hydroxyl group of Ser48, which in turn connects with the 2′-hydroxyl of the nicotinamide ribose. in $NADP^+$. However, the distance between this group and the hydroxyl of Ser51 is too large to allow efficient proton transfer. Interestingly, in ADH8, a water molecule bridges the gap between the coenzyme and Ser51, which would facilitate the connection of the active site with the solvent. A similar proton relay pathway has been proposed for mouse ADH2, where an asparagine residue is found at position 51.[10]

The $NADP^+$ structure and binding interactions

In the crystal of the ADH8–$NADP^+$ complex, a well defined electron density, corresponding to a $NADP^+$ molecule, was located between the catalytic and the coenzyme-binding domains in the two crystallographically independent protein subunits (Figures 1(b)). The $NADP^+$ shows an extended conformation, with both ribose moieties presenting C2′-*endo* sugar ring puckering, as also found in the NAD(H) molecules of NAD(H)-dependent ADH complexes.[13,21] The $NADP^+$ molecule shows significant conformational deviations with respect to the NAD(H) molecules found in ADH–NAD^+ complexes only for the adenosine moiety.

NAD(H)-dependent enzymes often have a conserved negatively-charged residue at the C-terminal end of the second β-strand,[32] which is Asp223 in NAD(H)-dependent medium-chain ADHs.[27] In contrast, proteins with preference for NADP(H) have a neutral residue at this position,[33] in particular a glycine in ADH8. Asp223 side-chain forms hydrogen bonds with the 2′- and 3′-hydroxyl groups of the adenosine ribose from the NAD(H) coenzyme. Since the Asp223 side-chain would sterically and electrostatically interfere with the 2′-phosphate group,[34] the sequence exchange Asp223Gly had been suggested to be the

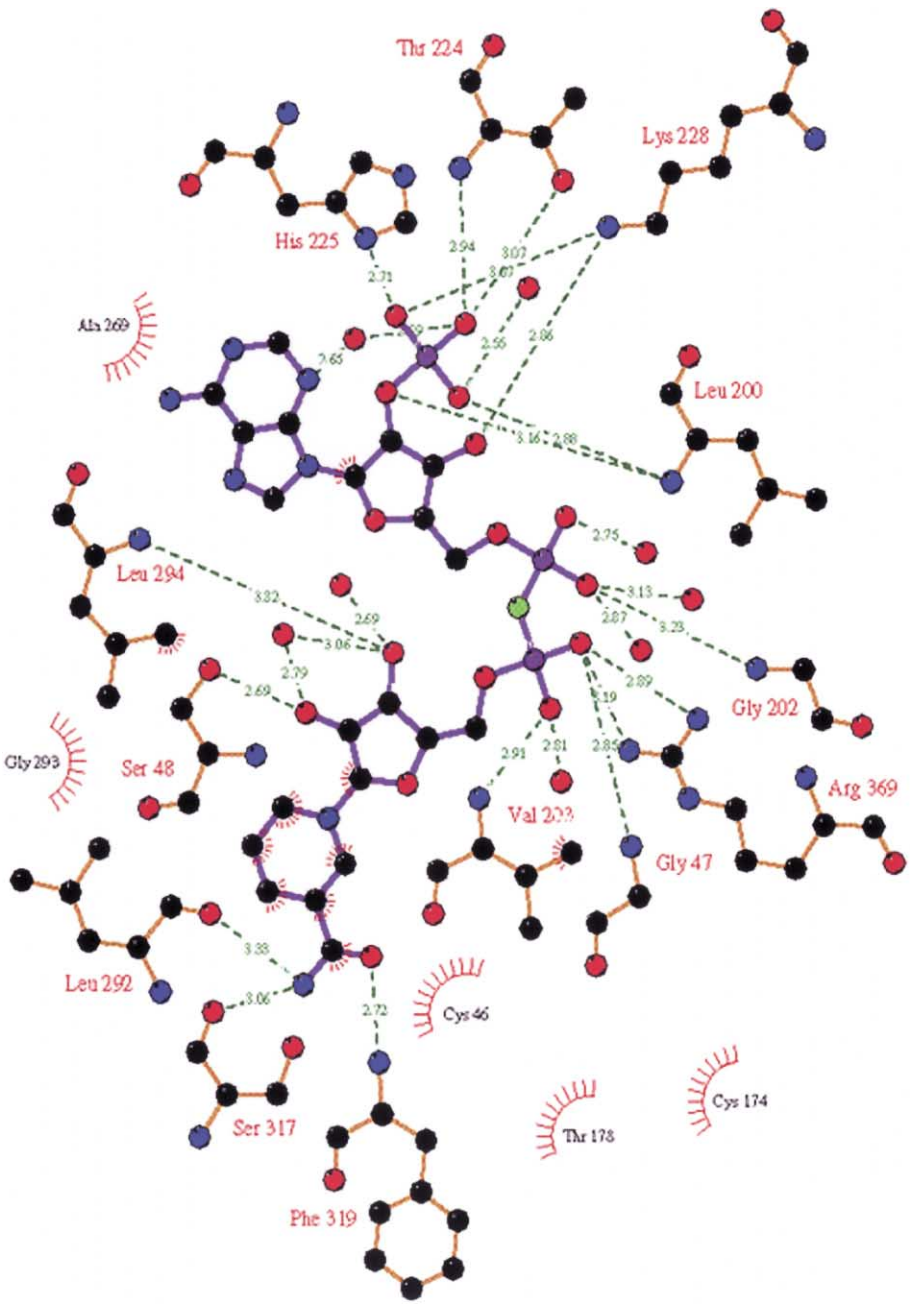

Figure 4. LIGPLOT[49] describing interactions of the $NADP^+$ molecule found in the structure of the ADH8–$NADP^+$ complex. Only side-chains of residues Thr224, His225 and Lys228 interact with the terminal phosphate group of the $NADP^+$ cofactor. Thr224 and His225 are sequence variations specific of ADH8 while Lys228 is conserved among NAD(H)-dependent ADHs (see in the text).

main reason of the coenzyme specificity in ADH8.[3] However, in the structure of the ADH8–$NADP^+$ complex, not only Gly223 but also Thr224, His225 together with Leu200 and Lys228, two highly conserved residues in NAD(H)-dependent ADHs, participate in the pocket for the $NADP^+$ extra phosphate group (Figures 4 and 5). Both the oxygen side chain and the nitrogen main chain of Thr224 are making hydrogen bonds with one of the oxygen atoms from the terminal phosphate group (Figure 4). A second oxygen atom from the terminal phosphate group is hydrogen bonded with the N^{δ} atom from His225 and with the side chain of Lys228, which in turn makes a second hydrogen bond, conserved in NAD(H)-dependent ADHs, with the hydroxyl group from the adenosine ribose. A third oxygen from the terminal phosphate group interacts with the nitrogen main chain atom of Leu200 and with a solvent molecule (Figure 4). Adenine atom N3 binds a water molecule which in turn interacts with the terminal phosphate group. Thr224 and His225 represent interesting residue changes with respect to the conserved Ile/Leu224 and Asn225 in NAD(H)-dependent ADHs, resulting in a more polar, favorable, environment for phosphate binding. It

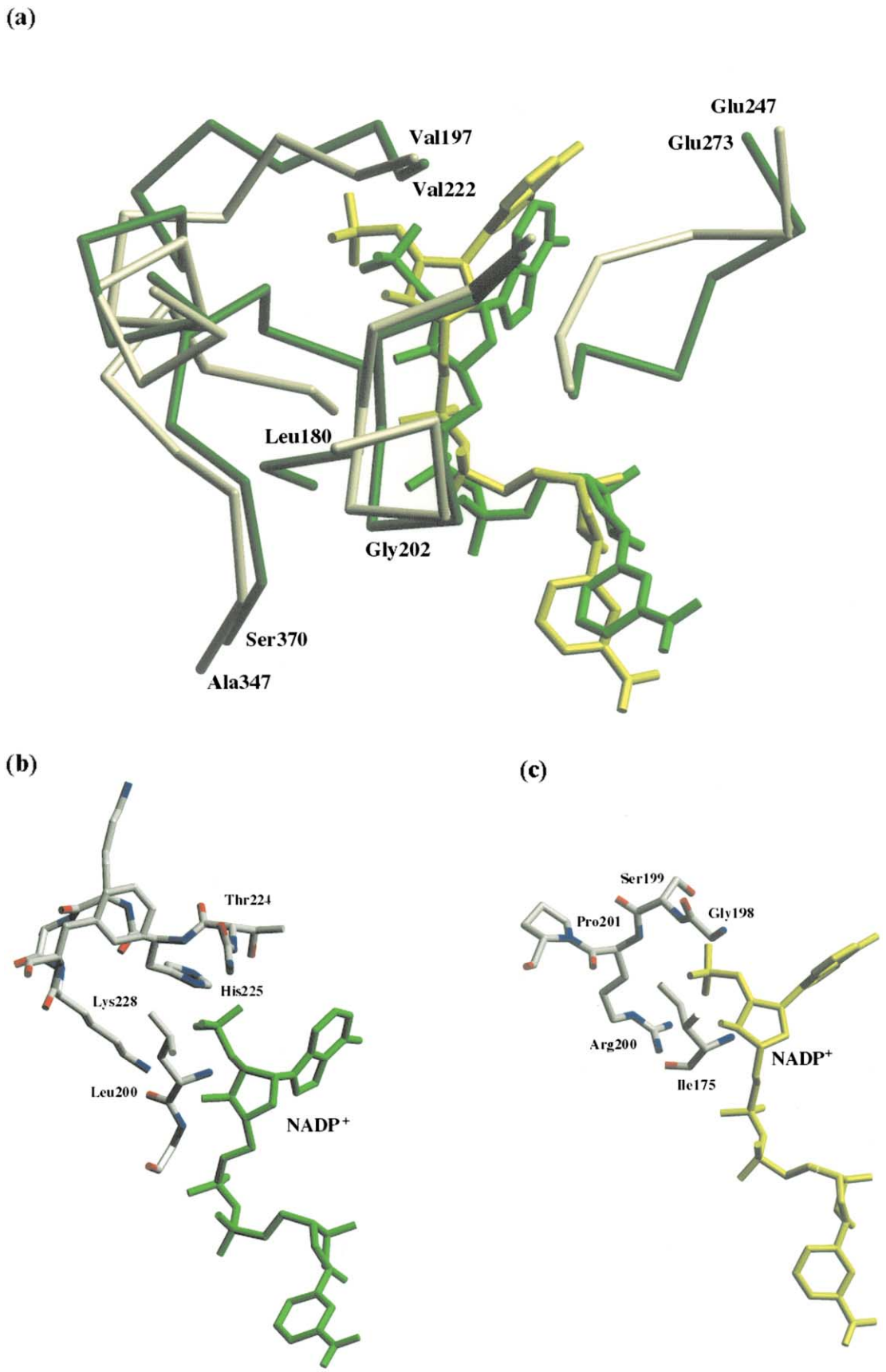

Figure 5. (a) Superimposition of ADH8 with the prokaryotic NADP(H)-dependent ADH from *Clostridium beijerinckii* (PDB entry 1KEV), in the vicinity of the NADP(H)-binding pocket. Protein main-chain tracings are represented as colored rods (green for ADH8). The corresponding NADP(H) molecules are also displayed with a stick representation. Terminal phosphate environment in the NADP(H)-binding pockets of ADH8 (b) and of the bacterial NADP(H)-dependent ADH from *Clostridium beijerinckii* (c). Differences in the NADP(H) conformation and in their interactions with the protein show two alternative ways to achieve NADP(H) specificity in ADHs (see in the text).

has been suggested that the presence of one or two basic residues interacting with the extra phosphate group is important for NADP(H) specificity.[35] Remarkably, in ADH8 the basic residue interacting with the terminal phosphate is Lys228 which, as indicated before, is a highly conserved residue among NAD(H)-dependent ADHs. Therefore, a few residue changes (Asp223Gly, Ile224Thr and Asn225His) and recruitment of conserved residues (in particular Lys228) allow the ADH molecular architecture to adapt, in a unique way, to the different coenzyme requirements. This type of adaptation imposes only minimal conformational rearrangements between ADH cofactors NAD(H) and $NADP^+$ which, in turn, explains why ADH8 still binds NAD(H).

In the structures of NAD(H)-dependent ADHs, adenine is sandwiched by hydrophobic interactions mainly with the highly conserved residues Ile224 and Ile269.[13,21,26,36] In ADH8 the corresponding residues Thr224 and Ala269 cannot provide such strong interactions with the adenine (Figure 4). Weakening the protein–coenzyme binding might facilitate the release of coenzyme which would explain the higher k_{cat} values of ADH8,[3] similarly to what has been reported for yeast and mutated horse ADHs.[37–39]

In the crystal of *apo*-ADH8 some extra electron density, found at the location corresponding to the pyrophosphate moiety in the cofactor-binding site, was interpreted as a phosphate group (Figure 1(a)). This phosphate interacts with Gly47, Gly202, Val203 and Arg369, which are the same residues that interact with the pyrophosphate of the cofactor in the ADH–$NADP^+$ complex (Figure 4). Extra electron density, interpreted as a glycerol molecule, was also found at the location corresponding to the terminal phosphate group. This glycerol molecule interacts with Gly223, Thr224, His225 and Lys228. The simultaneous presence of a glycerol and a phosphate group in the structure of *apo*-ADH8 suggests that the affinity for phosphate is lower in the pocket of the terminal phosphate group than in the site corresponding to the pyrophosphate. It is also interesting to notice that interactions stabilizing the glycerol found in the terminal phosphate pocket correspond to those of a primary alcohol. Therefore, competition between the terminal phosphate of the NADP(H) cofactor and alcohols may offer some subtle enzyme regulation. However, ADH8 activity assays in the presence of glycerol (0–500 mM) at various cofactor concentrations did not show any significant inhibition.

NADP(H)-dependent ADHs from microorganisms, *Thermoanaerobacter ethanolicus*,[40] *Thermoanaerobacter brockii*, *Clostridium beijerinckii*,[41] and *Entamoeba histolytica*,[42] also have a glycine, a hydrophilic and a basic residues at positions 223, 224 and 225, respectively (Figure 5). However, despite these similarities the $NADP^+$-binding pocket in ADH8 shows important differences with respect to the ones known from the prokaryotic NADP(H)-dependent ADHs of *C. beijerinckii* and *T. brockii* (PDB entries 1KEV and 1BXZ, respectively).[41] Some of the largest differences are located in the loops surrounding the cofactor-binding pocket which reflects that different strategies have been followed by members of the medium-chain-dehydrogenase/reductase superfamily to achieve specific recognition for the NADP(H) cofactor (Figure 5).

Conclusions

When ADH8 was initially characterized it was classified as a class IV-like enzyme because of its general substrate specificity and gastric localization, similar to those of mammalian class IV. However, the possibility that the enzyme constituted a new class (class VIII or ADH8) was also considered mainly due to its distinct cofactor specificity and primary-structure features.[3] Several structural properties, now determined, appear consistent with the notion of a separate ADH class, in particular: (i) the large active site pocket, (ii) the likely different proton-relay pathway, (iii) the very specific rearrangements in the cofactor phosphate-binding site, and (iv) the weak interactions of the adenine moiety. Nevertheless, the ADH8 nomenclature should be further validated by additional research on the ADH lines from lower vertebrates.

The two ADH8 structures now available, besides explaining the cofactor specificity, allow rationalizing the distinct kinetic features of this enzyme such as the high k_{cat} and K_m values for ethanol, and the high catalytic efficiency with retinals that results in one of the most efficient retinal reductases known so far. Subtle but concerted changes, in a very narrow region of the primary sequence, seem to allow the versatility for the cofactor used by ADHs. In view of these unique features kinetic and mutational studies are underway, particularly for the ADH8 residues participating in the coenzyme specificity.

Material and Methods

Protein purification and crystallization

Samples of recombinantly expressed and purified *R. perezi* ADH8 were used in crystallization screenings with the hanging-drop vapor-diffusion method, as reported previously.[43] Attempts to prepare binary complexes of ADH8 with $NADP^+$ and NADPH either by soaking or by co-crystallization resulted in high resolution diffracting crystals only for $NADP^+$ complexes.

Data collection and structure determination

Diffraction data sets from both the *apo*-ADH8 and the ADH8–$NADP^+$ crystals were collected at 100 K from a single crystal each, on a MarCCD detector using synchrotron radiation at the ESRF (Grenoble) beam line ID14.4. Images were evaluated and scaled internally

with programs DENZO and SCALEPACK,[44] respectively (Table 1). Crystals of the *apo*-ADH8 and ADH8–$NADP^+$ were isomorphous, space group *C*2, and contained two subunits per asymmetric unit with a solvent content of about 50%. Completeness of the two data set sets were 99% and 98%, with internal agreement factors (R_{sym}) of 7.6% and 5.0% at 2-Å and 1.8-Å resolution, respectively.

Molecular replacement calculations, using the program AMoRe[45] and the human ADH1B1 structure as a searching model, resulted in a clean initial solution with a correlation coefficient of 0.7 and an *R*-factor of 35% in the resolution shell from 3.5 Å to 20 Å. Refinement was done following standard protocols using iteratively the program CNS[46] with the amplitude-based maximum likelihood target function and alternating with manual rebuilding in the interactive graphics program O.[47] Bulk solvent correction and restrained, isotropic individual *B*-factor were used in the final rounds of refinement and model building. The refinement coordinates of the *apo*-ADH8 crystal were then used to start the determination of the ADH8–$NADP^+$ complex.

The stereochemistry of the structures determined were analyzed with the program PROCHECK.[48] Of the non-Gly residues 85% fall within the most favored region of the Ramachandran plot and the rest are inside the additional allowed regions. Structural comparisons were performed with the program SHP (D. Stuart, unpublished results).

Coordinates of both structures are deposited in the Protein Data Bank with ID codes 1POC and 1POF.

Enzyme activity assays

Alcohol dehydrogenase activity was determined at 25 °C by monitoring the change in absorbance at 340 nm, with a Cary 400 Bio (Varian) spectrophotometer. Glycerol oxidation was performed in 0.1 M glycine/NaOH, pH 10.0, using 1.2 mM $NADP^+$ as a coenzyme. Inhibition assays were carried out in 0.1 M glycine/NaOH, pH 10.0 using 1 M ethanol as a substrate, $NADP^+$ as a coenzyme and from 0 M to 0.5 M glycerol as an inhibitor. Each individual rate measurement was run in duplicate.

References

1. Duester, G., Farrés, J., Felder, M. R., Holmes, R. S., Höög, J. O., Parés, X. *et al.* (1999). Recommended nomenclature for the vertebrate alcohol dehydrogenase gene family. *Biochem. Pharmacol.* **58**, 389–395.
2. Nordling, E., Persson, B. & Jörnvall, H. (2002). Differential multiplicity of MDR alcohol dehydrogenases: enzyme genes in the human genome *versus* those in organisms initially studied. *Cell. Mol. Life Sci.* **59**, 1070–1075.
3. Peralba, J. M., Cederlund, E., Crosas, B., Moreno, A., Julià, P., Martínez, S. E. *et al.* (1999). Structural and enzymatic properties of a gastric NADP(H)-dependent and retinal-active alcohol dehydrogenase. *J. Biol. Chem.* **274**, 26021–26026.
4. Duester, G. (2000). Families of retinoid dehydrogenases regulating vitamin A function. Production of visual pigment and retinoic acid. *Eur. J.Biochem.* **267**, 4315–4324.
5. Bannister, W. H. (1967). The oxidation–reduction state of pyridine nucleotide in isolated frog gastric mucosa. *Experientia (Basel)*, **23**, 715–716.
6. Scadding, S. R. & Maden, M. (1994). Retinoic acid gradients during limb regeneration. *Dev. Biol.* **162**, 608–617.
7. Costaridis, P., Horton, C., Zeitlinger, J., Holder, N. & Maden, M. (1996). Endogenous retinoids in the zebrafish embryo and adult. *Dev. Dynam.* **205**, 41–51.
8. Niederhut, M. S., Gibbons, B. J., Pérez-Miller, S. & Hurley, T. D. (2001). Three-dimensional structures of the three human class I alcohol dehydrogenases. *Protein Sci.* **10**, 697–706.
9. Ramaswamy, S., El-Ahmad, M., Danielsson, O., Jörnvall, H. & Eklund, H. (1996). Crystal structure of cod liver class I alcohol dehydrogenase: substrate pocket and structurally variable segments. *Protein Sci.* **5**, 663–671.
10. Svensson, S., Höög, J. O., Schneider, G. & Sandalova, T. (2000). Crystal structures of mouse class II alcohol dehydrogenase reveal determinants of substrate specificity and catalytic efficiency. *J. Mol. Biol.* **302**, 441–453.
11. Yang, Z. N., Bosron, W. F. & Hurley, T. D. (1997). Structure of human XX alcohol dehydrogenase: a glutathione-dependent formaldehyde dehydrogenase. *J. Mol. Biol.* **265**, 330–343.
12. Sanghani, P. C., Robinson, H., Bosron, W. F. & Hurley, T. D. (2002). Human glutathione-dependent formaldehyde dehydrogenase. Structures of apo, binary, and inhibitory ternary complexes. *Biochemistry*, **41**, 10778–10786.
13. Xie, P., Parsons, S. H., Speckhard, D. C., Bosron, W. F. & Hurley, T. D. (1997). X-ray structure of human class IV σσ alcohol dehydrogenase. Structural basis for substrate specificity. *J. Biol. Chem.* **272**, 18558–18563.
14. Rossmann, M. G., Moras, D. & Olsen, K. W. (1974). Chemical and biological evolution of a nucleotide-binding protein. *Nature*, **250**, 194–199.
15. Eklund, H. & Brändén, C. I. (1979). Structural differences between *apo*- and holoenzyme of horse liver alcohol dehydrogenase. *J. Biol. Chem.* **254**, 3458–3461.
16. Eklund, H., Samama, J. P., Wallén, L., Brändén, C. I., Åkeson, Å. & Jones, T. A. (1981). Structure of a horse triclinic ternary complex with liver alcohol dehydrogenase at 2.9 Å. *J. Mol. Biol.* **146**, 561–587.
17. Eklund, H., Nordström, B., Zeppezauer, E., Söderlund, G., Ohlsson, I., Boiwe, T. *et al.* (1976). Three-dimensional structure of horse liver alcohol dehydrogenase at 2.4 Å resolution. *J. Mol. Biol.* **102**, 27–59.
18. Hurley, T. D., Bosron, W. F., Stone, C. L. & Amzel, L. M. (1994). Structures of three human β alcohol dehydrogenase variants: correlations with their functional differences. *J. Mol. Biol.* **239**, 415–429.
19. Colonna-Cesari, F., Perahia, D., Karplus, M., Eklund, H., Brändén, C. I. & Tapia, O. (1986). Interdomain motion in liver alcohol dehydrogenase. Structure and energetic analysis of the hinge bending mode. *J. Biol. Chem.* **261**, 15273–15280.
20. Eklund, H. & Brändén, C. I. (1987). Alcohol dehydrogenase. In *Biological Macromolecules and Assemblies* (Jurnak, F. A. & McPherson, A., eds), pp. 73–142, Wiley, London.
21. Hurley, T. D., Bosron, W. F., Hamilton, J. A. & Amzel, L. M. (1991). Structure of human β1β1 alcohol dehydrogenase: catalytic effects of non-active-site substitutions. *Proc. Natl Acad. Sci. USA*, **88**, 8149–8153.
22. Al-Karadaghi, S., Cedergren-Zeppezauer, E. S., Petrantos, K., Hovmöller, S., Terry, H., Dauter, Z. & Wilson, K. S. (1994). Refined crystal structure of

liver alcohol dehydrogenase–NADH complex at 1.8 Åresolution. *Acta Crystallog. sect. D*, **50**, 793–807.
23. Farrés, J., Moreno, A., Crosas, B., Peralba, J. M., Allali-Hassani, A., Hjelmqvist, L. *et al.* (1994). Alcohol dehydrogenase of class IV (σσ-ADH) from human stomach. cDNA sequence and structure/function relationships. *Eur. J. Biochem.* **224**, 549–557.
24. Crosas, B., Allali-Hassani, A., Martínez, S. E., Martras, S., Persson, B., Jörnvall, H. *et al.* (2000). Molecular basis for differential substrate specificity in class IV alcohol dehydrogenases: a conserved function in retinoid metabolism but not in ethanol metabolism. *J. Biol. Chem.* **275**, 25180–25187.
25. Allali-Hassani, A., Crosas, B., Parés, X. & Farrés, J. (2001). Kinetic effects of a single-amino acid mutation in a highly variable loop (residues 114–120) of class IV ADH. *Chem. Biol. Interact.* **130–132**, 435–444.
26. Yang, Z. N., Davis, G. J., Hurley, T. D., Stone, C. L., Li, T. K. & Bosron, W. F. (1994). Catalytic efficiency of human alcohol dehydrogenase of retinol oxidation and retinal reduction. *Alcohol. Clin. Expt. Res.* **18**, 587–591.
27. Sun, H. W. & Plapp, B. V. (1992). Progresive sequence alignment and molecular evolution of the Zn-containing alcohol dehydrogenase family. *J. Mol. Evol.* **34**, 522–535.
28. Davis, G. J., Carr, L. G., Hurley, T. D., Li, T. K. & Bosron, W. F. (1994). Comparative roles of histidine 51 in human beta 1 beta 1 and threonine 51 in pi pi alcohol dehydrogenases. *Arch. Biochem. Biophys.* **311**, 307–312.
29. Yasunami, M., Chen, C. S. & Yoshida, A. (1991). A human alcohol dehydrogenase gene (ADH6) encoding an additional class of isozyme. *Proc. Natl Acad. Sci. USA*, **88**, 7610–7614.
30. Höög, J. O. & Brandt, M. (1995). Mammalian class VI alcohol dehydrogenase. Novel type of the rodent enzymes. In Enzymology and Molecular Biology of Carbonyl Metabolism (Weiner, H., Holmes, R. S. & Wermuth, B., eds), vol. 5, pp. 355–364, Plenum Press, New York.
31. Svensson, S., Hedberg, J. J. & Höög, J. O. (1998). Structural and functional divergence of class II alcohol dehydrogenase-cloning and characterization of rabbit liver isoforms of the enzyme. *Eur. J. Biochem.* **251**, 236–243.
32. Bellamacina, C. R. (1996). The nicotinamide dinucleotide binding motif: a comparison of nucleotide binding proteins. *FASEB J.* **10**, 1257–1269.
33. Wierenga, R. K., Terpstra, P. & Hol, W. G. J. (1986). Prediction of the occurrence of the ADP-binding beta alpha beta-fold in proteins, using an amino acid sequence fingerprint. *J. Mol. Biol.* **187**, 101–107.
34. Fan, F., Lorenzen, J. A. & Plapp, B. V. (1991). An aspartate residue in yeast alcohol dehydrogenase I determines the specificity for coenzyme. *Biochemistry*, **30**, 6397–6401.
35. Carugo, O. & Argos, P. (1997). NADP-dependent enzymes. I: conserved stereochemistry of cofactor binding. *Proteins: Struct. Funct. Genet.* **28**, 10–28.
36. Cho, H., Ramaswamy, S. & Plapp, B. V. (1997). Flexibility of liver alcohol dehydrogenase in stereoselective binding of 3-butylthiolane 1-oxides. *Biochemistry*, **36**, 382–389.
37. Fan, F. & Plapp, B. V. (1995). Substitutions of isoleucine residues at the adenine binding site activate horse liver alcohol dehydrogenase. *Biochemistry*, **34**, 4709–4713.
38. Fan, F. & Plapp, B. V. (1999). Probing the affinity and specificity of yeast alcohol dehydrogenase I for coenzymes. *Arch. Biochem. Biophys.* **367**, 240–249.
39. Fernández, M. R., Biosca, J. A., Torres, D., Crosas, B. & Parés, X. (1999). A double residue substitution in the coenzyme-binding site accounts for the different kinetic properties between yeast and human formaldehyde dehydrogenases. *J. Biol. Chem.* **274**, 37869–37875.
40. Burdette, D. S., Vieille, C. & Zeikus, J. G. (1996). Cloning and expression of the gene encoding the *Thermoanaerobacter ethanolicus* 39E secondary-alcohol dehydrogenase and biochemical characterization of the enzyme. *Biochem. J.* **316**, 115–122.
41. Korkhin, Y., Kalb, A. J., Peretz, M., Bogin, O., Burstein, Y. & Frolow, F. (1998). NADP-dependent bacterial alcohol dehydrogenases: crystal structure, cofactor-binding and cofactor specificity of the ADHs of *Clostridium beijerinckii* and *Thermoanaerobacter brockii*. *J. Mol. Biol.* **278**, 967–981.
42. Kumar, A., Shen, P. S., Descoteaux, S., Pohl, J., Bailey, G. & Samuelson, J. (1992). Cloning and expression of an $NADP^+$-dependent alcohol dehydrogenase gene of *Entamoeba histolytica*. *Proc. Natl Acad. Sci. USA*, **89**, 10188–10192.
43. Valencia, E., Rosell, A., Larroy, C., Farrés, J., Biosca, J. A., Fita, I. *et al.* (2003). Crystallization and preliminary X-ray analysis of NADP(H)-dependent alcohol dehydrogenases from *Saccharomyces cerevisiae* and *Ranaperezi*. *Acta Crystallog. sect. D*, **59**, 334–336.
44. Otwinowski, Z. (1993). Oscillation data reduction program. In *Proceedings of the CCP4 Study Weekend: Data Collection and Processing* (Sawyer, L., Isaacs, N. & Bailey, S., eds), pp. 56–62, SERC Daresbury Laboratory, England.
45. Navaza, J. (1994). AmoRe: an automated package for molecular replacement. *Acta Crystallog. sect. A*, **50**, 157–163.
46. Brünger, A. T., Adams, P. D., Clore, G. M., DeLano, W. L., Gros, P., Grosse-Kunstleve, R. W. *et al.* (1998). Crystallography & NMR system: a new software suite for macromolecular structure determination. *Acta Crystallog. sect. D*, **54**, 905–921.
47. Jones, T. A., Zou, J. Y., Cowan, S. & Kjeldgaard, M. (1991). Improved methods for building protein models in electron density maps and the location of errors in these models. *Acta Crystallog. sect. A*, **47**, 110–119.
48. Laskowski, R. A., MacArthur, M. W., Moss, D. S. & Thornton, J. M. (1993). PROCHECK: a program to check the stereochemical quality of protein structure. *J. Appl. Crystallog.* **26**, 283–291.
49. Wallace, A. C., Laskowski, R. A. & Thornton, J. M. (1995). LIGPLOT: a program to generate schematic diagrams of protein-ligand interactions. *Protein Eng.* **8**, 127–134.

Edited by R. Huber

(Received 24 September 2002; received in revised form 19 March 2003; accepted 19 March 2003)

ARTICLE III

THE JOURNAL OF BIOLOGICAL CHEMISTRY
Vol. 278, No. 42, Issue of October 17, pp. 40573–40580, 2003

Printed in U.S.A.

Complete Reversal of Coenzyme Specificity by Concerted Mutation of Three Consecutive Residues in Alcohol Dehydrogenase*

Received for publication, July 10, 2003, and in revised form, August 4, 2003
Published, JBC Papers in Press, August 4, 2003, DOI 10.1074/jbc.M307384200

Albert Rosell‡, Eva Valencia§, Wendy F. Ochoa§, Ignacio Fita§, Xavier Parés‡, and Jaume Farrés‡¶

From the ‡Department of Biochemistry and Molecular Biology, Universitat Autònoma de Barcelona, E-08193 Bellaterra (Barcelona), Spain and the §IBMB-Consejo Superior de Investigaciones Científicas, Jordi-Girona 18–26, E-08034 Barcelona, Spain

Gastric tissues from amphibian *Rana perezi* express the only vertebrate alcohol dehydrogenase (ADH8) that is specific for NADP(H) instead of NAD(H). In the crystallographic ADH8-NADP$^+$ complex, a binding pocket for the extra phosphate group of coenzyme is formed by ADH8-specific residues Gly^{223}-Thr^{224}-His^{225}, and the highly conserved Leu^{200} and Lys^{228}. To investigate the minimal structural determinants for coenzyme specificity, several ADH8 mutants involving residues 223 to 225 were engineered and kinetically characterized. Computer-assisted modeling of the docked coenzymes was also performed with the mutant enzymes and compared with the wild-type crystallographic binary complex. The G223D mutant, having a negative charge in the phosphate-binding site, still preferred NADP(H) over NAD(H), as did the T224I and H225N mutants. Catalytic efficiency with NADP(H) dropped dramatically in the double mutants, G223D/T224I and T224I/H225N, and in the triple mutant, G223D/T224I/H225N (k_{cat}/K_mNADPH = 760 mM^{-1} min^{-1}), as compared with the wild-type enzyme (k_{cat}/K_mNADPH = 133,330 mM^{-1} min^{-1}). This was associated with a lower binding affinity for NADP$^+$ and a change in the rate-limiting step. Conversely, in the triple mutant, catalytic efficiency with NAD(H) increased, reaching values (k_{cat}/K_mNADH = 155,000 mM^{-1} min^{-1}) similar to those of the wild-type enzyme with NADP(H). The complete reversal of ADH8 coenzyme specificity was therefore attained by the substitution of only three consecutive residues in the phosphate-binding site, an unprecedented achievement within the ADH family.

Coenzyme specificity is an important property of NAD(P)-dependent oxidoreductases that is linked to their metabolic function. Thus the type of coenzyme, NAD$^+$ or NADP$^+$, often distinguishes between enzymes involved in alternative pathways (*e.g.* oxidative *versus* reductive or degradative *versus* biosynthetic). Because NAD$^+$ and NADP$^+$ only differ structurally in the phosphate group esterified at the 2′ position of adenosine ribose, dehydrogenases must possess a limited number of residues to discriminate between the two coenzyme types. Moreover, among dehydrogenases from a given enzyme family, the same protein fold is often used to bind either coenzyme type and even some enzymes show dual activity, meaning that they can use both coenzymes with similar efficiency (1).

A rather unique NADP-dependent alcohol dehydrogenase (ADH8)[1] was discovered in the gastric tissues of amphibians (2). ADH8 belongs to the medium chain dehydrogenase/reductase (MDR) superfamily and is phylogenetically related to the NAD-dependent vertebrate ADH family. This enzyme is active with ethanol and functionally may participate in the reduction of retinal to retinol (k_{cat}/K_m all-*trans*-retinal = 33,750 mM^{-1} min^{-1}). Recently, the three-dimensional structure of the ADH8-NADP$^+$ binary complex was determined at 1.8-Å resolution (3). Structural data suggested that the preference for NADP(H) depends on the segment Gly^{223}-Thr^{224}-His^{225} (Asp^{223}-Ile/Leu^{224}-Asn^{225} in most vertebrate NAD-dependent ADHs; Ref. 4), which together with Leu^{200} and Lys^{228}, define a binding pocket for the terminal phosphate group of NADP(H). Henceforth residue numbering will correspond to that of horse ADH1 with the Swiss Prot entry P00327. Interestingly, NADP-dependent ADHs from distantly related microorganisms (5–7), also have a glycine and two more hydrophilic residues at the positions corresponding to 223, 224, and 225, respectively. In ADHs, residue 223 is located at the C-terminal end of the second β-strand of the Rossmann fold (8) and classically is considered as determinant for coenzyme specificity. The substitution D223G, as found in ADH8, would avoid the possible steric and electrostatic hindrances because of the extra phosphate group of NADP(H). In fact, different attempts to switch the coenzyme specificity in medium chain ADHs have been focused on mutations involving residue 223 (9–12). However, full reversal of coenzyme specificity, in terms of having a mutant enzyme as catalytically efficient as the wild type, has been rarely achieved. This implies that conversion of coenzyme specificity may require multiple substitutions in the coenzyme-binding domain. Other residues found in ADH8, such as Thr^{224} and His^{225}, which are making hydrogen bonds with the oxygen atoms from the terminal phosphate group (3), could also be important in defining coenzyme specificity of ADH8.

In the present work, we have investigated, by means of site-directed mutagenesis, steady-state kinetics, and computer modeling, the individual and combined contribution of the adjacent residues Gly^{223}-Thr^{224}-His^{225} of ADH8 to coenzyme specificity. Moreover, because the ADH8 sequence is only 30% deviant from the closest NAD-dependent ADH structure (*Rana perezi* ADH1, Ref. 13), it was a suitable candidate for attempting the redesign of coenzyme specificity.

* This work was supported by grants from the Dirección General de Investigación Científica: BMC2000-0132 (to J. F.), BMC2002-02659 (to X. P.), and BIO2002-04419-C02-01 (to I. F.). The costs of publication of this article were defrayed in part by the payment of page charges. This article must therefore be hereby marked "*advertisement*" in accordance with 18 U.S.C. Section 1734 solely to indicate this fact.

¶ To whom correspondence should be addressed: Dept. of Biochemistry and Molecular Biology, Universitat Autònoma de Barcelona, E-08193 Bellaterra (Barcelona), Spain. Tel.: 34-93-5812557; Fax: 34-93-5811264; E-mail: jaume.farres@uab.es.

[1] The abbreviations used are: ADH, alcohol dehydrogenase; K_{ia}, dissociation constant for coenzyme; K_a, K_m for coenzyme; K_b, K_m for ethanol; MDR, medium chain dehydrogenase/reductase.

TABLE I
Kinetic constants of wild-type and mutant ADH8 with NAD$^+$ and NADP$^+$ at pH 10.0
Activities were measured with 1 M ethanol and 0.1 M glycine/NaOH at pH 10.

Enzyme	Coenzyme	K_m	k_{cat}	k_{cat}/K_m
		mM	*min^{-1}*	*mM^{-1} min^{-1}*
Wild-type	NADP$^+$	0.050 ± 0.002	1,600 ± 80	32,000 ± 6,600
	NAD$^+$	0.50 ± 0.05	1,490 ± 60	2,980 ± 295
G223D	NADP$^+$	0.08 ± 0.01	600 ± 50	7,500 ± 1,100
	NAD$^+$	0.42 ± 0.06	1,550 ± 50	3,690 ± 530
T224I	NADP$^+$	0.20 ± 0.01	900 ± 170	4,500 ± 890
	NAD$^+$	0.44 ± 0.03	2,370 ± 10	5,390 ± 320
H225N	NADP$^+$	0.16 ± 0.01	1690 ± 76	10,560 ± 640
	NAD$^+$	1.7 ± 0.4	1,820 ± 280	1,050 ± 270
G223D/T224I	NADP$^+$	NS[a]	NS	9.0 ± 0.3[b]
	NAD$^+$	0.130 ± 0.002	1,227 ± 40	9,440 ± 360
T224I/H225N	NADP$^+$	1.37 ± 0.30	50 ± 3	36 ± 9
	NAD$^+$	0.20 ± 0.04	1,850 ± 70	9,250 ± 1,840
G223D/T224I/H225N	NADP$^+$	NS	NS	15 ± 2[b]
	NAD$^+$	0.020 ± 0.003	2,275 ± 70	113,750 ± 10,700

[a] NS, no saturation up to 4.8 and 9.6 mM NADP$^+$ for G223D/T224I and G223D/T224I/H225N, respectively.
[b] k_{cat}/K_m was calculated as the slope of the linear plot of *V versus* [S].

EXPERIMENTAL PROCEDURES

Site-directed Mutagenesis—G223D, T224I, H225N, G223D/T224I, and T224I/H225N mutants were obtained using the wild-type ADH8 cDNA cloned into pGEX 4T-2 as a template. The mutations were introduced by sequential steps of PCR. In a first round, two reactions, 1 and 2, were performed with the following primers: 1) RanaL primer, 5′-TTATAGGATCCATGTGCACTGCGGGAAAAGAT-3′, and one of the antisense primers containing the mutations (underlined): 223R, 5′-GTCTTTATGGGTATCAACCCCTATAATACG-3′; 224R, 5′-GTCTTTATGGATTCCAACCCCTATAATAC-3′; 225R, 5′-GTCTTTATTGGTTCCAACCCCTATAATACG-3′; 224/225R, 5′-GTCTTTATTGATTCCAACCCCTATAATAC-3′; 2) RanaR primer, 5′-CCACCTGAATTCTTAGTATATCATAATGCTTCG-3′ and one of the primers containing the sense mutations. In a final amplification step, purified overlapping PCR products were used as templates, using RanaL and RanaR primers. All reactions were performed in a DNA thermal cycler (MJ Research) with High Fidelity DNA polymerase (Roche Diagnostics) under the following conditions: hot start at 95 °C for 1 min, annealing at 55 °C for 1 min, extension at 68 °C for 12 min (11 cycles to step 2), and a final extension step. All PCR products were purified and cloned into pGEX 4T-2 as for wild-type cDNA (14).

The G223D/T224I and G223D/T224I/H225N mutants were obtained using a method based on the QuikChange XL site-directed mutagenesis kit (Stratagene). Full-length pGEX 4T-2, containing G223D and T224I/H225N cDNAs, were used as templates to obtain the double and triple mutants, respectively. Mutagenesis was performed by means of a single PCR using an antisense primer containing the mutation (223/224R, 5′-GTCTTTATGGATATCAACCCCTATAATAC-3′ or TMR, 5′-GTCTTTATTGATATCAACCCCTATAATACG-3′) and primers containing either sense mutation. PCR conditions were the same as above except for the use of Expand Long Template polymerase (Roche). PCR products were incubated with *Dpn*I at 37 °C for 60 min. This treatment ensured the digestion of the *dam*-methylated parental strand (15). The resulting nicked circular mutagenic strands were transformed into *Escherichia coli* BL21, where bacterial DNA ligase repaired the nick and allowed normal replication to occur. Prior to expression, all mutated DNAs were completely sequenced, to ensure that unwanted mutations were absent.

Protein Expression and Purification—All mutants were expressed using the conditions previously described for the wild-type enzyme (14). Batch-wise purification of wild-type and T224I enzymes followed identical procedures (14). For G223D, H225N, G223D/T224I, T224I/H225N, and G223D/T224I/H225N mutants, the only difference was the matrix used in the last affinity chromatography step (Cibacron Blue 3-GA; Sigma). The degree of purity for each protein was assessed by means of SDS-polyacrylamide gel electrophoresis and Coomassie Blue staining. Protein concentration was determined using the Bio-Rad assay, based on the method of Bradford (16).

Enzyme Activity Assays—Alcohol dehydrogenase activity was determined at 25 °C by monitoring the change in absorbance at 340 nm, using a Cary 400 Bio (Varian) spectrophotometer. One unit of activity corresponds to 1 μmol of reduced coenzyme formed or utilized per min, based on an absorption coefficient of 6220 M^{-1} cm^{-1} at 340 nm for NADH or NADPH. Cuvette path length was 1 cm in oxidation reactions and 0.2 cm in reduction reactions. Alcohol oxidation was performed in 0.1 M glycine/NaOH, pH 10.0, or in 0.1 M sodium phosphate/NaOH, pH 7.5, using 1 M ethanol or 1.5 mM octanol as a substrate, respectively. For aldehyde reduction, 0.1 M sodium phosphate/NaOH, pH 7.5, and 0.2 mM *m*-nitrobenzaldehyde were used. When saturation could be reached, kinetic parameters were obtained from activity measurements with substrate or coenzyme concentrations that ranged from 0.1 × K_m to 10 × K_m. Each individual rate measurement was run in duplicate. Three determinations were performed for each kinetic constant. Kinetic constants were obtained with the non-linear regression program Grafit 5.0 (Erithacus Software Ltd.) and expressed as the mean ± S.D. Bisubstrate kinetic constants were calculated by fitting data to a Bi-Bi sequential mechanism (17). The standard assays were performed using 1 M ethanol as a substrate in 0.1 M glycine/NaOH, pH 10.0, and 1.2 mM NADP$^+$ for wild-type and G223D mutants; 2.4 mM NADP$^+$ for T224I and H225N mutants; 0.4 mM NAD$^+$ for G223D/T224I/H225N; and 2.4 mM NAD$^+$ for G223D/T224I and T224I/H225N mutants.

Deuterium Kinetic Isotope Effect—Kinetic constants for NAD$^+$ and NADP$^+$ were determined in 0.1 M Gly/NaOH, pH 10.0, with 1 M ethanol-d_6 (Merck) or ethanol as a substrate at different coenzyme concentrations, depending on the enzyme assayed. For the G223D/T224I and G223D/T224I/H225N mutants, saturation with NADP$^+$ could not be achieved, and thus a single concentration of 4.8 mM NADP$^+$ was used to measure enzyme activity. Assay buffer and ethanol-d_6 solution were prepared in deuterated water.

Structural Modeling of the Variants—The structures of all the variants were modeled using the available coordinates of the binary complex ADH8-NADP$^+$ (Protein Data Bank entry 1P0F, Ref. 3), where the corresponding substituted residues were introduced with the graphics program O (18). Conformations of the replaced residues were initially assumed to be the rotamers that presented less steric constraints. The geometry of the models was then regularized and refined throughout cycles of energy minimization with the program XPLOR (19).

RESULTS

Our study focused on residues 223 to 225 of ADH8, with the aim of testing their role in the phosphate-binding site and attempting the switch of coenzyme specificity. The obvious choice was to mutate Gly^{223}, Thr^{224}, and His^{225} to Asp, Ile, and Asn, respectively, because the sequence Asp^{223}-Ile/Leu^{224}-Asn^{225} is well conserved among vertebrate NAD-dependent ADHs (4). Therefore, single ADH8 mutants, G223D, T224I, and H225N, double mutants, G223D/T224I and T224I/H225N, and the triple mutant, G223D/T224I/H225N, were generated by

TABLE II
Kinetic constants of wild-type and mutant ADH8 with NAD^+ and $NADP^+$ at pH 7.5
Activities were measured with 1.5 mM octanol and 0.1 M sodium phosphate/NaOH at pH 7.5.

Enzyme	Coenzyme	K_m	k_{cat}	k_{cat}/K_m
		mM	min^{-1}	$mM^{-1}\ min^{-1}$
Wild-type	$NADP^+$	0.045 ± 0.007	640 ± 35	14,220 ± 2,330
	NAD^+	2.0 ± 0.2	640 ± 15	320 ± 33
G223D	$NADP^+$	0.090 ± 0.008	160 ± 9	1,780 ± 430
	NAD^+	0.64 ± 0.02	420 ± 50	655 ± 80
T224I	$NADP^+$	0.07 ± 0.01	330 ± 11	4,715 ± 730
	NAD^+	0.36 ± 0.06	560 ± 38	1,555 ± 272
H225N	$NADP^+$	0.11 ± 0.01	590 ± 37	5,360 ± 640
	NAD^+	3.0 ± 0.2	450 ± 48	150 ± 21
G223D/T224I	$NADP^+$	NS[a]	NS	1.3 ± 0.1[b]
	NAD^+	0.25 ± 0.03	330 ± 17	1,500 ± 220
T224I/H225N	$NADP^+$	9.0 ± 0.7	95 ± 5	10 ± 1
	NAD^+	0.34 ± 0.03	580 ± 31	1,700 ± 160
G223D/T224I/H225N	$NADP^+$	NS	NS	6 ± 1[b]
	NAD^+	0.05 ± 0.01	785 ± 33	15,700 ± 2,890

[a] NS, no saturation up to 4.8 and 9.6 mM $NADP^+$ for G223D/T224I and G223D/T224I/H225N, respectively.
[b] k_{cat}/K_m was calculated as the slope of the linear plot of *V versus* [S].

site-directed mutagenesis. The expression level for the wild-type enzyme and mutants was ~30 mg/liter of culture. All enzymes were purified to homogeneity with a 10% yield, and they were stable for several weeks when stored at 4 °C.

Steady-state Kinetics of Wild-type and Mutant Enzymes—Steady-state kinetic constants of wild-type and substituted ADH8 with NAD^+ and $NADP^+$, at pH 10.0 and 7.5, determined under saturating concentrations of substrate, are presented in Tables I and II, respectively. Kinetic constants in the reductive direction for NADH and NADPH, at pH 7.5, are shown in Table III.

In the wild-type recombinant ADH8, the kinetic constants were similar to those previously reported for the native enzyme purified from frog stomach tissue (2). At a given pH and with the same substrate, the k_{cat} values attained with NADP(H) and NAD(H) were similar, suggesting a common rate-limiting step, independent of the cofactor used. By contrast, K_m values for NADP(H) were 10–40-fold lower than those for NAD(H). This resulted in an enzyme much more specific for NADP(H), especially at pH 7.5.

Regarding the effect of substitutions on coenzyme kinetics, most of the observations made at pH 10.0 (Table I) could be confirmed at pH 7.5, for both the oxidation (Table II) and the reduction (Table III) reactions. This suggests that the introduced mutations had a similar effect on each coenzyme kinetics, independently of pH and whether the cofactor used was in its oxidized or reduced form. However, the substitutions did have a different effect on whether the cofactor used was NADP(H) or NAD(H).

Single mutations only produced a small decrease (2–8-fold) in the catalytic efficiency (k_{cat}/K_m) with NADP(H). Generally, this was because of an increase in K_m values, whereas k_{cat} values did not significantly change in the mutants. The substitution G223D did not hamper $NADP^+$ binding (see below) or change the catalytic rate significantly, as would have been anticipated, but resulted in an enzyme that still preferred NADP(H) over NAD(H). Similar results were obtained for the T224I mutant. The H225N substitution was well tolerated as it had the least effect on NADP(H) kinetics. No pH-dependent effect was observed associated with this mutation, perhaps because in the enzyme the His residue is deprotonated at both pH 7.5 and 10.0.

Single mutations provided a positive effect on NAD(H) kinetics, with a moderate increase in k_{cat}/K_m values. T224I showed the best catalytic efficiency for a single mutant, whereas H225N displayed the lowest catalytic efficiency, mostly due to its high K_m values for this coenzyme. In all single mutants, k_{cat} values for NAD(H) remained essentially constant, which is suggestive of a common rate-limiting step. At any pH employed, none of the three mutants showed a reversal of coenzyme specificity. Only the mutant T224I showed a very similar catalytic efficiency with the two cofactors at pH 10.0 (Table I).

A double mutation, G223D/T224I or T224I/H225N, was the minimal change to show a clearcut effect on coenzyme specificity, both at pH 7.5 and 10.0. The effect was most marked on NADP(H) kinetic constants, especially in the G223D/T224I mutant. This mutant could not be saturated with NADP(H) and thus K_m and k_{cat} values could not be determined. Kinetic constants could only be accurately measured for the T224I/H225N mutant in the oxidative direction: K_m values for NADP(H) increased dramatically (up to 200-fold) and k_{cat} values dropped down 30-fold. Catalytic efficiency with NADP(H) decreased from 1,500 to 10,000-fold for G223D/T224I and from 100 to 1,400-fold for T224I/H225N. Both mutants showed a moderate increase in k_{cat}/K_m values for NAD(H), mostly because of a small decrease in K_m values (more marked in G223D/T224I), with respect to the single mutant T224I. Overall, the double mutants showed a switch in coenzyme specificity, but without reaching full catalytic efficiency with NAD(H), which was only observed in the triple mutant.

The G223D/T224I/H225N triple substitution produced a complete reversal of coenzyme specificity, both at pH 7.5 and 10.0. In comparison with the double mutants, the effect was most marked on the NAD(H) kinetics. Thus, the catalytic efficiency of the triple mutant with NAD(H) increased 30–50-fold with respect to that of the wild-type enzyme, and it was even higher than the k_{cat}/K_m value of the wild-type enzyme with NADP(H). This was mainly provoked by a decrease in K_m values for NAD(H), which paralleled an increase in the affinity for the coenzyme (see below). On the other hand, the triple mutant could not be saturated by NADP(H) and the catalytic efficiency with NADP(H) decreased to about the same order of magnitude as those of the double mutants. Overall, the triple

TABLE III
Kinetic constants of wild-type and mutant ADH8 with NADH and NADPH at pH 7.5
Activities were measured with 0.2 mM *m*-nitrobenzaldehyde and 0.1 M sodium phosphate/NaOH at pH 7.5.

Enzyme	Coenzyme	K_m	k_{cat}	k_{cat}/K_m
		mM	min^{-1}	$mM^{-1}\ min^{-1}$
Wild-type	NADPH	0.030 ± 0.006	4,000 ± 10	133,330 ± 26,670
	NADH	0.44 ± 0.07	2,455 ± 190	5,580 ± 990
G223D	NADPH	0.110 ± 0.008	1,765 ± 120	16,050 ± 1,590
	NADH	0.150 ± 0.006	1,610 ± 50	10,735 ± 550
T224I	NADPH	0.050 ± 0.001	1,920 ± 80	38,400 ± 1,720
	NADH	0.110 ± 0.008	1,920 ± 10	17,455 ± 1,260
H225N	NADPH	0.080 ± 0.003	4,605 ± 110	57,560 ± 2,535
	NADH	0.660 ± 0.016	2,350 ± 70	3,560 ± 140
G223D/T224I	NADPH	NS[a]	NS	89 ± 7[b]
	NADH	0.040 ± 0.002	1,500 ± 190	37,550 ± 5,100
T224I/H225N	NADPH	NS	NS	1,250 ± 50[b]
	NADH	0.150 ± 0.016	2,805 ± 100	18,700 ± 2,100
G223D/T224I/H225N	NADPH	NS	NS	760 ± 21[b]
	NADH	0.040 ± 0.001	6,200 ± 150	155,000 ± 4,100

[a] NS, no saturation up to 1.2 mM NADPH.
[b] k_{cat}/K_m was calculated as the slope of the linear plot of *V versus* [S].

TABLE IV
Bisubstrate kinetics of wild-type and mutant ADH8 with NAD^+ and $NADP^+$ at pH 10.0
Activities were measured in 0.1 M glycine/NaOH at pH 10.0, with ethanol as a substrate. Standard errors of fits were less than 20%, except for the indicated values.

Enzyme	Coenzyme	K_{ia}	K_a	K_b	k_{cat}	$k_{cat}/K_{ia}K_b$
		mM	*mM*	*mM*	min^{-1}	$mM^{-2}\ min^{-1}$
Wild-type	$NADP^+$	0.02	0.042	25	1,520	3,040
	NAD^+	0.56	0.83	31	1,790	103
G223D	$NADP^+$	0.037[a]	0.14	109	570	141
	NAD^+	0.22[a]	0.33	35	1,100	143
T224I	$NADP^+$	0.028	0.12	98	900	328
	NAD^+	0.12[a]	0.20	41	2,250	457
H225N	$NADP^+$	0.16	0.10	40	1,700	265
	NAD^+	0.71	0.88	39	1,795	65
T224I/H225N	$NADP^+$	1.22	1.16	56	76	1
	NAD^+	0.12	0.23	68	2,090	256
G223D/T224I/H225N	$NADP^+$	NS[b]	NS	NS	NS	NS
	NAD^+	0.017[a]	0.04	45	2450	3,200

[a] Standard errors of fits were 20-30%.
[b] NS, no saturation up to 9.6 mM $NADP^+$.

mutant was much more NAD(H) specific than wild-type ADH8 was with NADP(H).

Bisubstrate kinetics were performed by covarying the concentrations of ethanol and either coenzyme, and were compatible with a Bi-Bi sequential kinetic mechanism (Table IV). In the enzymatic forms tested, K_m values for ethanol (K_b) ranged between 25 and 110 mM. Single substitutions had modest effects on the k_{cat} value with $NADP^+$ but this dropped ~20-fold in the T224I/H225N double mutant and could not be determined in the triple mutant because saturation could not be reached. For the double mutant, this dramatic change in the k_{cat} value with $NADP^+$ paralleled an increase in the dissociation (K_{ia}) and Michaelis constant (K_a) values for $NADP^+$ by 60- and 30-fold, respectively. In contrast, the k_{cat} value with NAD^+ remained relatively unchanged in all the substituted forms, suggesting a common rate-limiting step. Catalytic efficiency for NAD^+, as measured by $k_{cat}/K_{ia}K_b$ (20), increased by 30-fold,

TABLE V
Deuterium kinetic isotope effects of wild-type and mutant ADH8 at pH 10.0
Activities were measured with 1 M ethanol-d_6 or ethanol as a substrate and 0.1 M glycine/NaOH at pH 10.0.

Enzyme	$NADP^+$		NAD^+	
	k_{catH}/k_{catD}	$(k_{catH}/K_{mH})/(k_{catD}/K_{mD})$	k_{catH}/k_{catD}	$(k_{catH}/K_{mH})/(k_{catD}/K_{mD})$
Wild-type	1.99	1.99	1.85	2.02
G223D	2.04	1.95	1.72	1.86
T224I	1.94	2.04	1.88	2.04
H225N	2.11	2.04	1.87	1.81
G223D/T224I	1.31[a]	1.15[b]	1.78	1.57
T224I/H225N	1.03	1.08	1.60	1.80
G223D/T224I/H225N	0.90[a]	1.02[b]	2.08	1.66

[a] Activity ratio was calculated from a single concentration of coenzyme (4.8 mM $NADP^+$) because saturation could not be reached.
[b] k_{cat}/K_m was calculated as the slope of the linear plot of *V versus* [S], since saturation could not be reached.

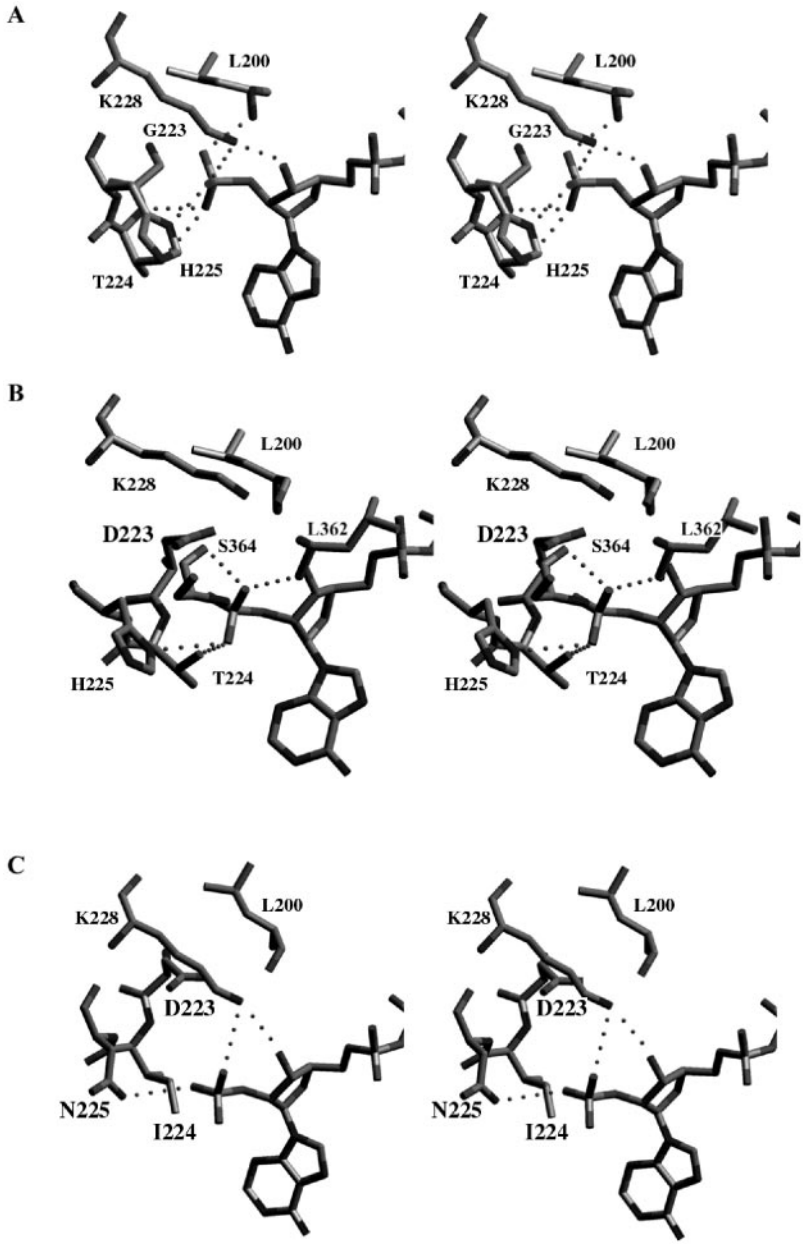

FIG. 1. **Stereo views of the adenosine-phosphate moiety of NADP$^+$ bound to wild-type and mutant forms of ADH8.** Interaction through hydrogen bonds is represented with *dotted lines*. *A*, crystallographic binary complex of wild-type ADH8 (Protein Data Bank code 1P0F, Ref. 3). Docking of NADP$^+$ inside the coenzyme-binding pocket of ADH8 mutants: *B*, G223D; *C*, G223D/T224I/H225N.

reaching the same level as that of the wild-type enzyme for NADP$^+$.

The kinetic isotope effect was studied with deuterated ethanol in the presence of either coenzyme. A substrate kinetic isotope effect of ~2-fold was observed with either NADP$^+$ or NAD$^+$ in the wild-type ADH8 (Table V), suggesting that hydride transfer may be the rate-limiting step during catalysis. When using NADP$^+$ as a cofactor, the same increase was only seen in the single mutant forms. In contrast, the double and triple mutants did not display any significant isotope effect, indicating that hydride transfer was no longer rate-limiting. With NAD$^+$ as a coenzyme, the 2-fold isotope effect was obtained for all the mutant forms.

Computer Modeling of Binary Complexes—Docking simulations of NADP$^+$ and NAD$^+$ to the wild-type and mutant enzymes were performed based on the three-dimensional structure of the binary complex ADH8-NADP$^+$ (3). In this structure, the oxygen atoms from the extra phosphate group interact through five hydrogen bonds with the side chains of Thr^{224}, His^{225}, Lys^{228}, and the nitrogen main chain atoms of Leu^{200} and Thr^{224} (Fig. 1*A*). In the G223D-NADP$^+$ complex, steric and electrostatic hindrances by the side chain of Asp^{223} force the coenzyme phosphate to relocate in the binding site, moving away from Lys^{228} (compare Fig. 1, *B* and *A*). Thus, as a result of the G223D mutation, hydrogen bonds with Leu^{200}, Lys^{228}, and the nitrogen main chain atom of Thr^{224} are missing. But these losses are partially compensated by the existence of two new hydrogen bonds between the same oxygen atom of the terminal phosphate and the carbonyl oxygen atom of Leu^{362} and the oxygen atom of Ser^{364}. Thus, one oxygen atom of the extra phosphate group is left without interacting, although it could do so through a water molecule. Small differences are observed in T224I-NADP$^+$ and H225N-NADP$^+$ complexes with respect to NADP$^+$ docked to the wild-type enzyme. In both cases, two hydrogen bond interactions involving the extra phosphate are lost, but a new hydrogen bond is formed in such a way that all the oxygen atoms of the extra phosphate group are interacting with some residue (data not shown). When comparing NADP$^+$ binding to the T224I/H225N mutant with respect to the wild-type enzyme, an oxygen atom of the extra phos-

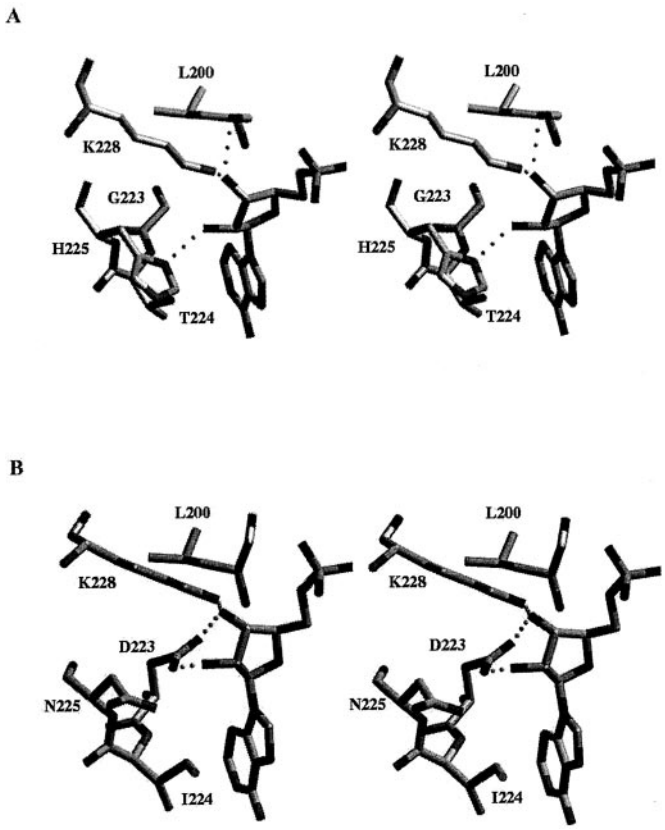

FIG. 2. **Stereo views of the adenosine moiety of NAD$^+$ docked inside the coenzyme-binding pocket of wild-type ADH8 and triple mutant.** Interaction through hydrogen bonds is indicated with *dotted lines*. *A*, wild-type ADH8; *B*, G223D/T224I/H225N.

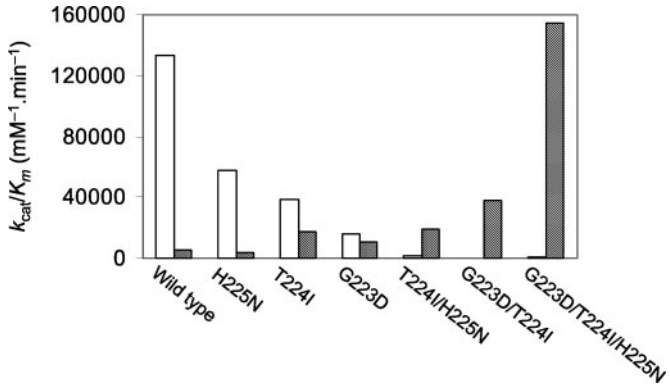

FIG. 3. ***Bar graph* representing the catalytic efficiency (k_{cat}/K_m) for each coenzyme of the wild-type and ADH8 mutants.** NADPH, *white bars*; NADH, *hatched bars*. Data are taken from Table III.

phate group would not interact with any residue, but it is conceivable that it could do so through a water molecule (data not shown).

In the simulation of docking NADP$^+$ to the G223D/T224I/H225N mutant, as it was previously observed for the G223D mutant, there is a relocation of the coenzyme. In this case, although, several protein-phosphate interactions (three hydrogen bonds) are lost and they are not compensated by new hydrogen bond formation. As a result, an oxygen atom of the extra phosphate group does not interact with any residue, although interaction through water molecules is still possible (compare Fig. 1, *C* and *A*).

Remarkably, in the binary complex of the triple mutant with NAD$^+$, Asp^{223} interacts with the 2′ and 3′ oxygen atoms of ribose, and Lys^{228} is hydrogen bonded with the 3′ oxygen (compare Fig. 2, *B* and *A*). These features are characteristic of NAD-dependent ADHs (21–24). Likewise, a hydrophobic interaction is gained between the adenine ring and Ile^{224}, which is not seen in the complex of the triple mutant with NADP$^+$ (compare Figs. 2*B* and 1*C*). This hydrophobic interaction is also typical of NAD-dependent ADHs and other NAD-dependent enzymes (25).

DISCUSSION

ADH8 is unique within the vertebrate ADH family in that it uses preferentially NADP(H) as a cofactor (2). ADH8 also binds NAD(H), but with K_m values that are 10 to 40 times higher than those for NADP(H). Structural studies on the binary complex ADH8-NADP$^+$ suggested that a phosphate binding pocket is configured by non-conserved residues 223, 224, and 225, and the highly conserved Leu^{200} and Lys^{228} (3). However, the contribution of these residues to the discrimination between NAD(H) and NADP(H) remains unknown. This fundamental question and the challenge of reverting coenzyme specificity prompted us to perform the present site-directed mutagenesis study. Therefore adjacent residues 223, 224, and 225 were systematically mutated and checked, separately or in different combinations.

Effect of Substitutions on the Rate-limiting Step and Catalytic Constant—In ADH8 single mutants, k_{cat} values for NADP(H) decreased slightly, whereas a moderate increase in K_{ia} values for NADP$^+$ was observed. Hydride transfer appeared to be the rate-limiting step. In contrast, in the T224I/H225N mutant, k_{cat} values for NADP$^+$ suffered a sharp decrease, which was associated with a marked increase in the K_{ia} value for NADP$^+$. In this regard, in double and triple mutants, the catalytic efficiency dropped dramatically, reflecting the fact that K_m values for NADP(H) increased, and even in most cases saturation could not be reached, and apparent k_{cat} values likely decreased. In concordance with this observation, the kinetic isotope effect was lost, indicating a change in the rate-limiting step, no longer being hydride transfer. A slower limiting step, such as a conformational change associated with coenzyme binding could be involved. However, at this time, we have no evidence for a conformational change upon coenzyme binding, because the crystal structure of the apoenzyme showed a closed conformation (3). On the other hand, it is likely that coenzyme dissociation was not the new rate-limiting step because the increase in K_{ia} values was not followed by an increase in k_{cat} values.

The k_{cat} values for NAD(H) remained relatively unchanged for the mutant enzymes with respect to the wild-type recombinant ADH8, indicating that the rate-limiting step was likely the same for all the enzymatic forms when NAD(H) was the coenzyme. This result was consistent with the finding of a slight deuterium kinetic isotope effect whenever NAD$^+$ was the coenzyme, suggesting that hydride transfer was rate-limiting. Hydride transfer has also been found limiting in other ADHs using ethanol as a substrate, such as human ADH3 (26) and horse liver I269S (27). The finding in ADH8 differs from what has been described for horse liver ADH and other ADH forms, with ethanol and other aliphatic alcohols as substrates, where the rate-limiting step is NADH dissociation (28, 29). In those cases, an increase in K_{ia} and K_{iq} (dissociation constants for NAD and NADH, respectively) often parallels an increase in k_{cat} values, which is not observed in ADH8.

Residue 223 Is Not the Only Discriminating Residue for Coenzyme Specificity—In the coenzyme-binding domain of NAD-dependent dehydrogenases with the Rossmann fold, an acidic residue (Asp^{223} in NAD-dependent ADHs, Ref. 4) is located at

the C-terminal end of the second β-strand (30). Asp^{223} is doubly hydrogen bonded to the adenine ribose diol in ADH-NAD^+ complexes (21–24). The significance of this acidic residue has been observed long ago and has been considered a fingerprint for NAD(H) binding pockets (8, 31). In ADHs, it has been proposed as the residue that discriminates against NADP(H) (9). NADP-dependent enzymes exhibit a smaller and uncharged residue, usually Gly, Ala, or Ser (3, 10, 32–34), that would reduce steric and electrostatic hindrances on binding of the extra phosphate group of NADP(H). Thus, to reverse coenzyme specificity, several studies have targeted this residue by site-directed mutagenesis. In one case, the homologous Asp residue in yeast ADHI was substituted by Gly and the resulting D223G mutant utilized the two coenzymes with similar but very low efficiency (9). In cinnamyl alcohol dehydrogenase, an NADP-dependent enzyme from the MDR superfamily, the equivalent reverse mutation S212D did not change the coenzyme specificity either (10). Similarly, the substitution of the corresponding Asp in other NAD-dependent dehydrogenases having the Rossmann fold did not generate NADP-dependent enzymes, although substitution improved the catalytic efficiency for $NADP^+$ and made it worse for NAD^+ (35, 36).

In the present paper, single mutations G223D, T224I, and H225N only provided small changes to coenzyme kinetics, which were slightly detrimental for NADP(H) and beneficial for NAD(H). For NADP(H), in general, there existed a good correlation between the loss of a few hydrogen bonds and electrostatic interactions, and a modest increase in K_m and K_{ia} values, as predicted by molecular docking simulations. In particular, the substitution G223D did not greatly hamper $NADP^+$ binding as it would have been anticipated but resulted in an enzyme that still preferred NADP(H) over NAD(H) (Fig. 3) although with a lower catalytic constant. The modeling results for the G223D mutant confirm the generation of unfavorable steric and electrostatic conditions on NADP(H) binding. But interestingly, the extra phosphate group of coenzyme can still be accommodated in the coenzyme binding pocket by moving away from Asp^{223} and Lys^{228}, at the expense of losing some hydrogen bonds and favorable electrostatic interactions. According to these results and confirming previous findings in other ADHs (9–12), Asp^{223} alone cannot be considered the discriminating residue in the coenzyme specificity of ADH8, and thus the combined substitutions in other positions along with that of residue 223 would be important as well.

Complete Reversal of Coenzyme Specificity in the Triple Mutant—In the triple mutant, the attained K_m, k_{cat}, and k_{cat}/K_m values for NAD(H) and K_{ia} for NAD^+ are in the same order of magnitude as those for NADP(H) in the wild-type enzyme. Thus, complete reversal of coenzyme specificity has been achieved (Fig. 3). Moreover, the k_{cat}/K_m values with NAD(H) obtained in the triple mutant are similar to those of typical NAD-dependent ADHs (37–42). It is conceivable that some kind of threshold in catalytic power has been attained in many ADHs regarding coenzyme usage. Overall, the triple mutant is much more "coenzyme specific" than the wild-type enzyme, as illustrated by the ratio $k_{cat}/K_{m(NADH)}/k_{cat}/K_{m(NADPH)}$ (Fig. 3). This behavior is typical of NAD-dependent vertebrate ADHs, which frequently are highly specific for NAD(H) although some have residual activity with NADP(H). In the triple mutant, the extra phosphate group poses steric and electrostatic problems for NADP(H) binding, especially because of the presence of both Asp^{223} and a less hydrophilic environment at positions 224 and 225. In contrast, NAD(H) can easily be accommodated in the vacant phosphate-binding site (with Gly) and interact with His^{225} and Lys^{228} in the NADP-dependent wild-type enzyme.

Synergistic Effects between Adjacent Residues Determine Coenzyme Specificity—Our results highlight the importance of cooperative or synergistic effects between two or more adjacent amino acid residues. Single amino acid substitutions had only very limited effects, whereas double and triple mutations involving the same residues caused great changes on coenzyme binding and kinetics. In ADH8, it is the combined contribution of these groups, interacting with one another and with the coenzyme, that provides alternative binding sites for the adenosine/adenosine-phosphate moiety of NAD(H)/NADP(H). NAD(H) requires the simultaneous presence of Asp^{223}, Ile^{224}, and Asn^{225}, although it does not interact with Asn^{225} in ADH8 nor in other ADH structures. NADP(H) needs Gly^{223}, Thr^{224}, and His^{225}, but it does not interact with Gly^{223}. Apparently, in ADH8, the small side chain of Gly^{223} provides additional space for the phosphate group of NADP(H) to interact with Lys^{228}, while in the triple mutant Asn^{225} leaves more space than His, for the adenine ring of NAD(H) to interact hydrophobically with Ile^{224}. Asp^{223} helps discriminate against NADP(H) and provides hydrogen bonding at the precise distance for NAD(H) to interact properly with Ile^{224} and Lys^{228}. Lys^{228} is a versatile highly conserved residue that performs a dual function, *i.e.* the electrostatic interaction with the extra phosphate of NADP(H) or the hydrogen bond interaction with the 3′ oxygen of NAD(H) ribose. It is clear that each of these residues has in ADH8 a different function from that in NAD-dependent ADHs. As expected, ionic interactions play a predominant role in NADP(H) binding, whereas hydrogen bonding and hydrophobic interactions are more prevalent for NAD(H) binding. The present results are consistent with the previous finding that $NADP^+$ binds to ADH8 in a similar conformation to that of NAD^+ found in ADH binary complexes, showing small differences only in the adenosine moiety of coenzyme (3).

The most effective switches in coenzyme specificities have come from multiple mutations in different regions of the primary structure of dehydrogenases (43–46). In contrast, the complete reversal of coenzyme specificity in ADH8 has been obtained by means of substitution of only three consecutive amino acid residues. The absence of an acidic residue together with the presence of polar residues around the extra phosphate group contribute to the NADP(H) specificity of ADH8. ADH architecture appears to be flexible enough to satisfy changes in coenzyme requirements and thus NADP-dependent enzymes have convergently evolved within the MDR superfamily at different times using seemingly different strategies and independent pathways: *e.g.* secondary ADH in bacteria (5–7), cinnamyl ADH in plants and fungi (10), quinone oxidoreductase in animals and bacteria (33), sorbitol dehydrogenase in insects (34), and ADH8 in amphibians (3). Our data support that concerted evolution of adjacent amino acid residues (223 to 225) within a short sequence segment, requiring minimally four point mutations in the gene sequence, has allowed coenzyme specificity in amphibian ADH to switch. This may reflect ADH8 late enzymogenesis, with a relatively recent evolutionary origin of this NADP-dependent structure from an ancestral NAD(H)-specific structure (class I ADH, 70% identity), as well as a fast functional adaptation to different metabolic needs (*i.e.* reduction of aldehydes, such as retinal, instead of oxidation of alcohols) (2). Undoubtedly, the simplicity of these evolutionary changes has contributed to facilitate the redesign of the coenzyme-binding site and to achieve the complete reversal of coenzyme specificity reported here.

Acknowledgment—We thank A. A. Santos for performing site-directed mutagenesis, expression, and purification of T224I and H225N mutants.

REFERENCES

1. Backer, P. J., Britton, K. L., Rice, D. W., Rob, A., and Stillman, T. J. (1992) *J. Mol. Biol.* **228,** 662–671
2. Peralba, J. M., Cederlund, E., Crosas, B., Moreno, A., Julià, P., Martínez, S. E., Persson, B., Farrés, J., Parés, X., and Jörnvall, H. (1999) *J. Biol. Chem.* **274,** 26021–26026
3. Rosell, A., Valencia, E., Parés, X., Fita, I., Farrés, J., and Ochoa, W. F. (2003) *J. Mol. Biol.* **330,** 75–85
4. Sun, H. W., and Plapp, B. V. (1992) *J. Mol. Evol.* **34,** 522–535
5. Burdette, D. S., Vieille, C., and Zeikus, J. G. (1996) *Biochem. J.* **316,** 115–122
6. Korkhin, Y., Kalb, A. J., Peretz, M., Bogin, O., Burstein, Y., and Frolow, F. (1998) *J. Mol. Biol.* **278,** 967–981
7. Kumar, A., Shen, P. S., Descoteaux, S., Pohl, J., Bailey, G., and Samuelson, J. (1992) *Proc. Natl. Acad. Sci. U. S. A.* **89,** 10188–10192
8. Rossmann, M. G., Moras, D., and Olsen, K. W. (1974) *Nature* **250,** 194–199
9. Fan, F., Lorenzen, J. A., and Plapp, B. V. (1991) *Biochemistry* **30,** 6397–6401
10. Lauvergeat, V., Kennedy, K., Feuillet, C., McKie, J. H., Gorrichon, L., Baltas, M., Boudet, A. M., Grima-Pettenati J., and Douglas, K. T. (1995) *Biochemistry* **34,** 12426–12434
11. Metzger, M. H., and Hollenberg, C. P. (1995) *Eur. J. Biochem.* **228,** 50–54
12. Fan, F., and Plapp, B. V. (1999) *Arch. Biochem. Biophys.* **367,** 240–249
13. Cederlund, E., Peralba, J. M., Parés, X., and Jörnvall, H. (1991) *Biochemistry* **30,** 2811–2816
14. Valencia, E., Rosell, A., Larroy, C., Farrés, J., Biosca, J. A., Fita, I., Parés, X., and Ochoa, W. F. (2003) *Acta Crystallogr. Sect. D Biol. Crystallogr.* **59,** 334–337
15. Nelson, M., and McClelland, M. (1992) *Methods Enzymol.* **216,** 279–303
16. Bradford, M. M. (1976) *Anal. Biochem.* **72,** 248–254
17. Cleland, W. W. (1979) *Methods Enzymol.* **63,** 103–138
18. Jones, T. A., Zou, J. Y., Cowan, S. W., and Kjeldgaard, M. (1991) *Acta Crystallogr. Sect. A* **47,** 110–119
19. Brünger, A. T., Adams, P. D., Clore, G. M., DeLano, W. L., Gros, P., Grosse-Kunstleve, R. W., Jiang, J. S., Kuszewski, J., Nilges, M., Pannu, N. S., Read, R. J., Rice, L. M., Simonson, T., and Warren, G. L. (1998) *Acta Crystallogr. Sect. D Biol. Crystallogr.* **54,** 905–921
20. Plapp, B. V. (1995) *Methods Enzymol.* **249,** 91–119
21. Eklund, H., Samama, J. P., and Jones, T. A. (1984) *Biochemistry* **23,** 5982–5996
22. Hurley, T. D., Bosron, W. F., Hamilton, J. A., and Amzel, L. M. (1991) *Proc. Natl. Acad. Sci. U. S. A.* **88,** 8149–8153
23. Xie, P., Parsons, S. H., Speckhard, D. C., Bosron, W. F., and Hurley, T. D. (1997) *J. Biol. Chem.* **272,** 18558–18563
24. Svensson, S., Höög, J. O., Schneider, G., and Sandalova, T. (2000) *J. Mol. Biol.* **302,** 441–453
25. Carugo, O., and Argos, P. (1997) *Proteins* **28,** 10–28
26. Lee, S. L., Wang, M. F., Lee, A. I., and Yin, S. J. (2003) *FEBS Lett.* **544,** 143–147
27. Fan, F., and Plapp, B. V. (1995) *Biochemistry* **34,** 4709–4713
28. Brändén, C. I., and Eklund, H. (1980) *Experientia Suppl.* (*Basel*) **36,** 40–84
29. Stone, C. L., Bosron, W. F., and Dunn, M. F. (1993) *J. Biol. Chem.* **268,** 892–899
30. Bellamacina, C. R. (1996) *FASEB J.* **10,** 1257–1269
31. Ohlsson, I., Nordstrom, B., and Brändén, C. I. (1974) *J. Mol. Biol.* **89,** 339–354
32. Lesk, A. M. (1995) *Curr. Opin. Struct. Biol.* **5,** 775–783
33. Edwards, K. J., Barton, J. D., Rossjohn, J., Thorn, J. M., Taylor, G. L., and Ollis, D. L. (1996) *Arch. Biochem. Biophys.* **328,** 173–183
34. Banfield, M. J., Salvucci, M. E., Baker, E. N., and Smith, C. A. (2001) *J. Mol. Biol.* **306,** 239–250
35. Feeney, R., Clarke, A. R., and Holbrook, J. J. (1990) *Biochim. Biophys. Res. Commun.* **166,** 667–672
36. Chen, Z., Lee, W. R., and Chang, S. H. (1991) *Eur. J. Biochem.* **202,** 263–267
37. Bosron, W. F., Li, T. K., Dafeldecker, W. P., and Vallee, B. L. (1979) *Biochemistry* **20,** 1101–1105
38. Bosron, W. F., Magnes, L. J., and Li, T.-K. (1983) *Biochemistry* **22,** 1852–1857
39. Burnell, J. C., and Bosron, W. F. (1989) in *Human Metabolism of Alcohol* (Crow, K. E., and Batt, R. D., eds) Vol. II, pp. 65–75, CRC Press, Inc., Boca Raton, FL
40. Farrés, J., Moreno, A., Crosas, B., Peralba, J. M., Allali-Hassani, A., Hjelmqvist, L., Jörnvall, H., and Parés, X. (1994) *Eur. J. Biochem.* **224,** 549–557
41. Peralba, J. M., Crosas, B., Martínez, S. E., Julià, P., Farrés, J., and Parés, X. (1999) *Adv. Exp. Med. Biol.* **463,** 343–350
42. Crosas, B., Allali-Hassani, A., Martínez, S. E., Martras, S., Persson, B., Jörnvall, H., Parés, X., and Farrés, J. (2000) *J. Biol. Chem.* **275,** 25180–25187
43. Scrutton, N. S., Berry, A., and Perham, R. N. (1990) *Nature* **343,** 38–43
44. Mittl, P. R. E., Berry, A., Scrutton, N. S., Perham, R. N., and Schulz, G. E. (1993) *J. Mol. Biol.* **231,** 191–201
45. Mittl, P. R. E., Berry, A., Scrutton, N. S., Perham, R. N., and Schulz, G. E. (1994) *Protein Sci.* **3,** 1504–1514
46. Bocanegra, J. A., Scrutton, N. S., and Perham, R. N. (1993) *Biochemistry* **32,** 2737–2740